The QCD Quark Propagator in Coulomb Gauge and some Implications for Hadronic Physics

Dissertation

zur Erlangung des Grades eines Doktors
der Naturwissenschaften

der Fakultät für Mathematik und Physik
der Eberhard-Karls-Universität zu Tübingen

vorgelegt von
Markus Kloker
aus Blaubeuren

2007

Tag der mündlichen Prüfung: 22.06.2007

Dekan: Prof. Dr. Nils Schopohl

1. Berichterstatter: Prof. Dr. Herbert Müther / Prof. Dr. Reinhard Alkofer
2. Berichterstatter: Prof. Dr. Kurt Langfeld

Abstract

We present approximate non-perturbative solutions for the quark propagator in Coulomb gauge of Quantum Chromo Dynamics and explore implications of these findings for hadronic physics, namely meson and diquark properties and nucleon form factors. For the latter case we use a Poincaré-covariant diquark-quark model.

In the limit of a vanishing infrared regulator we solve a system of renormalised, truncated Dyson-Schwinger equations for the quark propagator in two different truncations in the chiral limit, where we have to sidestep into Euclidean space-time only for the more involved one. Contrary to previous approaches we employ a MOM scheme for renormalisation and include also transverse gluons and retardation. We use a gluon propagator that is in accordance with recent lattice calculations and with computations in a Hamiltonian approach. For the quark-gluon vertex we adopt the rainbow truncation.

We start with solely keeping the instantaneous time-time component of the gluon propagator in the gap equation. With an ansatz for the occurring colour Coulomb potential that reflects confinement and asymptotic freedom we find that two propagator functions diverge for the infrared regulator going to zero. Nevertheless in this limit their ratio defines a finite mass function that acquires about a third of the desired value in the infrared. In the second truncation we include transverse components of the gluon propagator with retardation and gain no considerable rise in the constituent quark mass. Hence at the moment we can only perform qualitative calculations of observables in this approach.

Doing so we solve meson and diquark Bethe-Salpeter equations. With vanishing infrared regulator we find finite masses for mesons and diverging ones for diquarks, what explicates confinement, and in *both* cases finite charge radii.

With this motivation we utilise a Poincaré-covariant diquark-quark model in order to compute nucleon form factors. We solve the resulting Faddeev equations to obtain masses and Faddeev amplitudes for the nucleon and Δ. The amplitudes are a component of a nucleon-photon vertex that automatically fulfills a Ward-Takahashi identity for on-shell nucleons. With these elements we compute the quark core contribution to the nucleons electromagnetic form factors. The incorporation of meson-loop contributions reduces the errors in the static properties considerably. Since these contributions vanish for higher momenta we can compare our results with recent data for the ratio of the Sachs form factors of the proton. We attribute the agreement with the available polarization transfer data to correlations in the proton's amplitude.

Zusammenfassung

In der vorliegenden Arbeit stellen wir näherungsweise Lösungen für den Quarkpropagator in Coulombeichung der Quantenchromodynamik vor und untersuchen Folgen dieser Ergebnisse im Rahmen der Hadronphysik. Hier werden Meson- und Diquark-Eigenschaften beleuchtet und elektromagnetische Nukleonformfaktoren mit Hilfe eines Poincaré-kovarianten Diquark-Quark Modells berechnet.

Wir lösen ein System renormierter Dyson-Schwinger Gleichungen des Quarkpropagators im Limes eines verschwindenden Infrarotregulators in zwei verschiedenen Trunkierungen im chiralen Limes. Dabei müssen wir nur im komplizierteren Fall im Euklidischen arbeiten. Im Gegensatz zu früheren Vorgehensweisen verwenden wir ein MOM-Schema zur Renormierung und berücksichtigen transversale Gluonen mit Retardierung. Der verwendete Gluonpropagator stimmt mit aktuellen Gitterrechnungen und mit Resultaten im Hamiltonzugang gut überein. Den Quark-Gluon Vertex behandeln wir in Regenbogennäherung.

Zuerst verwenden wir ausschließlich die Zeit-Zeit Komponente des Gluonpropagators. Mit einem Ansatz für das Coulomb-Potential, der asymptotische Freiheit und Confinement enthält, erhalten wir zwei mit verschwindendem Infrarotregulator divergierende Propagatorfunktionen. Das Verhältnis dieser Funktionen definiert in demselben Grenzwert aber eine endliche Massenfunktion, die im Infraroten etwa ein Drittel der Konstituentenquarkmasse annimmt. In der zweiten Trunkierung berücksichtigen wir transversale Komponenten des Gluonpropagators mit Retardierung, was aber zu keiner nennenswerten Erhöhung der berechneten Konstituentenquarkmasse führt. Daher können wir in diesem Zugang im Moment nur qualitative Rechnungen für Observable durchführen.

Dies äußert sich bei den Bethe-Salpeter Gleichungen für Diquarks und Mesonen. Bei verschwindendem Infrarotregulator finden wir endliche Massen für Mesonen und divergierende für Diquarks, was deren Confinement aufzeigt. In *beiden* Fällen sind die Ladungsradien aber endlich.

Da dieses Ergebnis auf gute Erfolgsaussichten eines Poincaré-kovarianten Diquark-Quark Modells bei der Beschreibung von Baryonen hindeutet, berechnen wir mit einem solchen die elektromagnetischen Nukleonformfaktoren. Wir lösen dessen Faddeev-Gleichungen und erhalten Massen und Amplituden für das Nukleon und das Δ. Die Amplituden sind Teil eines Nukleon-Photon Vertex, der automatisch eine Ward-Takahashi Identität für Nukleonen auf der Massenschale erfüllt. Mit diesen Komponenten berechnen wir den Beitrag des Quarkkerns zu den Nukleonformfaktoren. Die Berücksichtigung mesonischer Beiträge verringert die Fehler in den statischen Observablen beträchtlich. Da solche Effekte aber für höhere Impulse verschwinden, können wir unsere Ergebnisse mit

aktuellen Daten für das Verhältnis der Sachs Formfaktoren des Protons vergleichen. Die Übereinstimmung mit den Polarisationstransferdaten schreiben wir Korrelationen in den Protonamplituden zu.

Contents

1 Prologue **1**

2 Chiral Symmetry Breaking in QCD **5**

2.1 Chiral symmetry of the QCD Lagrangian 5

2.2 Constituent and current quark mass 8

2.3 The pion as a Goldstone boson and PCAC 11

3 Remarks on QCD in Coulomb Gauge **15**

3.1 Motivation 15

3.2 Coulomb gauge and renormalisation 16

3.3 Approaches in Coulomb gauge 17

3.4 Quantisation of Maxwell theory 19

3.4.1 Canonical quantisation of Maxwell theory 20

3.4.2 Path integral quantisation of Maxwell theory in Coulomb gauge 24

3.5 Quantisation of Yang-Mills theory 25

3.6 The confinement scenario of Gribov and Zwanziger 28

3.6.1 Ambiguities in Coulomb gauge 28

3.6.2 Coulomb confinement as a necessary confinement condition 30

3.6.3 Quark-antiquark potentials and signals for confinement 32

3.6.4 Confinement in Coulomb gauge 33

4 The Quark Dyson-Schwinger Equation **35**

4.1 From the QCD action to the gap equation 35

4.2 The gap equation in Coulomb gauge 37

4.3 Considerations without transverse gluons 40

4.4 Numerical results 41

4.5 Adding transverse gluons and retardation 43

4.6 Numerical results 45

5 Meson Observables, Diquark Confinement and Radii 48

6 Nucleon Form Factors in a Covariant Diquark-Quark model 54
6.1 Introduction 54
6.2 Two-quark correlations 57
6.3 Covariant Faddeev equation 59
6.3.1 *Ansätze* for the nucleon and Δ 59
6.3.2 Propagators and diquark amplitudes 62
6.3.3 Solving the Faddeev equation and choices for nucleon and Δ masses 66
6.4 Electromagnetic current operator 67
6.4.1 Coupling to the quark 69
6.4.2 Coupling to the diquark 70
6.4.3 Coupling to the exchanged quark 72
6.4.4 Scalar $\leftrightarrow$ axialvector transition 72
6.4.5 Seagull contributions 73
6.5 Nucleon electromagnetic form factors: results 74
6.5.1 Remarks 74
6.5.2 Calculated results and discussion 75

7 Epilogue 91

A Units and Conventions 94
A.1 Conventions in Minkowski space 94
A.2 Euclidean conventions 94

B Gauge potential, field strength and E- and B-fields 96

C Numerical method employed in solving the gap equation with transverse gluons and retardation, eqs. (4.43)-(4.45) 97

Chapter 1

Prologue

Quantum Chromo Dynamics (QCD) is the SU(3) gauge theory of quarks and gluons and nowadays the widely accepted theory of strong interaction. Together with the Glashow-Salam-Weinberg Model of electroweak interactions, which succeeded in providing a unified description of the electromagnetic and weak interactions, QCD builds the so-called *Standard Model* of elementary particle physics. For high momenta, which correspond to low distances, the quarks behave like free particles, a phenomenon which is known as *asymptotic freedom*. In this momentum regime perturbative calculations have been carried out which agree well with the performed experiments. At low and intermediate momenta up to several GeV however the QCD coupling constant is too large in order to apply perturbation theory. This is physically required since neither quarks nor gluons have been detected as free particles so far. Therefore the *confinement hypothesis* was established: Only singlets of the gauge group occur as physical particles, which implies that both quarks and gluons should never appear individually. Up to the presence this statement still awaits a rigorous proof. Together with confinement *chiral symmetry breaking* is the outstanding fundamental low energy property of QCD. Hadron phenomenology, especially the low energy relations in pion physics, the sum rules derived from current algebra and the relations among meson masses left no doubt about the spontaneous breaking of chiral symmetry. Since neither quarks nor gluons can have nonvanishing vacuum expectation values, the breaking of chiral symmetry has to take place dynamically.

Our understanding of how observable properties of hadrons emerge from the underlying structure of the strong interaction is still far from complete. Nevertheless in the last years considerable progress has been achieved amongst others in lattice calculations. For example in [D$^+$04] an unquenched parameterfree calculation for a restricted set of observables testing several aspects of lattice QCD was reported. With u and d quark masses only about three times larger than the realistic value the agreement with experiment was

on the level of a few percent. Lattice QCD is used to compute a wide range of physical quantities, including the hadron mass spectrum, decay constants and form factors. The technique is not universally applicable, however, and quantities like the inelastic proton-proton scattering cross-section or the nucleon structure functions at small angles remain inaccessible.

Also for the calculation of Green's functions lattice Monte Carlo methods are the only *ab initio* approach so far. However, lattice results suffer potentially from finite volume effects in the infrared. One has to rely on extrapolation methods to obtain the infinite volume limit. For the implementation of realistic light quark masses still faster CPUs and better algorithms are needed.

Dyson-Schwinger and Bethe-Salpeter equations (DSEs/BSEs) are the equations of motion of the Green's functions of a quantum field theory. From a technical point of view they represent a method complementary to lattice simulations. The latter contains all effects from quantum fluctuations. However, the results are limited to a comparably small momentum range. DSEs and BSEs need for their solution a truncation scheme but provide us with a solution over a large momentum range.

In QCD the study of the nonperturbative behaviour of Green's functions is interesting for several reasons. Information on certain confinement mechanisms is encoded in specific two-point functions of the theory. Effects of dynamical chiral symmetry breaking are apparent in the quark propagator and the quark-gluon interaction. Furthermore quark and gluon propagators are vital ingredients for phenomenological models which describe low and medium energy hadron physics. Last but not least properties of bound states and resonances can be determined from the QCD n-point functions. The naturally embedded framework in the DSE context is the description of hadrons as bound states in relativistic Bethe-Salpeter/Faddeev equations for particle poles in quark correlation functions (in the colour singlet channel), the 4-point quark-antiquark Green's function for mesons, and the 6-quark Green's function for baryons. The aim is, of course, to use the results from DSEs, in particular the ones for the quark correlations, in the relativistic bound state equations.

The apparatus of DSEs and BSEs has been studied extensively in the last years [AS01, Fis06]. Since DSEs and BSEs need for their solution a truncation scheme one has to employ ansätze for higher correlation functions in order to obtain a closed system of equations. The quality of a truncation may be ascertained by comparison with lattice results and the conservation or violation of certain symmetries.

How the dynamical breaking of a symmetry can be achieved through the generation of a fermion pair condensate was shown in the classical papers of Nambu and Jona-Lasinio [NJL61a, NJL61b]. Their simple model containing a four fermion point interaction with

an ultraviolet cutoff differs in some respects from a complex non-abelian gauge theory like QCD. In a number of more realistic models which are based on approximations of the gluon sector of QCD it has however been shown, that chiral symmetry is broken in the manner as discussed by Nambu and Jona-Lasinio, if the attraction exceeds a critical level [ALYO$^+$83, FGMS83]. Particularly an instantaneous confining interaction always causes spontaneous breaking of chiral symmetry [DM85].

In Coulomb gauge such an interaction has been identified for heavy quarks, which is an advantage compared to covariant gauges. The approach to study QCD in different gauge fixed formulations is an interesting and well established endeavour. In general, Green's functions are gauge dependent objects. Of course confinement and dynamical mass generation are experimentally observable phenomena and as such must have gauge independent theoretical signatures. Confinement is reflected in the long distance behaviour of the (gauge invariant) Wilson loop and the strength of dynamical chiral symmetry breaking is determined by its (gauge invariant) order parameter, the chiral condensate. On the other hand it may very well be that the detailed mechanism that generates these quantities depends on the choice of gauge. Moreover possible order parameters separating the confining from the deconfining phase of gauge theories may only be identifiable after gauge fixing.

The next chapter reviews aspects of chiral symmetry breaking in QCD, which are vital for the following chapters. Starting with formal descriptions and implications we consider the definition of a mass function and its properties, PCAC and the special role of the pion.

The third chapter gives an overview concerning efforts in Coulomb gauge connected to this thesis. After a short motivation and comparison to Landau gauge DSE studies we report the status of the renormalisability proof. A brief discussion of different approaches in Coulomb gauge follows. The quantisation of Maxwell theory in comparison with Yang-Mills theory is demonstrated and the differences in the results are highlighted. In the remainder we review the Gribov-Zwanziger confinement scenario.

In chapter four we start out with deriving the quark Dyson-Schwinger equation from the QCD action and via Ward identities. We solve it in Coulomb gauge at first keeping only the time-time component of the gluon propagator in the instantaneous approximation. This improves on the approximation in ref. [Alk88] using the so-called Richardson potential in the gluon propagator and a MOM scheme for renormalisation. Improving the truncation we solve the gap equation including transverse gluons and retardation. The presented results are compared.

Chapter five utilises these solutions in order to gain qualitative information about meson and diquark properties. Explicitly we demonstrate that diquarks are confined and it is nevertheless possible to assign them a finite charge radius.

This motivates chapter six in which we point out the advantages of a Poincaré covariant diquark-quark model for baryons. We discuss approximations for the two-quark correlation matrix and introduce the model in some detail. We expand on the ingredients, namely the dressed quark propagator in Landau gauge, the diquark Bethe-Salpeter amplitudes and the diquark propagators. In order to calculate nucleon form factors we solve the truncated Faddeev equation and present an appropriate conserved current. We discuss the results and the influence of chiral corrections. A zero of the Sachs form factor ratio of the proton is predicted.

Chapter seven is an epilogue that is followed by an appendix, which describes amongst others the numerical methods applied in chapter four.

Chapter 2

Chiral Symmetry Breaking in QCD

2.1 Chiral symmetry of the QCD Lagrangian

Together with gauge invariance chiral symmetry is a further important symmetry of QCD in the limit of zero current quark mass. In this section we will discuss this feature and its connection to the phenomenology of hadrons and strong interaction. Starting with the general form of a Lagrangian density of a SU(3) gauge theory of quarks and gluons one can apply the Faddeev-Popov procedure in order to show that it can always be written as[1] [Ynd, PS, Pok]

$$\mathcal{L}_{QCD} = \sum_{f=1}^{N_f} \overline{\Psi}^f (i\gamma_\mu D^\mu - m_f)\Psi_f - \frac{1}{2}\mathrm{tr}(F_{\mu\nu}F^{\mu\nu}) + \mathcal{L}_{ghost} + \mathcal{L}_{g.f.} \ . \tag{2.1}$$

In this expression the variables Ψ_f are the quark fields, which occur in different flavours f=u,d,s,... . The masses m_f in the Lagrangian density are the current quark masses of a quark with flavour f. $\mathcal{L}_{g.f.}$ is the gauge fixing term and $\mathcal{L}_{ghost}$ contains the Faddeev-Popov ghosts, which are required in quantised gauge theories to cancel spurious gluon degrees of freedom. The gauge covariant derivative is given as

$$D^\mu = \partial^\mu - igA^\mu \ , \tag{2.2}$$

where g is the strong coupling constant, and the field strength tensor is defined in terms of the gluon fields as

$$F_{\mu\nu} = \partial A_\nu - \partial_\nu A_\mu - ig[A_\mu, A_\nu] \ . \tag{2.3}$$

The gauge covariant derivative and the field strength tensor are elements of the Lie algebra of SU(3) and are therefore matrices. Usually the gluon fields are expanded in terms of the

[1] In this chapter we work in Minkowski space, cf. A.1 .

generators of SU(3), which are the well-known Gell-Mann matrices:

$$\begin{aligned} A^{\mu}_{\alpha\beta} &= \frac{\lambda^{a}_{\alpha\beta}}{2}(A^{a})^{\mu} \ , \\ \alpha, \beta &= 1, 2, ..., N_c \ , \\ a &= 1, ..., (N_c^2 - 1) \ , \end{aligned}$$

where the Einsteinian summation convention is understood and N_c is the number of colours.

In order to discuss the symmetries of the quark fields we introduce left- and right-handed fields

$$\begin{aligned} \Psi^{f}_{R} &= \frac{1}{2}(1 + \gamma_5)\Psi^{f} \\ \Psi^{f}_{L} &= \frac{1}{2}(1 - \gamma_5)\Psi^{f} \ . \end{aligned}$$

Since γ_5 anticommutes with all gamma matrices this gives reason for the decomposition

$$\overline{\Psi}^{f} i\gamma_{\mu} D^{\mu} \Psi^{f} = \overline{\Psi}^{f}_{R} i\gamma_{\mu} D^{\mu} \Psi^{f}_{R} + \overline{\Psi}^{f}_{L} i\gamma_{\mu} D^{\mu} \Psi^{f}_{L} \ . \tag{2.4}$$

Regarding the Lagrangian density this means that in the limit of zero current quark masses left- and right-handed quarks propagate independently from each other. The Lagrangian is invariant under unitary transformations of the left- and right-handed quark field operators, which do not depend on each other. These transformations form the group $U_L(N_f) \times U_R(N_f)$. For the purpose of discussing the conserved charges we decompose this group in a first step into semisimple Lie sub-groups:

$$U_L(N_f) \times U_R(N_f) \cong U_{L+R}(1) \times U_{L-R}(1) \times SU_L(N_f) \times SU_R(N_f) \ . \tag{2.5}$$

The symmetry transformation of the subgroup $U_{L+R}(1)$ yields the conservation of baryon number whereas the divergence of the $U_{L-R}(1)$-current does not vanish even in the massless because of the Adler-Bell-Jackiw anomaly [Ynd, Pok]. *Chiral symmetry* is the invariance under the transformations $SU_L(N_f) \times SU_R(N_f)$. It implies the conservation of $2(N_f - 1)$ charges. The corresponding currents are

$$J^{r}_{L\mu}(x) = \overline{\Psi}^{f}_{L}(x)\gamma_{\mu}\frac{t^{r}_{fg}}{2}\Psi^{g}_{L} \ , \tag{2.6}$$

$$J^{r}_{R\mu}(x) = \overline{\Psi}^{f}_{R}(x)\gamma_{\mu}\frac{t^{r}_{fg}}{2}\Psi^{g}_{R} \ , \tag{2.7}$$

$$f, g = 1, ..., N_f \ , \ r = 1, ..., N_f^2 - 1 \ . \tag{2.8}$$

The matrices t^r are a basis of the fundamental representation of $SU(N_f)$. The resulting charges

$$Q_L^r = \int d^3x J_{L0}^r(\mathbf{x}, t) \tag{2.9}$$

$$Q_R^r = \int d^3x J_{R0}^r(\mathbf{x}, t) \tag{2.10}$$

fulfil the same commutation relations as the generators of the Lie algebra of $SU_L(N_f) \times SU_R(N_f)$. Under parity transformations they transform into each other, $\mathcal{P}Q_L\mathcal{P}^{-1} = Q_R$, which explains the name chiral transformations. The parity eigenstate are obtained by examining the diagonal subgroups $SU_{L+R}(N_f)$ and $SU_{L-R}(N_f)$ and the corresponding currents:

$$\begin{aligned} V_\mu^r(x) &= J_{R\mu}^r(x) + J_{L\mu}^r(x) \\ &= \overline{\Psi}^f(x)\gamma_\mu \frac{t_{fg}^r}{2}\Psi^g \ , \end{aligned} \tag{2.11}$$

$$\begin{aligned} A_\mu^r(x) &= J_{R\mu}^r(x) - J_{L\mu}^r(x) \\ &= \overline{\Psi}^f(x)\gamma_\mu\gamma_5 \frac{t_{fg}^r}{2}\Psi^g \ . \end{aligned} \tag{2.12}$$

They transform as vector and an axial-vector respectively under parity transformations. Their time components fulfil the equal time commutation relations

$$[V_0^r(\mathbf{x}, t), V_0^s(\mathbf{y}, t)] = if^{rst}V_0^t(\mathbf{x}, t)\delta^{(3)}(\mathbf{x} - \mathbf{y}) \ , \tag{2.13}$$

$$[V_0^r(\mathbf{x}, t), A_0^s(\mathbf{y}, t)] = if^{rst}A_0^t(\mathbf{x}, t)\delta^{(3)}(\mathbf{x} - \mathbf{y}) \ , \tag{2.14}$$

$$[A_0^r(\mathbf{x}, t), A_0^s(\mathbf{y}, t)] = if^{rst}V_0^t(\mathbf{x}, t)\delta^{(3)}(\mathbf{x} - \mathbf{y}) \ . \tag{2.15}$$

In these equations f^{rst} are the antisymmetric structure constants of the Lie algebra of $SU(N_f)$. The set of commutation relations is known as the current algebras. Since the left hand sides of the relations are quadratic in the currents and the right hand sides are linear, non-linear constraints for the currents follow. In particular their normalisation is determined by these equations. They also give (via the current algebra sum rules [IZ, CL, TW]) rise to relations between different cross sections of lepton-nucleon scattering, which are in good agreement with experiment.

Explicit breaking of chiral symmetry is caused by the fermionic mass terms in the Lagrangian (2.1). Nevertheless chiral symmetry is a good approximation concerning the light quarks due to the fact that their current quark masses are small compared to the typical energy scale of strong interaction. For the strange quark the concept of an approximate

chiral symmetry is not always suitable. For heavy quarks it is definitely not fruitful. Luckily the Applequist-Carazzone decoupling theorem states, that particles, which are heavy compared to the involved energies, decouple and therefore in low energy processes only the light quarks have to be taken into consideration. They are called the active flavours. Accordingly the hadron spectrum below one or two GeV has to reflect chiral symmetry $SU(2) \times SU(2)$ or $SU(3) \times SU(3)$ respectively. As hadrons do not occur in degenerate parity doublets, the symmetry is not realised in the Wigner-Weyl phase but in the Nambu-Goldstone phase and is thus spontaneously broken. If the current quark masses were zero, there would thus be $N_f^2 - 1$ massless Goldstone bosons with negative inner parity. Since chiral symmetry is only an approximate one, these bosons acquire masses, which are small compared to those of other mesons. Hence we can identify the isotriplet of pions and the octet of pseudoscalar mesons with these Goldstone bosons.

The gluons remain unaffected from the chiral transformations. It therefore seems to be a good approximation to assume that, though the gluon sector provides the mechanism for chiral symmetry breaking, it does not change qualitatively. This gets support from the fact that only a small fraction of the gluon condensate is due to chiral symmetry breaking. Even the entire suppression of instantons in the chiral limit, which selects the realisation $\theta = 0$ of the θ-vacuum, is no obstacle: The phenomenological value of θ is compatible with 0 [Pok]. Hence all facts support that the chiral limit is smooth and chiral symmetry is a good concept concerning the light quarks.

As a further consequence of chiral symmetry breaking the quarks receive a non-perturbative dynamical mass of the order of the typical energy scale of strong interaction. This mass is generally called the constituent quark mass. Its quantitative description is due to Politzer [Pol76] and will be shortly discussed in the next section.

2.2 Constituent and current quark mass

The starting point for the definition of the current quark mass is the full quark propagator for Euclidean momenta $-p^2 = P^2 > 0$ in Landau gauge,

$$S(p) = \frac{i}{\gamma_\mu p^\mu C(P^2) - B(P^2) + i\epsilon} \tag{2.16}$$

$$= \frac{i}{C(P^2)[\gamma_\mu p^\mu - M(P^2)] + i\epsilon} \ , \tag{2.17}$$

where we used the definition

$$M(P^2) := \frac{B(P^2)}{C(P^2)} \ . \tag{2.18}$$

Together with C and B the function M is a function of the spacelike squared momentum P^2, the renormalisation point and the renormalised current quark masses. There are two reasons for the definition (6.30) being the most suitable one for a mass function [Pol76]. Firstly $M(P^2)$ is the mass parameter for quarks, which appears in an operator product expansion of the quark propagator in the chiral limit. This means that it can be interpreted as the parton mass in lepton hadron scattering. Furthermore it will get apparent that for considerations in Coulomb gauge and a confining potential the functions C and B are divergent, whereas M can be finite. With this expression for M one has to keep in mind that the quark mass is a function of the momentum and thereby depends on the momentum scale of the process under consideration.
In the chiral limit the symmetry of the QCD Lagrangian under the axial $SU(N_f)$ assures, that in the fermion propagator no mass term can show up in each order in perturbation theory. The situation is analogous to BCS theory for superconductivity, where it is also impossible to obtain the energy gap in perturbation theory. Again like in BCS theory in our case the spontaneous breaking of chiral symmetry implies a non-perturbative mass term. Therefore a theory, which is eager to describe explicit and spontaneous breaking of chiral symmetry, has to be able to specify the behaviour of perturbative and non-perturbative masses. The non-trivial behaviour of QCD under scale transformations entails that the parameters of the Lagrangian, and with this also the current quark masses, turn into momentum dependent running quantities. This circumstance is described by the Callan-Symanzik equation. Unfortunately their coefficients are only known in perturbation theory, which means that we can use this equation only for large momenta, where the coupling constant is small, as one can infer from the Callan-Symanzik equation. In the lowest non-trivial order of perturbation theory it is possible to derive from the Callan-Symanzik equation the following equation for the momentum dependency of the perturbative quark mass $m_k(P^2)$ at large Euclidean momenta [Pol76]

$$P\frac{dm_k(P^2)}{dP} = -\frac{1}{2\pi^2}g^2(P^2)m_k(P^2)\left(1 - \frac{m_k^2(P^2)}{P^2}\ln\left(1 + \frac{P^2}{m_k^2(P^2)}\right)\right) \ , \tag{2.19}$$

where we used for the running coupling the expression of first order perturbation theory

$$g^2(P^2) = \frac{48\pi^2}{(11N_c - 2N_f)\ln(P^2/\Lambda^2)} \ . \tag{2.20}$$

In this context N_c is the number of colours and N_f is the number of active flavours. Λ is the QCD scale parameter. Since (2.19) is only valid for large momenta, the term proportional to $\frac{m^2}{P^2}$ can be neglected and one obtains

$$m_k = (P^2) = m_k(\nu^2)\left(\frac{g^2(P^2)}{g^2(\nu^2)}\right)^{d_m} \ , \tag{2.21}$$

where

$$d_m = \frac{12}{11N_c - 2N_f} \tag{2.22}$$

and is usually called the anomalous dimension of mass.

To identify the behaviour of the non-perturbative mass at hight energies we assume that the QCD vacuum is not chiral invariant. The axial unitary transformations are given as

$$U_5(\Phi^r) q U_5^{-1}(\Phi^r) = e^{i\Phi^r \gamma_5 t^r} q \tag{2.23}$$

$$U_5(\Phi^r) \overline{q} U_5^{-1}(\Phi^r) = \overline{q} e^{i\Phi^r \gamma_5 t^r} \ . \tag{2.24}$$

The assumption, that the vacuum is not chirally invariant,

$$U_5|\Omega> \neq |\Omega> \ , \tag{2.25}$$

has two essential consequences. Firstly the Goldstone theorem is applicable and one obtains $N_f^2 - 1$ pseudoscalar light mesons. Secondly the vacuum expectation value $\langle\Omega|\overline{\Psi}(x)\overline{\Psi}(x)|\Omega\rangle$ does not equal zero. Using an operator product expansion for the quark propagator

$$\langle\Omega|T\ \overline{\Psi}(x)\Psi(0)|\Omega\rangle \overset{x\to 0}{=} C_1(x)\langle\Omega|\Omega\rangle + C_2(x)\langle\Omega|\overline{\Psi}(x)\Psi(0)|\Omega\rangle + ... \tag{2.26}$$

and our definition for $M(P^2)$ we identify a non-perturbative contribution to the quark mass, which is for large momenta [Pol76]

$$M_f^{np}(P^2) \overset{P^2\to\infty}{\approx} -\frac{1}{3}\frac{g^2(P^2)}{P^2}\left(\frac{g^2(P^2))}{g^2(\nu^2)}\right)^{-d_m} \langle\Omega|\overline{\Psi}^f \Psi^f(\nu)|\Omega\rangle \ . \tag{2.27}$$

According to our considerations the non-perturbative mass contribution approaches zero a lot quicker for large momenta than the perturbative one. For large momenta the asymptotic behaviour of $M(P^2)$ is given as the sum of the perturbative and the non-perturbative contribution because of asymptotic freedom. This is not true for low and intermediate momenta, since in this regime the interaction is strong.

The asymptotic behaviour of the quark mass is independent of the flavour quantum number as long as the relevant momentum is sizeably bigger than the quark mass. In particular we have

$$\lim_{P^2\to\infty}\frac{M_f(P^2)}{M_g(P^2)} = \lim_{P^2\to\infty}\frac{m_f(P^2)}{m_g(P^2)} = \frac{m_f(\nu^2)}{m_g(\nu^2)} \ . \tag{2.28}$$

The meaning of these equations is that the ratio of the bare quark masses determines symmetry properties of the QCD Lagrangian. These ratios show up regularly in calculations utilising the current algebra. Therefore the masses are often called current quark masses.

As mentioned above the quantitative considerations of this subsection are all valid in Landau gauge. Nevertheless in Coulomb gauge we define a mass function in the same way as above and are able to show, that it exhibits a behaviour as the one in Landau gauge for low momenta.

2.3 The pion as a Goldstone boson and PCAC

From the fact that the vacuum expectation value $\langle\Omega|\overline{\Psi}\Psi|\Omega\rangle$ does not vanish we can conclude by considering the proof of the Goldstone theorem that the axial currents $A^r_\mu(x)$ couple the Goldstone bosons to the vacuum. If we denote the one particle states of the Goldstone bosons with momentum p as $|\pi^s(p)\rangle$, this is expressed as [Ynd, CL, Pok]

$$\langle\Omega|A^r_\mu(x)|\pi^s(p)\rangle = if^{rs}p_\mu e^{ipx} \ , \quad r,s = 1,2,3 \ , \tag{2.29}$$

where the f^{rs} are nonvanishing constants. If we assume that the $SU(N_f)$ isospin symmetry is unbroken, they may be written as

$$f^{rs} = \delta^{rs} f_\pi \ . \tag{2.30}$$

For $N_f = 2$ f_π is the pion decay constant. It can be measured in weak π decays, since the matrix element (2.29) enters there. For instance for the decay $\pi \to \mu\nu$ we have

$$\Gamma = f_\pi^2 \frac{G^2 m_\mu^2 (m_\pi^2 - m_\mu^2)^2}{4\pi m_\pi^2} \cos^2\theta_c \ , \tag{2.31}$$

where G is the the weak decay constant and θ_c the Cabibbo angle. From experiment $f_\pi \approx 92\,\mathrm{MeV}$ is known. For three flavours the kaon decay constant is approximately $f_K \approx 1.2 f_\pi$.

Applying the four divergence to equation (2.29) and using the Klein-Gordon equation one can derive

$$\langle\Omega|\partial^\mu A^r_\mu(x)|\pi^s(p)\rangle = \delta^{rs} f_\pi m_\pi^2 e^{ipx} \ . \tag{2.32}$$

If chiral symmetry of the QCD Lagrangian was exact, we could infer $m_\pi = 0$ or $f_\pi = 0$ from the conservation of the axial current. This is true in the Nambu-Goldstone and Wigner-Weyl realisation of chiral symmetry. Because both quantities do not vanish, it follows immediately that chiral symmetry is explicitly broken. Since on the other hand the pions are sizeably lighter than the rest of the mesons, the current quark masses of up and down quarks, which are responsible for this explicit breaking, are quite small compared to the typical energies of strong interaction. For the relevant case of explicit symmetry breaking

one can generalise equation (2.32) to an equation for operators in the following way. The pion field operator is normalised with respect to the one pion state,

$$\langle \Omega | \Phi_\pi^r(x) | \pi^s(p) \rangle = \delta^{rs} e^{ipx} \ . \tag{2.33}$$

Using this relation to recast (2.32) and generalising the result to an equation for operators, one obtains [CL, Pok]

$$\partial^\mu A_\mu^r(x) = m_\pi^2 f_\pi \phi_\pi^r(x) \ . \tag{2.34}$$

This equation is the so-called Partially Conserved Axial-vector Current (PCAC) hypothesis. Assuming that it is possible to extrapolate meson and baryon form factors in a reasonably smooth manner away from the mass shell, this hypothesis has far reaching consequences, since it relates parameters of strong and weak interaction. One implication is for instance the Goldberger-Treiman relation,

$$f_\pi g_{\pi NN} = m_N g_A \ , \tag{2.35}$$

which concatenates the weak axial vector coupling of the nucleon g_A and the pion-nucleon coupling $g_{\pi NN}$ with each other. This equation is fulfilled experimentally within ten percent, what highlights the validity of the PCAC hypothesis.

It is also possible to relate masses and decay constants of the pseudoscalar mesons on the one side with quark masses in the Lagrangian on the other side. From equation (2.32) it is possible to conclude by using the PCAC hypothesis and the LSZ formalism, that in the limit of low meson energies the relation

$$\delta^{rs} m_\pi^2 f_\pi^2 = i \int d^4x \langle \Omega | \delta(x_0) [A_0^r(x), \partial^\mu A_\mu^s(0)] | \Omega \rangle \tag{2.36}$$

holds [Ynd, CL, IZ]. Denoting the charge of the axial vector current with Q^{5r} and the Hamiltonian density with $\mathcal{H}(\mathbf{x})$ we can write this as

$$\delta^{rs} m_\pi^2 f_\pi^2 = \langle \Omega | [Q^{5r}, [Q^{5s}, \mathcal{H}(0)]] | \Omega \rangle \ . \tag{2.37}$$

For the Lagrangian (2.1) it is possible to work out the axial vector and the vector currents explicitly. For one matrix element in flavour space we obtain

$$\partial^\mu V_\mu^{kl} = i(m_k - m_l) \overline{q}^k q^l \tag{2.38}$$

$$\partial^\mu A_\mu^{kl} = i(m_k + m_l) \overline{q}^k \gamma_5 q^l \ . \tag{2.39}$$

For the case of identical nonvanishing current quark masses the vector current is conserved, whereas every nonvanishing current quark mass breaks axial symmetry explicitly. In order

to get further insight we have to phrase the symmetry breaking term in a group theoretical language. As an example we show how to do this with flavour SU(3) (the generalisation is trivial). At first one defines the $N_f^2 = 9$ scalar quark densities

$$u^r = \overline{q}\lambda q \ , \ r = 0, 1, ..., , 8 \ , \tag{2.40}$$

where λ^r are the famous Gell-Mann matrices and

$$\lambda^0 = \sqrt{\frac{2}{3}} \begin{pmatrix} 1 & 0 & 0 \\ 0 & 1 & 0 \\ 0 & 0 & 1 \end{pmatrix} \ . \tag{2.41}$$

With this definition one can recast the mass terms in the Lagrangian to yield

$$m_u \overline{u}u + m_d \overline{d}d + m_s \overline{s}s \ , \tag{2.42}$$

where the symmetry breaking parameters are linear combinations of the quark masses,

$$c_0 = \frac{1}{\sqrt{6}}(m_u + m_d + m_s) \tag{2.43}$$

$$c_3 = \frac{1}{2}(m_u - m_d) \tag{2.44}$$

$$c_8 = \frac{1}{2\sqrt{3}}(m_u + m_d - 2m_s) \ . \tag{2.45}$$

For the twofold commutator in (2.37) only the symmetry breaking term in the Hamiltonian contributes. With the well-known algebra of the Gell-Mann matrices this commutator can be calculated easily. Taking into consideration that for three flavours the twofold commutator in (2.37) is not diagonal in flavour space, one arrives at

$$\begin{aligned} f_\pi^2 m_\pi^2 &= \frac{1}{2}(m_u + m_d)\langle\Omega|\overline{u}u + \overline{d}d|\Omega\rangle \\ f_K^2 m_K^2 &= \frac{1}{2}(m_u + m_s)\langle\Omega|\overline{u}u + \overline{s}s|\Omega\rangle \\ f_\eta^2 m_\eta^2 &= \frac{1}{6}(m_u + m_d)\langle\Omega|\overline{u}u + \overline{d}d|\Omega\rangle + \frac{4m_s}{3}\langle\Omega|\overline{s}s|\Omega\rangle \ . \end{aligned} \tag{2.46}$$

For simplicity it was assumed that f_π is diagonal. From the definition of the decay constant (2.29) and the assumption

$$\langle\Omega|\overline{u}u|\Omega\rangle = \langle\Omega|\overline{d}d|\Omega\rangle = \langle\Omega|\overline{s}s|\Omega\rangle \tag{2.47}$$

we conclude that all decay constants are equal. Thereby we derive with (2.46) not only the famous, phenomenologically discovered mass relation of Gell-Mann and Okubo,

$$4m_K^2 = 3m_\eta^2 + m_\pi^2 \ , \tag{2.48}$$

but also a relation among the current quark masses,

$$\frac{m_u + m_d}{2m_s} = \frac{m_\pi^2}{2m_K^2 - m_\pi^2} \approx \frac{1}{25} \ . \tag{2.49}$$

Taking into account the breaking of isospin $m_u \neq m_d$ and an electromagnetic correction of the charged mesons it is possible to derive equations like (2.46) for the octet of the pseudoscalar mesons. Employing furthermore experimental data of other mesons one can estimate the current quark mass of all known quarks well. A caveat in this context is that only the ratio between current quark masses is uniquely defined since only these are scale invariant and do not have to be renormalised. It is however difficult to estimate the current quark masses, as one should know the relevant momentum scale for parameters of chiral symmetry breaking, which are extracted from hadron phenomenology. For a renormalisation scale of 2 GeV in a $\overline{\text{MS}}$-scheme the following values were found [E$^+$04]:

$$m_u \approx 2.5\,\text{MeV} \tag{2.50}$$

$$m_d \approx 6\,\text{MeV} \ . \tag{2.51}$$

For the strange quark mass there is a large fluctuation in the literature.

Chapter 3

Remarks on QCD in Coulomb Gauge

"*Yet, despite its headstart in an Abelian context, application of the Coulomb gauge to non-Abelian models remains as puzzling and problematic today as ever.*" This is a statement of [Lei] and is probably still up to date. The present chapter is devoted to point out that together with the difficulties outstanding features are connected to QCD in Coulomb gauge.

3.1 Motivation

For many years Landau gauge has been the most popular choice for non-perturbative QCD efforts. It imposes transversality of the gluon field in space-time and has proven to be practical. Feynman rules can be derived easily, it preserves Lorentz invariance of the theory and allows for simple ansätze in the truncation of the infinitely coupled system of DSEs.

Considerable advances in DSE Landau gauge studies have been achieved over the last years. For example in [Fis03] for the first time the coupled system of quark, gluon and ghost DSEs was solved. Such studies support a possible infrared effective theory which is given by the gauge-fixing parts of the action [Fis06]. Ghost degrees of freedom dominate in the infrared and are responsible for long range correlations whereas the gluon propagator vanishes at zero momentum. This property implies positivity violations in the gluon propagator and assures that transverse gluons are confined. The infrared analysis of the running coupling of SU(N)-Yang-Mills theory showed a fixed point which is qualitatively universal and invariant in a class of transverse gauges. The quark propagator exhibits dynamical chiral symmetry breaking and the chiral condensate can be extracted reliably. In the meson sector of QCD the approach naturally reproduces both the Goldstone nature

of the pion and resulting low energy theorems. Of course there are still a number of challenges in this approach. The gluon self-energy needs further investigation since it might be a key ingredient in our understanding of the transition from the perturbative to the non-perturbative region of Yang-Mills theory. The quark-gluon vertex and its consequences for the analytical structure of the quark propagator pose a hard problem for further progress (only very recently some light was shed on this [AFLE06]). Future advance can come from studies in other gauges and the comparison of the mentioned findings to their results.

There is an number of reasons for working in Coulomb gauge. One of the advantages of Coulomb gauge is the understanding of confinement. This physical phenomenon has two complementary aspects. A long range attractive potential between coloured sources is known to exist. However, the gluons, which mediate this force, are absent from the spectrum of physical states. Therefore the mechanism for confinement is not very transparent in covariant gauges [Zwa97]. In Coulomb gauge on the contrary these two aspects co-exist comfortably: The confining force is given by the instantaneous Coulomb interaction and is enhanced for small three-momenta, whereas the physical transverse gluon propagator is suppressed, which reflects the absence of coloured states in the observed spectrum.

In Coulomb gauge all degrees of freedom are physical. This makes the Hamiltonian approach resemble constituent quark models. Since this is an active research area for many years, intuition gained in this field can be applied. Furthermore Gauss's law is built into the Hamiltonian and retardation effects are minimised for heavy quarks. It is thus also a natural framework to study non-relativistic bound states.

3.2 Coulomb gauge and renormalisation

For QCD in Coulomb gauge renormalisability has not been proven yet though there have been a number of serious attempts. Reference [BZ99] is probably the most sophisticated approach. There interpolating gauges between Landau and Coulomb gauge, defined via

$$-a\partial_0 A_0 + \nabla \cdot \mathbf{A} = 0 \ , \tag{3.1}$$

are studied and shown to be renormalisable. Coulomb gauge is examined as the limit $a \to 0$ in the gauge parameter. The authors phrase the partition function as a functional integral in phase space and perform a linear shift in the field variables in order to exhibit a symmetry (called "r-symmetry") between the Fermi and Bose unphysical degrees of freedom. Individual closed Fermi-ghost loops and closed unphysical Bose loops diverge

like $1/\sqrt{a}$, but they cancel pairwise in each order in perturbation theory by virtue of the r-symmetry. Therefore in the Coulomb gauge limit the correlation functions are finite, which remains true for the renormalised correlation functions. However, one-loop graphs are identified that vanish like $\sqrt{a}$ and that do not exist in the *formal Coulomb gauge*, i.e. $a = 0$. These graphs cannot be neglected since they give a finite contribution when inserted into the graphs that diverge like $1/\sqrt{a}$. It is still possible that these two-loop graphs, which are not existent in the formal Coulomb gauge, are mere gauge artefacts and decouple from expectation values of all gauge-invariant quantities such as a Wilson loop. However, up to now it was not possible to show this.

3.3 Approaches in Coulomb gauge

Working perturbative calculations are desirable in every gauge. However, in Coulomb gauge no further insight has been achieved with the standard dimensional regularisation technique. The reason for this is, that the gauge boson propagator is of the form

$$G^{ab}_{\mu\nu}(q) = -\frac{i\delta^{ab}}{q^2}\left[g_{\mu\nu} + \frac{n^2}{\mathbf{q}^2}q_\mu q_\nu - \frac{q\cdot n}{\mathbf{q}^2}(q_\mu n_\nu + n_\mu q_\nu)\right] \ , \tag{3.2}$$

where $n_\mu = (1,0,0,0)$. It generates loop integrals with the expression

$$\int \frac{d^D q}{q^2(\mathbf{q}-\mathbf{p})^2} \ . \tag{3.3}$$

The energy integral is not defined, even if one uses dimensional regularisation.

A procedure called *split dimensional regularisation* for this ill-defined integrals was brought up in [LW96]. Here energy and 3-momentum integrals are separately dimensionally regularised. Two regulating parameters are introduced by splitting the dimensionality of space-time into two different sectors, namely, $D = 4 - 2\epsilon = \omega + \rho$ and the divergences contained in the energy integrals are expressed as poles in ρ besides the usual ones in terms of ω. In this approach Coulomb gauge integrals were studies up to one and two-loop level and results for the divergent part of several of them were obtained. This concept of splitting up the dimensions is also used together with the so-called negative dimensional integration method [SS01]. With these methods combined results at the one and two loop level for arbitrary exponents of propagators and dimension have been achieved.

In recent years the Yang-Mills sector of QCD was examined in the Schrödinger picture [FR04a, FR04b, RF05, ERS06]. Using canonical quantisation a combination of Coulomb and Weyl gauge is fixed with the Faddeev-Popov method. In this approach the functional

Yang-Mills Schrödinger equation is solved up to two loop level for the vacuum employing a variational principle. Since the field configurations at the Gribov horizon are important for the confinement mechanism in Coulomb gauge, an ansatz for the wave functional is made, which diverges at the boundary of the Gribov region. The condition, that the vacuum energy is supposed to be minimal, leads to a coupled system of non-linear Dyson-Schwinger equations for the gluon energy, the ghost and Coulomb form factor and the curvature in configurations space. The numerical solution of this system gives a diverging gluon energy in the infrared, which indicates the absence of gluons in the physical spectrum at low energies and hence gluon confinement. The ghost form factor is also diverging in the infrared and generates therefore a linearly rising heavy quark potential for large distances, i.e. quark confinement. The investigations show that the curvature of configuration space, which is given in terms of the Faddeev-Popov operator, is crucial for confinement of quarks and gluons in this approach. Allowing for general powers of the Faddeev-Popov determinant in the trial wave functionals very different probability amplitudes for the field configurations at the Gribov horizon are probed. As a result there is no change in the infrared for the gluon two-point function and the ghost propagator, which is responsible for the long distance heavy quark potential. Despite of these successes an inclusion of quarks in the calculations is desireable.

The most coherent efforts have been devoted to Coulomb gauge by lattice QCD [Cuc06]. The performed studies can be divided into two periods. In the first period the examinations focused on the infrared behaviour of ghost and gluon propagators and the long-distance behaviour of the colour-Coulomb potential. In $SU(2)$ lattice calculations of reference [CZ02b] analytic predictions about the infrared behaviour of the gluon propagator have been confirmed: The equal-time transverse propagator is suppressed, while the time-time component is enhanced. Furthermore it has been found [CZ02b, CMZ02] that in the infinite-volume limit the equal-time transverse gluon propagator is well described by a Gribov-like propagator characterised by a pair of purely imaginary poles. Up to now the ghost propagator $G(\mathbf{k}, t)$ has only been studied in reference [LM04]. There, it was found that $G(\mathbf{k}, t)$ has an infrared divergence stronger than $1/k^2$. At the same time, the running coupling, which one can define as

$$g^2_{\mathrm{Coul}}(\mathbf{k}) = \frac{11N_c - 2N_f}{12N_c}\ \mathbf{k}^2\ V_C(\mathbf{k})\ , \tag{3.4}$$

appears to be consistent [CZ03, LM04] with an infrared behaviour of the type $1/k^2$. The colour-Coulomb potential has been computed in $SU(2)$ and $SU(3)$ lattice studies [GO03, NS06]. The relation $\sigma_c \approx 2 - 3\sigma$ to the static inter-quark potential has been found,

whereas approximate equality was found with a different method for the $SU(2)$ group [CZ03]. In a second period of lattice calculations the eigenvalue spectrum of the Faddeev-Popov operator became the main topic of investigation. There confinement is related to the near-zero eigenmodes of the Faddeev-Popov operator [GOZ05] and relations to the vortex confinement scenario are found.

3.4 Quantisation of Maxwell theory

In the following we will show how to formulate Yang-Mills theory in Coulomb gauge. It will make apparent how this approach provides access to the Coulomb potential of colour charges in an elegant way. For the sake of comparison with the Abelian case we begin by quantising Maxwell theory in this gauge[1].

For the quantisation of gauge theories standard procedures are not applicable. Looking at the theory of electromagnetism this becomes clear. The Lagrangian density of this field theory is given by

$$\mathcal{L} = -\frac{1}{4} F_{\mu\nu} F^{\mu\nu} + g_0 A_\mu j^\mu \ . \tag{3.5}$$

Here the four-current $j^\mu = (\rho, \mathbf{j})$ is a function of the matter fields. Computing the conjugated momentum fields gives

$$\Pi_\mu = \frac{\partial \mathcal{L}}{\partial(\partial_0 A^\mu)} \ . \tag{3.6}$$

Explicitly they read

$$\Pi^0 = 0 \tag{3.7}$$

$$\Pi^i = F^{i0} \ . \tag{3.8}$$

Imposing usual rules of quantisation[2] , we set

$$[\hat{A}_\mu(\mathbf{x}, t), \hat{\Pi}^\nu(\mathbf{y}, t)] = i\delta_\mu^\nu \delta^{(3)}(\mathbf{x} - \mathbf{y}) \ . \tag{3.9}$$

Comparing this to (3.7) we have clearly a contradiction. Modified rules for quantisation with constraints are required. The origin of their formulation is due to Dirac [Dir].

From the viewpoint of Dirac quantisation, the choice of a gauge consists of the replacement of an arbitrary function by a well-defined one in the Hamiltonian. The gauge conditions can be classified into three classes.

- Class I: Gauge conditions involving only A_k^a and their canonically conjugate momenta π_k^a.

[1] This chapter employs the conventions A.1 and B .

[2] A hat " ˆ " over a quantity is supposed to denote the associated operator.

- Class II: Gauge conditions involving also A_0^a.
- Class III: Gauge conditions involving furthermore $\partial_0 A_0^a$.

Class III contains the most general conditions. Any gauge condition of class I or II leads to a condition of class III. In this class physical degrees of freedom cannot be directly separated. With the help of a Class I gauge condition it is in general possible to get an effective Hamiltonian in terms of physical degrees of freedom only. Coulomb gauge is a class I gauge.

Before we quantise Yang-Mills theory we will start out with the canonical quantisation of electromagnetism in Coulomb gauge. These considerations can be collected from the literature [Kug, GT, Bur82, Moy04].

3.4.1 Canonical quantisation of Maxwell theory

At first we will briefly describe the quantisation procedure with constraints. In this procedure differences are made concerning the constraints. *Primary constraints* are conditions, which are derived in the process of calculating the Hamiltonian from the Lagrangian density. *Secondary constraints* are created by demanding that the primary constraints and all derived constraints are valid for all times. Let us denote the ensemble of all constraints, i.e. also the gauge condition and its stability condition, by $\{\varphi_\alpha\}$. The maximal ensemble of constraints $\{\phi_\alpha\} \subseteq \{\varphi_\alpha\}$ for which the matrix of the Poisson brackets

$$C_{ij} = \{\phi_i, \phi_j\}_P \tag{3.10}$$

is non-singular is called *second-class ensemble*. For any dynamical variable A let us define an associated *first-class* quantity A' by

$$A' = A - \{A, \phi_m\}_P C^{-1}_{mn} \phi_n \ . \tag{3.11}$$

An important property of this quantity is, that A' is compatible with all constraints of the second-class ensemble,

$$\{A', \phi_i\}_P = 0 \ . \tag{3.12}$$

Furthermore we need to define the Dirac bracket $\{...\}_D$ for variables A and B by

$$\{A, B\}_D := \{A', B'\}_P \ , \quad \{A', B'\}_P = \{A, B\}_P - \{A, \phi_m\}_P C^{-1}_{mn} \{\phi_n, B\}_P \ . \tag{3.13}$$

The procedure of quantising the theory is now defined as *replacing the Dirac bracket by the commutator*, i.e.

$$\{A, B\}_D \to -i[\hat{A}, \hat{B}] \ , \tag{3.14}$$

and setting all constraints of the second-class ensemble in the Hamiltonian to zero.

We will now apply this to Maxwell theory. The Hamiltonian density is given as[3]

$$\mathcal{H}_\Lambda = \frac{1}{2}(\mathbf{\Pi}^2 + \mathbf{B}^2) - (g_0 J_0 + \Pi \cdot \nabla)A_0 + \Lambda \Pi_0 + g_0 \mathbf{A} \cdot \mathbf{J} \ , \tag{3.15}$$

where Λ is the unknown velocity $\dot{A}_0$. Because $\mathcal{H}$ is a Hamiltonian density, integrating by part under the assumpion that the surface term vanishes does not change the Hamiltonian and yields

$$\mathcal{H}_\Lambda = \frac{1}{2}(\mathbf{\Pi}^2 + \mathbf{B}^2) - (g_0 J_0 - \nabla \cdot \Pi)A_0 + \Lambda \Pi_0 + g_0 \mathbf{A} \cdot \mathbf{J} \ . \tag{3.16}$$

By temporal derivation of (3.7) and demanding stability for the constraints we can derive a chain of secondary constraints,

$$\Pi_0 = 0 \ \Rightarrow \ \partial_i \Pi^i = g_0 J_0 \ \Rightarrow \ 0 = 0 \ . \tag{3.17}$$

Since we are dealing with a gauge theory, this chain does not provide any condition for Λ. For the purpose of eliminating the arbitrariness we have to fix the gauge. As we are interested in Coulomb gauge, we impose transversality of the spatial components of the photon field by the condition

$$\partial_i A^i = 0 \ . \tag{3.18}$$

By demanding that the gauge condition is valid for all times we get the stability chain

$$\partial_i A^i = 0 \ \Rightarrow \ \Delta A_0 = -\partial_i \Pi^i \ \Rightarrow \ \Delta \Lambda = 0 \ . \tag{3.19}$$

The constraints (3.17) and (3.19) are second-class, which means, that the dimension of the matrix C of the Poisson brackets is maximum. If we choose $\phi_1 = \Pi_0$, $\phi_2 = \partial_i \Pi^i - g_0 J_0$, $\phi_3 = \partial_i A^i$ and $\phi_4 = \Delta A_0 + \partial_i \Pi^i$, this matrix reads

$$C = \begin{pmatrix} 0 & 0 & 0 & -\Delta \\ 0 & 0 & \Delta & 0 \\ 0 & -\Delta & 0 & -\Delta \\ \Delta & 0 & \Delta & 0 \end{pmatrix} \delta^{(3)}(\mathbf{x} - \mathbf{y}) \ . \tag{3.20}$$

Thus Coulomb gauge belongs to the class I type of gauge conditions. The inverse of C is

$$C^{-1} = \begin{pmatrix} 0 & -\Delta^{-1} & 0 & \Delta^{-1} \\ \Delta^{-1} & 0 & \Delta^{-1} & 0 \\ 0 & \Delta^{-1} & 0 & 0 \\ -\Delta^{-1} & 0 & 0 & 0 \end{pmatrix} \delta^{(3)}(\mathbf{x} - \mathbf{y}) \ . \tag{3.21}$$

[3]For the necessary conventions see appendix B .

Employing (3.11) we can derive the first-class quantities

$$A_0' = -g_0\Delta^{-1}J_0 \ , \tag{3.22}$$
$$\Pi_0' = 0 \ , \tag{3.23}$$
$$A_k' = A_k - \partial_k\partial_l\Delta^{-1}A_l \ , \tag{3.24}$$
$$\Pi^{k'} = \Pi^k - \partial_k\partial_l\Delta^{-1}\Pi^l + g_0\partial_k\Delta^{-1}J_0 \ , \tag{3.25}$$

and the non-vanishing Dirac brackets are

$$\{A_k(x), \Pi^l(y)\}^{x_0=y_0} = (\delta_k^l - \partial_k\partial_l\Delta^{-1})\delta^{(3)}(\mathbf{x}-\mathbf{y}) \ . \tag{3.26}$$

As we already mentioned we have to set all constraints to zero in the Hamiltonian density. This at first eliminates the second and third term in (3.16). We then have to express the remainder

$$\mathcal{H} = \frac{1}{2}(\mathbf{\Pi}^2 + \mathbf{B}^2) + g_0\mathbf{A}\cdot\mathbf{J} \tag{3.27}$$

by 2×2 independent variables, e.g. A_1, A_2, Π_1, Π_2, whereas A_3 and Π_3 are solutions of $\phi_3 = 0$ and $\phi_2 = 0$ respectively. The dependence on the matter field J_0 is now hidden in the term Π^2 and the equation $\phi_2 = 0$. It is however possible to derive a more transparent expression for the Hamiltonian density. This can be done by replacing the variables $\mathbf{A}$ and $\mathbf{\Pi}$ by the corresponding first-class quantities. This is possible since these quantities differ from the original ones only by terms containing the constraints, which are set to zero. Expressing the transversal part of any field φ as

$$\varphi_k^\perp := \varphi_k - \partial_k\partial_l\Delta^{-1}\varphi_l \ , \tag{3.28}$$

we substitute

$$A_k \to A_k^\perp \tag{3.29}$$
$$\Pi^k \to \Pi_\perp^k + g_0\partial_k\Delta^{-1}J_0 \ . \tag{3.30}$$

This entails the substitution of the first term in (3.27) by

$$\frac{1}{2}\left[\mathbf{\Pi}_\perp^2 + \mathbf{B}^2 + (g_0\partial_l\Delta^{-1}J_0)^2 - 2g_0\Pi_\perp^l\partial_l\Delta^{-1}j_0\right] \ . \tag{3.31}$$

Integrating the last two terms by part yields the substitutions

$$(g_0\partial_l\Delta^{-1}J_0)^2 \ \to \ -J_0\Delta^{-1}J_0 \ , \tag{3.32}$$
$$\Pi_\perp^l\partial_l\Delta^{-1}J_0 \to \partial_l\Pi_\perp^l\Delta^{-1}J_0 = 0 \tag{3.33}$$

and therefore we get

$$\mathcal{H}_\perp = \frac{1}{2}\left[\mathbf{\Pi}_\perp^2 + \mathbf{B}^2\right] - \frac{1}{2}g_0^2 J_0 \Delta^{-1} J_0 + g_0 \mathbf{A}_\perp \cdot \mathbf{J} \ . \tag{3.34}$$

If we use the equality $\mathbf{E}_\perp = \mathbf{\Pi}_\perp$ and integrate over the spatial coordinates, we get the following expression for the Hamiltonian:

$$H = \int d^3x \left[\frac{1}{2}(\mathbf{E}_\perp^2 + \mathbf{B}^2) + g_0 \mathbf{A}_\perp \cdot \mathbf{J}\right] + H_{\text{Coul}} \ , \tag{3.35}$$

where we defined

$$H_{\text{Coul}} := \frac{1}{2}g_0^2 \int d^3x d^3y \ \rho(\mathbf{x}) \mathcal{V}_{\text{Coul}}(\mathbf{x}, \mathbf{y}) \rho(\mathbf{y}) \tag{3.36}$$

and used the notation

$$\mathcal{V}_{\text{Coul}}(\mathbf{x}, \mathbf{y}) = -\Delta^{-1}|_{(\mathbf{x},\mathbf{y})} \ . \tag{3.37}$$

This is our *final expression* for the *Hamiltonian of Maxwell theory* and will be compared later to the Hamiltonian of Yang-Mills theory in Coulomb gauge.

Some remarks are in order at this point. The fields $\mathbf{A}_\perp$ and $\mathbf{\Pi}_\perp$ possess only two linearly independent components due to the transversality conditions

$$\partial_i A_\perp^i = 0 \ , \ \partial_i \Pi_\perp^i = 0 \ . \tag{3.38}$$

These components represent the two transversal photon polarisations. Using the Coulomb gauge eliminates the unphysical degrees of freedom at the level of the Hamiltonian, which means that timelike and longitudinal photons are no more present in the quantised theory. Furthermore we notice, that the constraint ϕ_2 is Gauss's law. It is therefore automatically satisfied and does not have to be imposed after the quantisation as a constraint in terms of operators on the physical states.

Our introduction of the first-class fields into the Hamiltonian made the quantity J_0 reappear in the expression

$$-\frac{1}{2}g_0^2 J_0 \Delta^{-1} J_0 = \frac{1}{2}g_0^2 \int d^3y \frac{J_0(\mathbf{x}) J_0(\mathbf{y})}{4\pi|\mathbf{x} - \mathbf{y}|} \ . \tag{3.39}$$

This term is the well-known *Coulomb energy density*. The inverse of the Laplacian is thereby known to be

$$\Delta^{-1}|_{(\mathbf{x},\mathbf{y})} = -\frac{1}{4\pi}\frac{1}{|\mathbf{x} - \mathbf{y}|} \ . \tag{3.40}$$

We already mentioned that the gauge condition (3.18) eliminates the unphysical degrees of freedom. Therefore Coulomb gauge is called a physical gauge. The price we have to pay for this feature is the violation of Lorentz invariance of Maxwell theory. However, the

terms hindering Lorentz invariance should vanish when physical observables are computed due to gauge invariance.

The last aspect is less complicated in *covariant gauges*. They are given by

$$\partial_\mu A^\mu = \omega(x) \ , \tag{3.41}$$

where $\omega(x)$ is a scalar function. This equation can be cast into the form

$$\dot{A}_0 = -\partial_i A^i + \omega(x) \ , \tag{3.42}$$

from which we recognise, that the quantity Λ in (3.16) is directly fixed by the gauge condition. Any covariant gauge of the form (3.41) is thus a class III gauge, in which all degrees of freedom evolve dynamically. In a covariant gauge it is not trivial to eliminate non-physical states of the Hilbert space. It is described by the Gupta-Bleuler formalism in QED and in the BRST formalism in quantised Yang-Mills theories.

3.4.2 Path integral quantisation of Maxwell theory in Coulomb gauge

The Feynman path integral quantisation procedure needs to modified in the case of a gauge theory. Let us denote the set of constraints by

$$\phi_\alpha = 0 \ , \ \alpha = 1, ..., M \ . \tag{3.43}$$

Since Coulomb gauge is a class I gauge, this set is second-class. The modified expression for the partition function in phase space is [Kug]

$$Z = \int \mathcal{D}A\mathcal{D}\Pi \prod_{\alpha=1}^{M} \delta(\phi_\alpha) \mathrm{Det}^{\frac{1}{2}}[C](A,\Pi) \exp\left\{ i \int dx \left[\Pi_\mu \dot{A}^\mu - \frac{1}{2}(\mathbf{\Pi}^2 + \mathbf{B}^2) - g_0 \mathbf{A}\cdot\mathbf{J} \right] \right\} \ . \tag{3.44}$$

We can omit the determinant of the matrix C, because it does not depend on the fields. The partition function will be transformed in two steps. At first we integrate over A_0 and Π_0,

$$Z = \int \mathcal{D}\mathbf{A}\mathcal{D}\mathbf{\Pi} \exp\left\{ i \int dx \left[\Pi_i \dot{A}^i - \frac{1}{2}(\mathbf{\Pi}^2 + \mathbf{B}^2) - g_0 \mathbf{A}\cdot\mathbf{J} \right] \right\} \delta(\partial_i A^i) \delta(\partial_i \Pi^i - g_0 J_0) \ . \tag{3.45}$$

Then we represent $\delta(\partial_i \Pi^i - g_0 J_0)$ as an integral, for which the field A_0 is reintroduced as the integration variable:

$$\delta(\partial_i \Pi^i - g_0 J_0) = \int \mathcal{D}A_0 \exp\left\{ -i \int A_0 (\partial_i \Pi^i - g_0 J_0) dx \right\} \ . \tag{3.46}$$

If we insert this expression in the partition function, we find

$$Z = \int \mathcal{D}A\mathcal{D}\mathbf{\Pi} \exp\left\{ i \int dx \left[\Pi_i(\dot{A}^i - \partial^i A_0) - \frac{1}{2}(\mathbf{\Pi}^2 + \mathbf{B}^2) + g_0 A_\mu J^\mu \right] \right\} \delta(\partial_i A^i) \ . \quad (3.47)$$

Performing the Gaussian integral over $\mathbf{\Pi}$ we obtain the final result:

$$Z = \int \mathcal{D}A \exp\left\{ i \int \mathcal{L} dx \right\} \delta(\partial_i A^i) \ , \quad \mathcal{L} = -\frac{1}{4} F_{\mu\nu} F^{\mu\nu} + g_0 A_\mu J^\mu \ . \quad (3.48)$$

Our transformations end with the appearance of the Maxwell Lagrangian and the Coulomb gauge condition as the only constraint in form of a delta function. It is possible to recast this in a way, which emphasises the physical degrees of freedom $\mathbf{A}_\perp$ and $\mathbf{\Pi}_\perp$. To this end we start from (3.45) and separate the transverse and longitudinal parts of the $\mathbf{\Pi}$ field, $\mathbf{\Pi} = \mathbf{\Pi}_\perp - \nabla\phi$. The integration measure thus becomes $\mathcal{D}\mathbf{\Pi} \simeq \mathcal{D}\mathbf{\Pi}_\perp \mathcal{D}\phi$. Reintroducing the irrelevant factor $\mathrm{Det}[-\Delta]$, we can use

$$\mathrm{Det}[-\Delta]\delta(\partial_i \Pi^i - g_0 J_0) = \mathrm{Det}[-\Delta]\delta(-\Delta^{-1}\phi - g_0 J_0) = \delta(\phi + g_0 \Delta^{-1} J_0) \ . \quad (3.49)$$

and perform the ϕ-integration to obtain

$$Z = \int \mathcal{D}\mathbf{A}_\perp \mathcal{D}\mathbf{\Pi}_\perp \exp\left\{ i \int dx (\Pi_{\perp,i} \dot{A}^i - \mathcal{H}_\perp) \right\} \ , \quad (3.50)$$

where $\mathcal{H}_\perp$ is the Hamiltonian density (3.34).

3.5 Quantisation of Yang-Mills theory

At this point we are ready to quantise a non-Abelian gauge theory of the gauge group $SU(N)$ in Coulomb gauge.

We start with the Lagrangian density

$$\mathcal{L} = -\frac{1}{4} F^a_{\mu\nu} F_a^{\mu\nu} + g_0 A^a_\mu J^\mu_a \ . \quad (3.51)$$

The conjugate momenta are

$$\Pi^0_a = 0 \ , \Pi^i_a = F^{i0}_a \ , \quad (3.52)$$

and thus we obtain a primary constraint as we did in (3.7). Postulating the stability of this condition gives us the chain of secondary constraints

$$\Pi^0_a = 0 \ \Rightarrow \ [D_i \Pi^i]_a = g_0 J^0_a \ \Rightarrow 0 = 0 \ . \quad (3.53)$$

For the Hamiltonian density we get

$$\mathcal{H} = \frac{1}{2}(\mathbf{\Pi}^2 + \mathbf{B}^2) - (g_0 J_0^a + \mathbf{\Pi}^b \cdot \mathbf{D}^{ab}) A_0^a + \Lambda^a \Pi_0^a + g_0 \mathbf{A}^a \cdot \mathbf{J}^a \ , \tag{3.54}$$

where for all quantities X the product $\mathbf{X}^2$ now stands for $X_a^i X_a^i$. In Coulomb gauge our gauge condition reads

$$\partial_i A_a^i = 0 \ . \tag{3.55}$$

The stability of (3.55) provides a secondary constraint and a condition for Λ:

$$\partial_i A_a^i = 0 \ \Rightarrow \ \nabla \cdot \mathbf{D}^{ab} A_0^b = -\partial_i \Pi_a^i \ \Rightarrow \ \nabla \cdot \mathbf{D}^{ab} \Lambda^b = 0 \ . \tag{3.56}$$

Our set of constraints is second-class and therefore Coulomb gauge is a class I gauge. We could now employ the canonical quantisation procedure and calculate the matrix of the Poisson brackets, invert it, calculate the first-class quantities, the Dirac brackets and in the end the Hamiltonian density. The constraint chain makes clear, that the matrix of the Poisson brackets contains the differential operator $\nabla \cdot \mathbf{D}$. The computation of the Dirac brackets requires the inversion of this operator, which is not easy. The canonical quantisation procedure is usually performed in the temporal gauge $A_0^a = 0$ or in the axial gauge $A_3^a = 0$. We choose to follow the path integral approach, which leads to

$$Z = \int \mathcal{D}A \exp\left\{ i \int \mathcal{L} \ dx \right\} \delta(\partial_i A_a^i) \mathrm{Det}[-\nabla \cdot \mathbf{D}] \ , \qquad \mathcal{L} = -\frac{1}{4} F_{\mu\nu}^a F_a^{\mu\nu} + g_0 A_\mu^a J_a^\mu \tag{3.57}$$

as the pendant of (3.48).

We recognise that this expression differs from the Abelian analogue by the determinant $\mathrm{Det}[-\nabla \cdot \mathbf{D}]$. In the Abelian case it is possible to neglect the determinant since it does not depend on a dynamical variable.

In order to make the expression more transparent we try to cast the partition function in a form with $\mathbf{A}_\perp$ and $\mathbf{\Pi}_\perp$ as integration variables. This is analogous to the transformations which lead to the Abelian expression (3.50). We linearise the factor

$$\exp\left\{ i \int \left(-\frac{1}{2} F_{0i}^a F_a^{0i} \right) dx \right\} \simeq \int \mathcal{D}\mathbf{\Pi} \exp\left\{ i \int \left(\Pi_i^a F_a^{0i} - \frac{1}{2} \mathbf{\Pi}^2 \right) \right\} \tag{3.58}$$

using the new variables $\mathbf{\Pi}$, which are interpreted as the conjugated momenta. Thus the generating functional becomes

$$Z = \int \mathcal{D}A \mathcal{D}\mathbf{\Pi} \exp\left\{ i \int \left[\Pi_i^a (\dot{A}_a^i - [D^i A_0]_a) - \frac{1}{2}(\mathbf{\Pi}^2 + \mathbf{B}^2) + g_0 A_0^a J_0^a - g_0 \mathbf{A}^a \cdot \mathbf{J}^a \right] \right\} \cdot \\ \delta(\partial_i A_a^i) \mathrm{Det}[-\nabla \cdot \mathbf{D}] \ . \tag{3.59}$$

Integrating over A_0^a leads to

$$Z = \int \mathcal{D}\mathbf{A}\mathcal{D}\mathbf{\Pi} \exp\left\{ i \int \left[\Pi_i^a \dot{A}_a^i - \frac{1}{2}(\mathbf{\Pi}^2 + \mathbf{B}^2) - g_0 \mathbf{A}^a \cdot \mathbf{J}^a \right] \right\} \cdot \\ \delta(\partial_i A_a^i)\ \delta([D_i \Pi^i]^a - g_0 J_0^a) \mathrm{Det}[-\nabla \cdot \mathbf{D}] \ , \tag{3.60}$$

what exhibits the validity of Gauss's law in the integrand. This expression is the analogue to (3.45). If we separate the transverse and longitudinal parts of the conjugated fields,

$$\mathbf{\Pi}^a = \mathbf{\Pi}_\perp^a - \nabla \phi^a \ , \tag{3.61}$$

the integration measure factorises to $\mathcal{D}\mathbf{\Pi}_\perp \mathcal{D}\phi$. Using $\nabla \cdot \mathbf{D} = \mathbf{D} \cdot \nabla$, which is due to the transversality of the gauge fields, and the definition of the colour-charge density of the gluons $\rho_{\mathrm{gl}}^a = f^{abc} A_i^b E_c^i$ we can absorb the determinant in the delta function of (3.60), which enforces Gauss's law. Integrating over ϕ yields finally

$$Z = \int \mathcal{D}\mathbf{A}_\perp \mathcal{D}\mathbf{\Pi}_\perp \exp\left\{ i \int (\Pi_{\perp,i}^a \dot{A}^{i,a} - \mathcal{H}_\perp) \right\} \ . \tag{3.62}$$

The Hamiltonian density $\mathcal{H}_\perp$ is derived from (3.54) by substituting $\mathbf{A} \to \mathbf{A}_\perp$ and $\mathbf{\Pi} \to \mathbf{\Pi}_\perp$ and setting all constraints to zero. Supressing colour indices it is

$$\mathcal{H}_\perp = \frac{1}{2}(\mathbf{\Pi}_\perp^2 + \mathbf{B}^2) - \frac{1}{2} g_0^2 (\rho_{\mathrm{gl}} + J_0)(-\nabla \cdot \mathbf{D})^{-1} \Delta (-\nabla \cdot \mathbf{D})^{-1} (\rho_{\mathrm{gl}} + J_0) + g_0 \mathbf{A}_\perp \cdot \mathbf{J} \ . \tag{3.63}$$

Therefore the Yang-Mills analogues to (3.35) and (3.36) are

$$H = \int d^3x \left[\frac{1}{2}(\mathbf{E}_\perp^2 + \mathbf{B}^2) + g_0 \mathbf{A}_\perp^a \cdot \mathbf{J}^a \right] + H_{\mathrm{Coul}} \tag{3.64}$$

and

$$H_{\mathrm{Coul}} = \frac{1}{2} g_0^2 \int d^3x d^3y \rho^a(\mathbf{x}) \mathcal{V}_{\mathrm{Coul}}^{ab}(\mathbf{x}, \mathbf{y}) \rho^b(\mathbf{y}) \ . \tag{3.65}$$

Thereby we used the definitions

$$\mathcal{V}_{\mathrm{Coul}}^{ab}(\mathbf{x}, \mathbf{y}) := M^{-1}(-\Delta) M^{-1}|_{(\mathbf{x},\mathbf{y})}^{ab} \ , \tag{3.66}$$

$$\rho := \rho_{\mathrm{gl}} + J_0 \ , \tag{3.67}$$

$$M := -\nabla \cdot \mathbf{D} \ . \tag{3.68}$$

The operator M is called the *Faddeev-Popov operator* and plays an important role in the Gribov-Zwanziger scenario of colour confinement. In the Abelian case of Maxwell theory the Faddeev-Popov operator reduces simply to the Laplacian, $M = -\Delta$, and $\mathcal{V}_{\mathrm{Coul}}^{ab}(\mathbf{x}, \mathbf{y})$, which is the analogue of (3.37), becomes the Coulomb potential of electrodynamics.

3.6 The confinement scenario of Gribov and Zwanziger

3.6.1 Ambiguities in Coulomb gauge

Eventually the question has to be addressed, if the Coulomb gauge condition fixes the gauge completely or if it allows for gauge copies [Gri78]. Starting with a gauge potential $\mathbf{A}$, which fulfils the gauge condition (3.55), we examine the gauge-transformed potential

$$\mathbf{A}^g = g\mathbf{A}g^{-1} - \frac{i}{g_0}(\nabla g)g^{-1} \ , \tag{3.69}$$

where g is an element of the gauge group. If the condition (3.55) fixes the gauge completely, it should not be possible to find a further transversal gauge configuration on the gauge orbit of $\mathbf{A}$. Assuming suitable conditions at spatial infinity the solution of the equation

$$\nabla \cdot \mathbf{A}^g = 0 \tag{3.70}$$

for g should be the identity.

The Abelian case is easy. With $g = \exp\{ig_0\Lambda\}$ the gauge-transformed potential is given by $\mathbf{A}^g = \mathbf{A} + \nabla\Lambda$ and the equation (3.70) simplifies to

$$\Delta\Lambda = 0 \ . \tag{3.71}$$

If we demand that Λ vanishes at spatial infinity, it is zero everywhere and we get $g = 1$. Consequentially there are no gauge copies in Coulomb gauge for Maxwell theory.

In the non-Abelian case, the transformed potential is (3.69) with $g = \exp\{ig_0\alpha^a T^a\}$. Expanding to first order in the parameter α casts (3.70) into $\nabla \cdot \mathbf{D}\alpha^a = 0$. This result can be interpreted as a Schrödinger-type equation for the Faddeev-Popov operator with zero eigenvalue, i.e. $\epsilon[\mathbf{A}] = 0$:

$$-\Delta\alpha^a - g_0 f^{abc}\mathbf{A}^b \cdot \nabla\alpha^c = \epsilon[\mathbf{A}]\alpha^a \ . \tag{3.72}$$

A non-trivial solution for sufficiently small potentials can only be achieved with $\epsilon > 0$. For perturbation theory gauge copies are therefore of no relevance. For a potential with bigger magnitude the lowest eigenvalue of the Faddeev-Popov operator vanishes and gives a non-trivial solution of (3.70). For increasing magnitude of $\mathbf{A}$ the eigenstate transforms to one with negative ϵ and after this to another state with $\epsilon = 0$ and so on. The space of gauge field configurations can then be divided into regions C_n according to the number of negative eigenvalues of the Faddeev-Popov operator. This is illustrated in figure 3.1.

Gribov was able to show that for a configuration in C_0 and close to its boundary an infinitesimal gauge transformation has the effect of putting the potential in the region

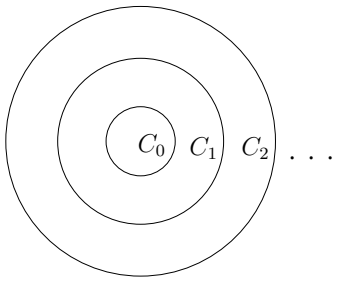

Figure 3.1: The space of gauge field configurations is divided in regions C_n depending on the number n of negative eigenvalues of the Faddeev-Popov operator. On each single boundary this operator possess a non-trivial zero mode.

C_1. Gribov hoped that such relations hold for general gauge transformations and that the configurations outside of C_0 are merely copies (*Gribov copies*) and therefore redundant. In order to get rid of the ambiguities he suggested to restrict functional integrations in the space of gauge configurations to the *Gribov region* C_0. The functional integrals should be cut off at the boundary, where the lowest non-trivial eigenvalue of the Faddeev-Popov operator vanishes, also known as the first *Gribov horizon*.

Further studies showed that in the region C_0 there are still Gribov copies present. This can be illuminated by following the gauge fixing procedure of Zwanziger [Zwa82]. It consists of choosing elements g of the gauge group minimising the functional

$$F_A[g] = \int d^3x \ \mathrm{tr}[\mathbf{A}^g(x) \cdot \mathbf{A}^g(x)] \ , \ g = \exp\{ig_0\alpha^a T^a\} \ , \tag{3.73}$$

which is the L^2 norm of the potential along the gauge orbit. Expanding to second order in the parameter α gives

$$F_A[g] = F_A[1] + 2\int d^3x \ \mathrm{tr}[\partial_i A_i(\mathbf{x})\alpha(\mathbf{x})] + \int d^3x \mathrm{tr}[\alpha^\dagger(\mathbf{x})(-\partial_i D_i)\alpha(\mathbf{x})] + \mathcal{O}(\alpha^3) \ . \tag{3.74}$$

We recognise that for a minimum of (3.73) we have transversality of the potential $\partial_i A_i^a = 0$ and positivity of the Faddeev-Popov operator $-\nabla \cdot \mathbf{D}[A^g] \geq 0$, because the Hessian matrix is positive at a minimum. The set of these minima is by definition the Gribov region C_0, which is often denoted by Ω. Since on each gauge orbit there may be more than one local minimum there is obviously room for gauge copies in Ω.

The remaining gauge copies in the Gribov region can be eliminated with the help of an improved gauge condition. Instead of the Gribov region one considers the set of all absolute minima, which is obtained by minimising the norm (3.73) along the gauge orbits. It is called the *fundamental modular region* and is denoted by Λ. Functional integration

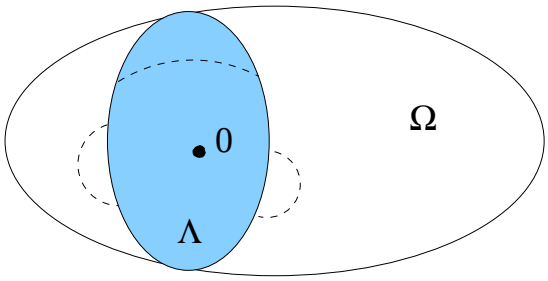

Figure 3.2: The Gribov region Ω contains the fundamental modular region Λ. The point $A = 0$ lies in both sets and points on the boundary of Λ have to be identified.

must now be restricted to this region. The gauge obtained by the described procedure is called *minimal Coulomb gauge*. Λ contains the point $A = 0$, is a subset of Ω, convex and points of its boundary have to be identified because of continuity reasons [Baa97, SBZ03]. This is demonstrated in figure 3.2.

3.6.2 Coulomb confinement as a necessary confinement condition

The Coulomb potential is derived from the partition function (3.57) by looking at the A_0A_0-correlator

$$g_0^2\langle A_0^a(x)A_0^b(y)\rangle = \frac{-1}{Z}\frac{\delta^2 Z}{\delta J_0^a(x)\delta J_0^b(y)} \ . \tag{3.75}$$

Using the more convenient expression (3.62) for the partition function this calculation yields [CZ02b]

$$\frac{-1}{Z}\frac{\delta^2 Z}{\delta J_0^a(x)\delta J_0^b(y)} = g_0^2\left\langle \mathcal{V}^{ab}_{\mathrm{Coul}}(\mathbf{x},\mathbf{y})\right\rangle \delta(x_0-y_0) - g_0^2\left\langle (\mathcal{V}\rho_{\mathrm{gl}})^a(x)(\mathcal{V}\rho_{\mathrm{gl}})^b(y)\right\rangle \ . \tag{3.76}$$

The instantaneous part of this correlation function represents the *Coulomb potential*

$$V_C(\mathbf{x}-\mathbf{y})\delta^{ab} = \mathcal{N} g_0^2\langle \mathcal{V}_{\mathrm{Coul}}(\mathbf{x},\mathbf{y})\rangle \ , \tag{3.77}$$

which is (up to a constant $\mathcal{N}$) the vacuum expectation value of the operator $\mathcal{V}_{\mathrm{Coul}}$.

The well-known *Wilson potential* V_W can be extracted from the vacuum expectation value of the Wilson loop. The *ground state energy* of the static $q\overline{q}$ pair is given as

$$E_{min}(R) = E_{self} + V_W(R) \ , \tag{3.78}$$

where E_{self} are the quark self energies.

It is possible to show that a confining Coulomb potential is necessary for the Wilson potential to be confining. We proof this statement with the help of group theory, following the derivation in [Zwa03]. To this end we examine the energy of the static $q\overline{q}$ state in Coulomb gauge. Explicitly it is

$$E_{qq} = \langle \Phi_{qq}|H|\Phi_{qq}\rangle - \langle 0|H|0\rangle \ , \tag{3.79}$$

where H is the Coulomb gauge Hamiltonian (3.64). The quark and antiquark of the $q\overline{q}$ pair live in the fundamental representation N and $\overline{N}$ of the gauge group $SU(N)$. Our trial states in terms of the wave functionals read

$$\Phi_{qq}[A] = \Psi^s_{qq}\Psi_0[A] \ . \tag{3.80}$$

The state $\Psi_0[A]$ is the wave functional of the vacuum state in the absence of external quarks and the state Ψ^s_{qq} belongs to the singlet part of the decomposition $N \times \overline{N} = 1 + (N^2 - 1)$. For the following considerations we use the convenient notation $|\Phi_{qq}\rangle = |s\rangle|0\rangle_A$ for the trial state and $\langle ...\rangle_A = \int \mathcal{D}A...$ for the expectation value. The Coulomb term H_{Coul} in the Hamiltonian contains with the colour-charge density J_0 the external quark fields. The infinitely massive quark and antiquark are treated as pointlike particles sitting at $\mathbf{x}$ and $\mathbf{y}$ respectively. Their colour charge density is given as

$$J^a_0(\mathbf{z}) = \lambda^a_q \delta(\mathbf{z} - \mathbf{x}) + \lambda^a_{\overline{q}}\delta(\mathbf{z} - \mathbf{y}) \ , \tag{3.81}$$

where λ^a_q and $\lambda^a_{\overline{q}}$ can be expressed through the Hermitian generators λ^a_N of the gauge group $SU(N)$ in the fundamental representation. Since the total colour charge density is given as the sum $\rho = \rho_{\text{gl}} + J_0$, the Coulomb term of the Hamiltonian can be written as

$$H_{\text{Coul}} = H_{\text{gl}} + H_{\text{gl qu}} + H_{\text{qu qu}} \ , \tag{3.82}$$

where H_{gl} is the Hamiltonian without external quarks, $H_{\text{gl qu}}$ is linear in J_0 and the last term is

$$H_{\text{qu qu}} = g_0^2 \frac{1}{2} \sum_{a,b} \int d\mathbf{z}_1 d\mathbf{z}_2 J^a_0(\mathbf{z}_1)\mathcal{V}^{ab}_{\text{Coul}}(\mathbf{z}_1, \mathbf{z}_2)J^b_0(\mathbf{z}_2) \ . \tag{3.83}$$

The first term is responsible for the vacuum energy without external quarks,

$$\langle \Phi_{qq}|H_{\text{gl}}|0\rangle_A = E_0 \ . \tag{3.84}$$

Because of $\langle s|\lambda^a_{q,\overline{q}}|s\rangle = 0$ ($|s\rangle$ is a colour-singlet state) the second term vanishes. The third term gives the most intriguing contribution, namely

$$\langle \Phi_{qq}|H_{\text{qu qu}}|\Phi_{qq}\rangle = \sum_{i,j\in\{q,\overline{q}\}} \sum_{a,b} \langle s|\lambda^a_i\lambda^b_j|s\rangle\langle 0|\mathcal{V}^{ab}_{\text{Coul}}(\mathbf{x},\mathbf{y})|0\rangle_A \ . \tag{3.85}$$

From group theory the identity $\langle s|\lambda^a\lambda^b|s\rangle = -\frac{1}{N^2-1}\delta^{ab}C_N$ is known (C_N is the Casimir of the representation N). Adding the mentioned contributions yields

$$E_{qq} = E'_{self} + V_C \ , \tag{3.86}$$

where again the Coulomb potential

$$V_C = -C_N g_0^2 \langle 0|\mathcal{V}^{aa}_{\text{Coul}}(\mathbf{x},\mathbf{y})|0\rangle_A \tag{3.87}$$

shows up. The first term in (3.86) contains the contributions $i = j = q$ and $i = j = \overline{q}$, which represent the quark self-energies. The R-dependent second term of E_{qq} is the Coulomb potential (3.77) of the massive quark-antiquark pair.

We are now in the position to compare the potentials $V_W(R)$ and $V_C(R)$. The former can be calculated from the *ground state energy* $E_{min}(R)$ of the static $q\overline{q}$ pair, which can be extracted from the expectation value of the Wilson loop. The latter is the R-dependent part of the *total energy* E_{qq} of the system, which we calculated by taking the expectation value (3.79) of the Coulomb gauge Hamiltonian. We start from the inequality

$$E_{min}(R) \leq E_{qq}(R) \ . \tag{3.88}$$

If the Wilson potential and the Coulomb potential are confining, we assume that the static quark self-energies E_{self} and E'_{self} can be neglected in comparison to the potentials at large R. Asymptotically this results in

$$V_W(R) \leq V_C(R) \ , \tag{3.89}$$

which means that Coulomb confinement is a necessary condition for confinement.

3.6.3 Quark-antiquark potentials and signals for confinement

Let us have a closer look at the meaning of the Wilson and the Coulomb potential in the context of lattice calculations. The Wilson potential is computed by averaging the Wilson loop operator over all gluonic and fermionic fluctuations,

$$\langle W_\Gamma[A]\rangle_{\text{Eucl.}} = \frac{\int \mathcal{D}A \ W_\Gamma[A]\text{Det}[K[A]]\exp(-S^{\text{Eucl.}}_{YM}[A])}{\int \mathcal{D}A \ \text{Det}[K[A]]\exp(-S^{\text{Eucl.}}_{YM}[A])} \ . \tag{3.90}$$

Here $K[A]$ is the matrix $K_{x\alpha,y\beta}[A] = [\gamma_\nu(\partial_\mu + iA_\mu) + m]_{\alpha\beta}\delta^{(4)}(x-y)$. Effects coming from dynamical fermions can be switched off by setting $\text{Det}[K] \equiv 1$, which is known as the *quenched approximation*.

In this approximation lattice calculations have shown that the Wilson potential signals confinement of two static quarks by rising linearly at large R,

$$V_W(R) = \sigma R \ , \tag{3.91}$$

where σ is the well-known *string tension*. The linearly rising energy is stored in the colour electric flux string connecting the two quarks. If dynamical quarks are present, which means $\mathrm{Det}[K] \neq 1$, the creation of a pair of dynamical quarks from the vacuum is energetically more appealing than the expansion of a string between the two static sources. Consequently a pair of mesons is formed at separation R. In this situation the Wilson potential describes no longer the interaction of two external quarks in the vacuum but the potential of two mesons at separation R and can be regarded as an analogue of a Van der Waals potential. A different quantity should be found, which does not lose its confining property in the presence of dynamical quarks.

Let us review the A_0A_0 correlator (3.76), which contains besides the Coulomb potential the quantity

$$P_0 := -g_0^2 \left\langle (\mathcal{V}\rho_{\mathrm{gl}})^a(x)(\mathcal{V}\rho_{\mathrm{gl}})^b(y) \right\rangle \ . \tag{3.92}$$

It describes the vacuum polarisation induced by the dynamical quarks, where the minus sign signals that it corresponds to screening. As we have seen the first term in (3.76) is confining in the absence of dynamical quarks. Allowing for those V_W is no longer confining indicating that the screening polarisation term dominates in (3.76). The Coulomb potential might still be confining, because the long range of V_C could be the reason that makes the creation of a dynamical quark pair preferable to an expansion of the flux tube [CZ02c]. The Coulomb potential is thus a candidate for an order-parameter of confinement in the presence of dynamical quarks. Recent lattice studies [NNST07], however, show that the Coulomb string tension does not vanish for temperatures far beyond the deconfinement transition, which suggests that the Coulomb potential cannot serve as an order parameter.

3.6.4 Confinement in Coulomb gauge

When Gribov wrote his famous paper [Gri78] about the problem of gauge copies and suggested the possible restriction of the gauge field integration to the Gribov region Ω, he already pointed out the possible relation between the restriction to Ω and the confinement problem by examining the infrared behaviour of the ghost propagator. This is given by the vacuum expectation value of the Faddeev-Popov operator $-\nabla \cdot \mathbf{D}$:

$$D^{ab}(\mathbf{x}-\mathbf{y}) = \langle M^{-1}[A]|^{ab}_{(\mathbf{x},\mathbf{y})} \rangle \ . \tag{3.93}$$

The confinement scenario is nowadays stated in the following way [AG06]. The Coulomb potential

$$V_C \propto \langle M^{-1}[A](-\Delta)M^{-1}[A]\rangle \tag{3.94}$$

is long range and thereby enhanced for small momenta because $M^{-1}[A]$ is long range. This follows from entropy considerations: Since the dimension of configuration space is quite large, it is reasonable that most of the configurations are located close to the horizon (just as the volume measure $r^{d-1}dr$ of a sphere in d dimensions is enhanced near the radius). This suggests that the near-zero eigenvalues of the Faddeev-Popov operator are dominating at large quark separations.

As already mentioned these questions have been examined via lattice Monte Carlo simulations in Coulomb gauge, which found that $V_C(R)$ does indeed rise linearly [NS06]. Furthermore the infrared divergent Coulomb energy of an isolated charge comes about by the mechanism suggested by Gribov and Zwanziger, namely a large density of eigenvalues of the Faddeev-Popov operator near the zero eigenvalue [GOZ05]. There is also a connection to a different confinement picture. If centre vortices are removed from lattice configurations, the Coulomb energy is not confining any more and the Faddeev-Popov eigenvalue distribution resembles that of the abelian theory. Together with the fact that centre vortices are field configurations lying on the boundary $\partial\Lambda$ of the fundamental modular region if they are gauge transformed to minimal Coulomb gauge, this suggests a close relationship between these two confinement scenarios.

On the contrary it also turns out that the Coulomb string tension is roughly three times larger than the string tension of the Wilson potential, so the behaviour of the Coulomb interaction energy cannot be the whole story describing confinement. An interesting investigation (e.g. in [SK06]) is to try to construct physical states in Coulomb gauge, whose energy is below that of a quark-antiquark pair plus their Coulomb field by adding constituent gluons. As a quark and an antiquark separate, they might pull out between them a "chain" of constituent gluons, where each gluon in this chain is supposed to be bound to its nearest neighbours by Coulomb interaction. This picture has the name "gluon chain model" [GT02], and it encourages an imagination of the QCD flux tube as a kind of discretised string. Alternatively such a picture might arise also from a recent worldsheet formulation of gauge theory quantised in light-cone gauge [Tho02].

Chapter 4

The Quark Dyson-Schwinger Equation

In this chapter we can use the insight we gained in the last one. The profit concerns mainly the parametrization of the gluon propagator. Its all-dominant part is the Coulomb potential, for which we employ an analytic ansatz. We start by deriving the quark Dyson-Schwinger equation with two different methods. We solve it numerically in two different truncations and compare the results.

4.1 From the QCD action to the gap equation

In this section we derive the quark Dyson-Schwinger equation from the QCD action. Because this is not rigorously possible in Coulomb gauge, we choose for this demonstration a linear covariant gauge and Euclidean space-time[1].

The starting point is the renormalised Lagrangian [AS01], which reads

$$\begin{aligned}\mathcal{L}_{\text{QCD}} &= Z_3 \frac{1}{2} A^a_\mu \left(-\partial^2 \delta_{\mu\nu} - \Big(\frac{1}{Z_3 \xi} - 1\Big) \partial_\mu \partial_\nu \right) A^a_\nu \\ &\quad + \widetilde{Z}_3 \, \bar{c}^a \partial^2 c^a + \widetilde{Z}_1 \, g f^{abc} \, \bar{c}^a \partial_\mu (A^c_\mu c^b) - Z_1 \, g f^{abc} \, (\partial_\mu A^a_\nu) \, A^b_\mu A^c_\nu \\ &\quad + Z_4 \frac{1}{4} g^2 f^{abe} f^{cde} \, A^a_\mu A^b_\nu A^c_\mu A^d_\nu + Z_2 \, \bar{q} \big(-\partial\!\!\!/ + Z_m m \big) q - Z_{1F} \, ig \, \bar{q} \gamma_\mu t^a q \, A^a_\mu \, .\end{aligned} \tag{4.1}$$

Employing the usual notation for the quark, gluon and ghost fields and using the notation ξ for the gauge parameter, this equation defines all multiplicative renormalisation constants. In the partiton function of course the source terms

$$A^a_\mu j^a_\mu + \overline{\eta} q + \overline{q} \eta + \overline{\sigma} c + \overline{c} \sigma \tag{4.2}$$

[1] Appropriately we use the conventions in A.2 .

are added to (4.1). We denote the generating functional for the connected Green's functions by W. A functional Legendre transform leads to the generating functional for the one-particle irreducible vertex functions, which we denote by Γ. The operators

$$\frac{\delta}{\delta(\overline{q},\overline{\eta})} \tag{4.3}$$

denote left derivatives and

$$\frac{\delta}{\delta(q,\eta)} \tag{4.4}$$

right ones.

The derivation of the quark Dyson-Schwinger equation is similar to the one of the ghost equation [Fis03]. The integral of a total derivative vanishes, therefore we have

$$\begin{aligned} 0 = \int \mathcal{D}\overline{q}\ \exp\{-S_{\mathrm{QCD}}[q,\overline{q},A,c,\overline{c}] + A^a_\mu j^a_\mu + \overline{\eta}q + \overline{q}\eta + \overline{\sigma}c + \overline{c}\sigma\}\cdot \\ \left(\frac{\delta}{\delta\overline{q}(x)} S_{\mathrm{QCD}}[q,\overline{q},A,c,\overline{c}] - \eta(x)\right) \\ =: \left\langle \left(\frac{\delta}{\delta\overline{q}(x)} S_{\mathrm{QCD}}[q,\overline{q},A,c,\overline{c}] - \eta(x)\right)\right\rangle\ . \end{aligned} \tag{4.5}$$

This can be cast into

$$\left(-\frac{\delta S_{\mathrm{QCD}}}{\delta\overline{q}(x)}\left[\frac{\delta}{\delta\overline{\eta}},\frac{\delta}{\delta\eta},\frac{\delta}{\delta j},\frac{\delta}{\delta\overline{\sigma}},\frac{\delta}{\delta\sigma}\right] + \eta(x)\right) Z[\overline{\eta},\eta,j,\overline{\sigma},\sigma] = 0\ . \tag{4.6}$$

Applying another derivative $\frac{\delta}{\delta\eta(y)}$ to this equation yields

$$\left\langle \frac{\delta S_{\mathrm{QCD}}}{\delta\overline{q}(x)}\overline{q}(y)\right\rangle = \mathbb{1}\delta^4\ (x-y)\ . \tag{4.7}$$

Calculating the vacuum expectation value results in

$$\begin{aligned} Z_2\left(-\partial\!\!\!/ + Z_m m\right) S(x-y) - Z_{1F}\, ig \int d^4z d^4z'\, \delta^4(x-z)\,\delta^4(x-z')\cdot \\ (\gamma_\mu t^a)\big\langle\, q(z)\,\bar{q}(y)\,A^a_\mu(z')\,\big\rangle = \mathbb{1}\delta^4\ (x-y)\ . \end{aligned} \tag{4.8}$$

In the covariant formalism full and connected 3-point functions are equivalent, and we thus obtain

$$\big\langle\, q(z)\,\bar{q}(y)\,A^a_\mu(z')\,\big\rangle = \big\langle\, q(z)\,\bar{q}(y)\,A^a_\mu(z')\,\big\rangle_{\mathrm{conn.}} = \frac{\delta^3 W}{\delta\overline{\eta}(z)\delta\eta(y)\delta j^a_\mu(z')}\ . \tag{4.9}$$

We are aiming to express this in terms of 2-point functions and the quark-gluon vertex. To this end we observe that

$$\frac{\delta W}{\delta\eta} = \overline{q} \qquad\qquad \frac{\delta W}{\delta\overline{\eta}} = q \tag{4.10}$$

$$\frac{\delta\Gamma}{\delta q} = \overline{\eta} \qquad\qquad \frac{\delta\Gamma}{\delta\overline{q}} = \eta\ , \tag{4.11}$$

which leads to the identity

$$\begin{aligned}\delta(x-y) &= \int d^4z \; \frac{\delta\overline{\eta}(y)}{\delta\overline{q}(z)} \; \frac{\delta\overline{q}(z)}{\delta\overline{\eta}(x)} \\ &= \int d^4z \frac{\delta^2\Gamma}{\delta\overline{q}(z)\delta q(y)} \frac{\delta^2 W}{\delta\overline{\eta}(x)\delta\eta(z)} \; . \end{aligned} \tag{4.12}$$

Together with the matrix relation

$$\frac{\delta\chi^{-1}}{\delta A} = -\chi^{-1}\frac{\delta\chi}{\delta A}\chi^{-1} \tag{4.13}$$

we can rephrase (4.9) in the following way:

$$\frac{\delta^3 W}{\delta\overline{\eta}(z)\delta\eta(y)\delta j^a_\mu(z')} = \frac{\delta}{\delta j^a_\mu}\left[\frac{\delta^2\Gamma}{\delta\overline{q}(z)\delta q(y)}\right]^{-1} \tag{4.14}$$

$$= \int d^4u_1 \frac{\delta A^d_\nu(u_1)}{\delta j^a_\mu(z')} \frac{\delta}{\delta A^d_\nu(u_1)}\left[\frac{\delta^2\Gamma}{\delta\overline{q}(z)\delta q(y)}\right]^{-1} \tag{4.15}$$

$$= -\int d^4u_1 d^4u_2 d^4u_3 \frac{\delta^2 W}{\delta j^a_\mu(z')\delta j^d_\nu(u_1)} \frac{\delta^2 W}{\delta\overline{\eta}(y)\delta\eta(u_2)} \frac{\delta^3\Gamma}{\delta A^d_\nu(u_1)\delta\overline{q}(u_2)\delta q(u_3)} \frac{\delta^2 W}{\delta\overline{\eta}(u_3)\delta\eta(z)} \tag{4.16}$$

$$= \int d^4u_1 d^4u_2 d^4u_3 D^{ad}_{\mu\nu}(z'-u_1)S(u_2-y)\Gamma^d_\nu(u_1,u_2,u_3)S(z-u_3) \; . \tag{4.17}$$

Performing a Fourier transform and using the colour structure of the quark-gluon vertex, which is [AS01]

$$\Gamma^a_\mu(k,q,p) = -igt^a(2\pi)^4\delta^4(k+q-p)\Gamma_\mu(q,p) \; , \tag{4.18}$$

we arrive at the quark Dyson-Schwinger equation in a linear covariant gauge:

$$S^{-1}(p) = Z_2 S_0^{-1}(p) + \frac{g^2}{16\pi^4} Z_{1F} C_F \int d^4q \; \gamma_\mu S(q)\Gamma_\nu(q,k)D_{\mu\nu}(k) \; . \tag{4.19}$$

The equation is represented conveniently in a graphical way (figure 4.1). In the next section we derive a version of the renormalised gap equation in Coulomb gauge, which is of an analogous structure.

4.2 The gap equation in Coulomb gauge

For a realistic potential these equations are UV divergent and have to be renormalised.

Looking at the theory of superconductivity, the gap equation is part of a more general system of equations for the electron propagator and the electron-photon vertex, in which the Ward identity is satisfied [Sch]. Therefore it seems natural concerning the quark DSE to proceed in an analogous fashion, using the Ward identities to derive the renormalised

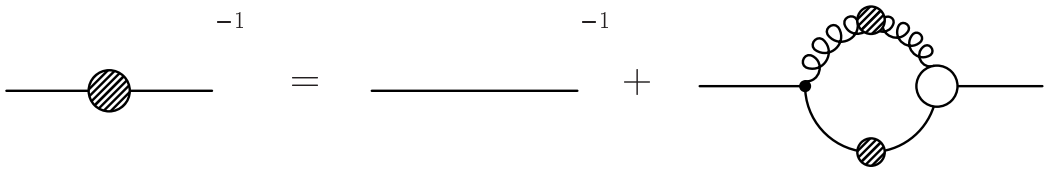

Figure 4.1: Diagrammatical representation of the quark Dyson-Schwinger equation. On the left hand side we have the inverse dressed quark propagator. The diagrams on the right hand side symbolise the inverse bare propagator and a dressing loop containing dressed quark and gluon propagators and one bare and one dressed quark-gluon vertex.(Adapted from reference [Fis06])

gap equation from suitable approximations to the vertex parts. Hence we start from the renormalised Dyson equation for the vector and axial-vector vertices, making the ladder approximation that the Bethe-Salpeter kernel depends only on the momentum transfer. Consistent with this approximation, we exclude quark annihilation graphs, so that there are no anomalies. Furthermore we neglect terms arising from the non-commutativity of colour matrices on the quark lines, which implies that we can use the Ward identities of QED rather than the more complicated Slavnov-Taylor identities of QCD and can omit all colour indices.

The starting points of our analysis are therefore the following equations for the renormalised vector, axial-vector and pseudoscalar vertex functions[2] [BD]

$$\begin{aligned}
\Gamma_\mu(p',p) &= Z_{(\mu)}\gamma_\mu + \int \frac{d^4q}{(2\pi)^4}[S(p'+q)\Gamma_\mu(p'+q,p+q)S(p+q)]\cdot \\
&\qquad K(p+q,p'+q,q)\ , \\
\Gamma_{\mu 5}(p',p) &= Z_{(\mu)5}\gamma_\mu\gamma_5 + \int \frac{d^4q}{(2\pi)^4}[S(p'+q)\Gamma_{\mu 5}(p'+q,p+q)S(p+q)]\cdot \\
&\qquad K(p+q,p'+q,q)\ , \\
\Gamma_5(p',p) &= Z_5\gamma_5 + \int \frac{d^4q}{(2\pi)^4}[S(p'+q)\Gamma_5(p'+q,p+q)S(p+q)]\cdot \\
&\qquad K(p+q,p'+q,q)\ .
\end{aligned} \tag{4.20}$$

Here $K(p,p',q)$ is the quark-antiquark Bethe-Salpeter kernel. In QCD the renormalisation constants $Z_{(\mu)}$ and $Z_{(\mu)5}$ are identical. If one employs only the zero-zero component of the gluon propagator, this is not the case. The inclusion of retarded transverse gluons cures this problem [Adl86]. In the absence of an axial U(1) anomaly, the vertex functions are

[2]For the rest of this chapter we use Minkowski space and employ the conventions A.1

related to the quark propagator by the non-anomalous Ward identities for the vector and axial vector currents [Adl69, BD, IZ]

$$\begin{aligned}(p'-p)^\mu\Gamma_\mu(p',p) &= iS^{-1}(p') - iS^{-1}(p) \ , \\ (p'-p)^\mu\Gamma_{\mu 5}(p',p) &= \gamma_5 iS^{-1}(p) + iS^{-1}(p')\gamma_5 + 2m\Gamma_5(p',p) \ . \end{aligned} \tag{4.21}$$

In order to derive the renormalised version of the gap equation we make the ladder approximation to the Bethe-Salpeter kernel

$$K(p+q,p'+q,q) \approx k(q) \ . \tag{4.22}$$

In lower order perturbation theory $k(q)$ is given by

$$k(q) = -iC_f g^2 \gamma_\mu \otimes \gamma_\nu D^{\mu\nu}(q) \ , \tag{4.23}$$

which means that in the case of keeping only the time-time component in the instantaneous approximation we are left with

$$k(q) = k(\mathbf{q}) = -4\pi C_f \gamma_0 \otimes \gamma_0 V_C(\mathbf{q}) \ , \tag{4.24}$$

where V_C is the famous colour Coulomb potential. We point out that in the ladder approximation, which is exclusively used in this work, $k(q)$ does not contain any quark propagators, and therefore there are no quark loops generated when we insert it in (4.20). Applying the equations (4.20) and (4.21) yields

$$\begin{aligned}(p'-p)^\mu\Gamma_{\mu 5}(p',p) &= \gamma_5 iS^{-1}(p) + iS^{-1}(p')\gamma_5 + 2m\Gamma_5(p',p) \\ &= Z_{(\mu)5}\gamma_\mu\gamma_5(p'-p)^\mu + \int \frac{d^4q}{(2\pi)^4}(S(p'+q)[\gamma_5 iS^{-1}(p+q) \\ &\quad + iS^{-1}(p'+q)\gamma_5 + 2m\Gamma_5(p'+q,p+q)]S(p+q))k(q) \\ &= \gamma_5\left(Z_{(\mu)5}\gamma_\mu p^\mu - Z_5 m + \int \frac{d^4q}{(2\pi)^4}S(p+q)k(q)\right) \\ &\quad + \left(Z_{(\mu)5}\gamma_\mu p'^\mu - Z_5 m + \int \frac{d^4q}{(2\pi)^4}S(p'+q)k(q)\right)\gamma_5 \\ &\quad 2m\Gamma_5(p',p) \ . \end{aligned} \tag{4.25}$$

It has to be stressed that the vector character of the renormalised quark propagator therefore satisfies the equation

$$iS^{-1}(p) = Z_{(\mu)5}\gamma_5 p^\mu - Z_5 m + \int \frac{d^4q}{(2\pi)^4}S(p+q)k(q) \ . \tag{4.26}$$

Using (4.23) this can be cast into

$$\Sigma(p) = (Z_{(\mu)} - 1)\gamma_\mu p^\mu - (Z_5 - 1)m + iC_F \int \frac{d^4q}{(2\pi)^4}\; g^2 \gamma_\mu S(q) \gamma_\nu D^{\mu\nu}(p-q)\;, \tag{4.27}$$

where Σ is the quark self energy and $C_f = \frac{4}{3}$. This equation is formally the same as (4.19) up to the bare quark-gluon vertex and constants.

4.3 Considerations without transverse gluons

Neglecting the transverse components of the gluon propagator we employ the parametrisation

$$S^{-1}(p) = -i \cdot (\gamma_0 p_0 \cdot A(|\mathbf{p}|) - \boldsymbol{\gamma} \cdot \mathbf{p}\; C(|\mathbf{p}|) - B(|\mathbf{p}|) + i\epsilon) \tag{4.28}$$

for the quark propagator. With the instantaneous approximation for the time-time component of the gluon propagator,

$$D^{00}(\mathbf{x}, t) = V_C(\mathbf{x}) \cdot \delta(t) \tag{4.29}$$

we can extract the following integral equations for the quark propagator functions by taking appropriate traces:

$$B(|\mathbf{p}|) = Z_5 m - \frac{C_F}{(2\pi)^3} \int dq_0 \int_0^\infty d|\mathbf{q}| \cdot |\mathbf{q}|^2 \int_{-1}^{1} d(\cos\theta) \cdot \\ 4\pi V_C(|\mathbf{k}|) \frac{B(|\mathbf{q}|)}{q_0^2 - |\mathbf{q}|^2 C^2(|\mathbf{q}|) - B^2(|\mathbf{q}|)} \tag{4.30}$$

$$C(|\mathbf{p}|) = Z_{(\mu)} - \frac{C_F}{|\mathbf{p}|(2\pi)^3} \int dq_0 \int_0^\infty d|\mathbf{q}| \cdot |\mathbf{q}|^3 \int_{-1}^{1} d(\cos\theta) \cdot \\ 4\pi V_C(|\mathbf{k}|) \cos\theta \frac{C(|\mathbf{q}|)}{q_0^2 - |\mathbf{q}|^2 C^2(|\mathbf{q}|) - B^2(|\mathbf{q}|)}\;. \tag{4.31}$$

It turns out that the A-function is identically 1. The only remaining unknown in (4.30) and (4.31) is now the colour Coulomb potential V_C. Its large momentum behaviour is constrained by perturbation theory, since the relation

$$V_C(\mathbf{p}) = \frac{\alpha(|\mathbf{p}|)}{\mathbf{p}^2} \tag{4.32}$$

holds ($\alpha(|\mathbf{p}|)$ is the running coupling). From lattice calculations we can infer the large distance behaviour [NS06], cf. sections 3.3 and 3.6.4. An analytic ansatz, which obeys both limiting behaviours and which we will employ, is the Richardson potential [Ric79]

$$V_C(\mathbf{q}) = \frac{12\pi}{(11N_c - 2N_f) \cdot \ln(1 + \mathbf{q}^2/\Lambda^2)} \ . \tag{4.33}$$

N_f and N_c are the number of colours and the number of flavours respectively. Here we use the values $N_f = 3$ and $N_c = 3$. Λ is a parameter which we can calculate from the string tension of lattice calculations by expanding V_C for large momenta. Defining the quark mass function as motivated in section 2.2 as the ratio

$$M(|\mathbf{p}|) := \frac{B(|\mathbf{p}|)}{C(|\mathbf{p}|)} \tag{4.34}$$

and performing the q_0-integral analytically we are able to express the equations (4.30) and (4.31) as a single integral equation

$$M(|\mathbf{p}|) = \frac{Z_5 m + \frac{2C_1}{3\pi} \int_0^\infty dq\ q^2 \frac{M(|\mathbf{q}|)}{\sqrt{M^2(|\mathbf{q}|)+\mathbf{q}^2}} \int_{-1}^1 d(\cos\theta) \frac{1}{|\mathbf{p}-\mathbf{q}|^2} \cdot \frac{1}{\ln(1+|\mathbf{p}-\mathbf{q}|^2/\Lambda^2)}}{Z_{(\mu)} + \frac{2C_1}{3\pi} \int_0^\infty dq\ q^2 \frac{|\mathbf{q}|}{|\mathbf{p}|\sqrt{M^2(|\mathbf{q}|)+\mathbf{q}^2}} \int_{-1}^1 d(\cos\theta) \frac{\cos\theta}{|\mathbf{p}-\mathbf{q}|^2} \cdot \frac{1}{\ln(1+|\mathbf{p}-\mathbf{q}|^2/\Lambda^2)}} \ , \tag{4.35}$$

where θ is the angle between $\mathbf{p}$ and $\mathbf{q}$ and the abbreviation $C_1 = \frac{12\pi}{(11N_c-2N_f)}$ was used. Because the integral equation is singular at $\mathbf{p} = \mathbf{q}$ we introduce a regulator μ_{IR} by using the substitution

$$|\mathbf{p} - \mathbf{q}|^2 \ \rightarrow \ |\mathbf{p} - \mathbf{q}|^2 + \mu_{\mathrm{IR}}^2 \tag{4.36}$$

for all terms in question. In order to calculate the solution for (4.35) we have to solve the equation for non-vanishing μ_{IR} and take the limit $\mu_{\mathrm{IR}} \rightarrow 0$. An analytic proof for the convergence of such a regularisation was already given in [Alk88]. Furthermore we observe, that both momentum integrals in (4.35) are divergent in the ultraviolet. The equation obviously has to be renormalised and in doing so we choose a MOM scheme and impose the conditions

$$B(|\boldsymbol{\nu}|) = m \tag{4.37}$$

$$C(|\boldsymbol{\nu}|) = 1 \ , \tag{4.38}$$

where $|\boldsymbol{\nu}|$ is the renormalisation point.

4.4 Numerical results

In figure 4.2 we display the results for the mass function in the chiral limit employing only the time-time component of the gluon propagator. As a renormalisation point we choose

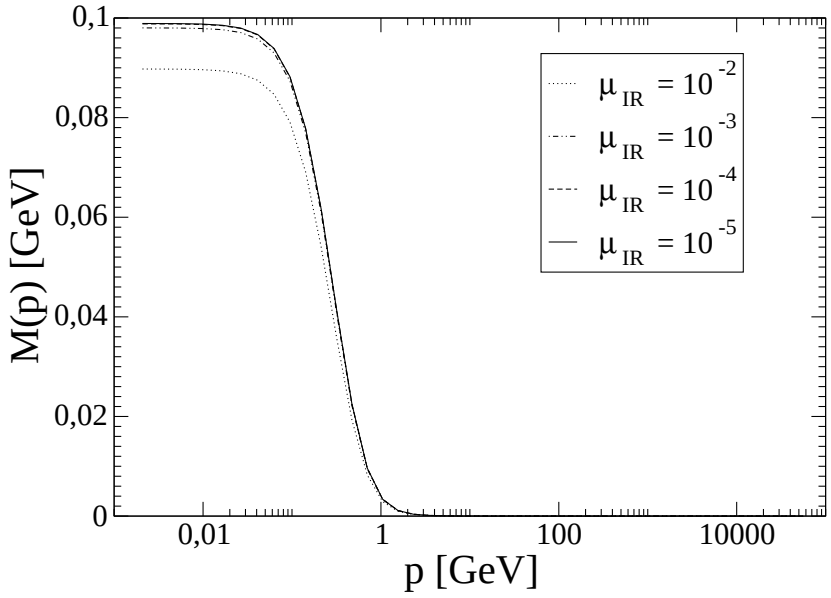

Figure 4.2: Shown are the mass functions in the chiral limit calculated with the rainbow truncation, a bare quark-gluon vertex and without transverse gluons. The results are converging in the limit of a vanishing infrared regulator μ_{IR}.

$|\boldsymbol{\nu}| = 45000\,\mathrm{GeV}$. We checked that the result stays stable if the renormalisation point is increased a few orders of magnitude. It was not possible to obtain a converging result with non-zero current quark mass. The value of the mass function in the deep infrared serves as a measure for the constituent quark mass as usual. With the string tension $\sigma_c = 0.5476\,\mathrm{GeV}^2$ taken from [NS06] we arrive at about a third of the desired value. In order to work on this handicap we seek to improve the level of sophistication with which we treat the gluon propagator in our computations. This is done in the following section by taking into account the transverse components of the gluon propagator in connection with retardation. We keep in mind that the infrared analysis for the quark-gluon vertex carried out in Landau gauge [AFLE06], which showed an infrared divergence, can be analogously performed in Coulomb gauge. This indicates that we have to expect an important contribution from a dressing of the quark-gluon vertex. However, these computations are tedious and even a one-loop calculation awaits completion [Lic].

4.5 Adding transverse gluons and retardation

In this section we improve the approximations, which led to (4.35), in two respects. We add transverse components of the gluon propagator and overcome the instantaneous approximation by taking into account retardation for these components. Explicitly we employ

$$D^{ij}(k_0, |\mathbf{k}|) = \frac{1}{g^2} \cdot \left(\delta^{ij} - \frac{k^i k^j}{\mathbf{k}^2}\right) \cdot \frac{-iZ(k_0, \mathbf{k})}{k_0^2 - \omega_g^2(|\mathbf{k}|) + i\epsilon} \ , \tag{4.39}$$

where for simplicity in this exploratory calculation we choose $Z(k_0, \mathbf{k}) = 1$, and the function ω_g is adjusted to calculations in the Hamiltonian approach [FR04b],

$$\omega_g(|\mathbf{k}|) = \frac{\Lambda^2}{|\mathbf{k}|} + |\mathbf{k}| \ , \tag{4.40}$$

where Λ is the same parameter as in the Richardson potential. This ansatz is furthermore in accordance with lattice calculations for the transverse equal-time gluon propagator [CZ02a]. In the present approximation the simple ansatz in equation (4.28) for the quark propagator has to be extended,

$$S^{-1}(p) = -i \cdot (\gamma_0 p_0 \cdot A(p_0, |\mathbf{p}|) - \boldsymbol{\gamma} \cdot \mathbf{p}\ C(p_0, |\mathbf{p}|) - B(p_0, |\mathbf{p}|) + i\epsilon) \ . \tag{4.41}$$

Solving the gap equation for the propagator functions and performing a Wick rotation

$$p_0 \to i p_E \ , \ \int dq_0 \to \int dq_E\ i \ , \ q_0 \to i q_E \quad , \tag{4.42}$$

yields (we define $k := p - q$ and $k_E := p_E - q_E$):

$$\begin{aligned} p_E A(p_E, |\mathbf{p}|) = Z_{(\mu)} p_E + \frac{C_F}{(2\pi)^3} \int dq_E \int_0^\infty d|\mathbf{q}| \cdot |\mathbf{q}|^2 \int_{-1}^{1} d(\cos\theta) \\ \left[4\pi V_C(|\mathbf{k}|) + \frac{2Z(k_E, \mathbf{k})}{-k_E^2 - \omega_g^2(\mathbf{k})}\right] \frac{q_E A(q_E, |\mathbf{q}|)}{\mathrm{denom}(q_E, |\mathbf{q}|)} \end{aligned} \tag{4.43}$$

$$\begin{aligned} B(p_E, |\mathbf{p}|) = Z_5 m - \frac{C_F}{(2\pi)^3} \int dq_E \int_0^\infty d|\mathbf{q}| \cdot |\mathbf{q}|^2 \int_{-1}^{1} d(\cos\theta) \\ \left[4\pi V_C(|\mathbf{k}|) - \frac{2Z(k_E, \mathbf{k})}{-k_E^2 - \omega_g^2(\mathbf{k})}\right] \frac{B(q_E, |\mathbf{q}|)}{\mathrm{denom}(q_E, |\mathbf{q}|)} \end{aligned} \tag{4.44}$$

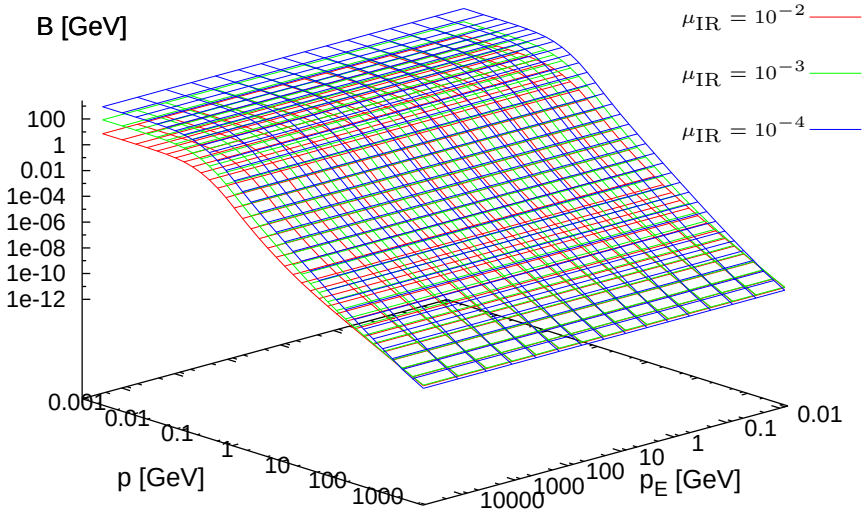

Figure 4.3: Shown are the propagator functions $B(p_E, |\mathbf{p}| = p)$ depending on μ_{IR} in the chiral limit calculated with the rainbow truncation employing a bare quark-gluon vertex and transverse gluons including retardation. They diverge with vanishing infrared regulator μ_{IR}.

$$C(p_E, |\mathbf{p}|) = Z_{(\mu)} - \frac{C_F}{|\mathbf{p}|(2\pi)^3} \int dq_E \int_0^\infty d|\mathbf{q}| \cdot |\mathbf{q}|^3 \int_{-1}^{1} d(\cos\theta)$$
$$\left[4\pi V_C(|\mathbf{k}|) \cos\theta + \frac{Z(k_E, \mathbf{k})}{-k_E^2 - \omega_g^2(\mathbf{k})} \left(-\cos\theta - \frac{-2|\mathbf{p}||\mathbf{q}| + \cos\theta \, (|\mathbf{p}|^2 + |\mathbf{q}|^2)}{|\mathbf{p}|^2 + |\mathbf{q}|^2 - 2|\mathbf{p}||\mathbf{q}|\cos\theta} \right) \right] \frac{C(q_E, |\mathbf{q}|)}{\text{denom}(q_E, |\mathbf{q}|)} \, . \tag{4.45}$$

Thereby we made the abbreviation

$$\text{denom}(q_E, |\mathbf{q}|) := -q_E^2 A^2(q_E, |\mathbf{q}|) - |\mathbf{q}|^2 C^2(q_E, |\mathbf{q}|) - B^2(q_E, |\mathbf{q}|) \quad .$$

Again all involved integrals diverge. For renormalisation we use as in the case without transverse gluons a MOM-scheme by imposing

$$S(\nu_E, \boldsymbol{\nu}) \stackrel{!}{=} S_0(\nu_E, \boldsymbol{\nu}) \tag{4.46}$$

for some renormalisation point $(\nu_E, \boldsymbol{\nu})$.

4.6 Numerical results

A description of the numerical methods can be found in appendix C. Parts of it apply also to calculations in the sections 4.3 and 5. All presented results are in the chiral limit. For the Coulomb string tension we employ the value as in section 4.4, namely $\sigma_c = 0.5476\,\mathrm{GeV}^2$. For non-vanishing current quark mass no converging result could be obtained. Figure 4.3 displays the propagator function $B(p_E, |\mathbf{p}|)$ in dependence of the infrared regulator. As already experienced in our calculation with the time-time component of the gluon propagator only we observe a diverging behaviour. The same is true for the propagator function $C(p_E, |\mathbf{p}|)$. The third propagator function $A(p_E, |\mathbf{p}|)$ deviates only very slightly from its value when only the time-time components of the gluon propagator is kept. This already hints that the changes in the mass function are not sizeable. Indeed in the computed result, illustrated in the figures 4.5 and 4.6, no considerable increase in the mass function compared to the case without transverse gluons and retardation is obtained. Also for all displayed functions we have a variation in the frequency coordinate p_E only up to the numerical accuracy. The p-axis is for all presented functions a symmetry axis. As a renormalisation point we choose $(\nu_E, |\boldsymbol{\nu}|) = (20000\mathrm{GeV}, 45000\mathrm{GeV})$. As in section 4.4 the results do not vary while increasing the renormalisation point a few orders of magnitude.

An increase of the factor Z in the equations (4.43)-(4.45) on the percentage level increases the mass function slightly but has no impact on the frequency dependence.

Evidently with the current results for the quark Dyson-Schwinger equation a realistic calculation and description of observables is not possible. Further progress in this direction has to come from a more realistic version of the quark-gluon vertex.

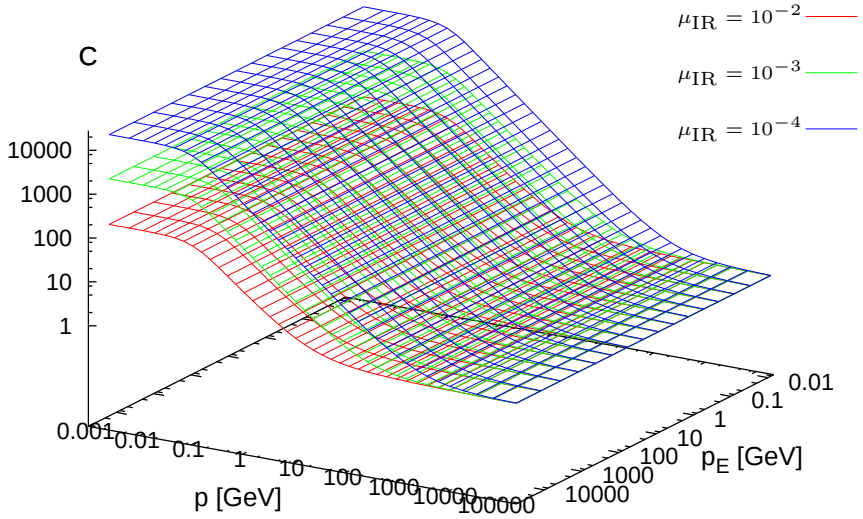

Figure 4.4: Analogous to figure 4.3 for the $C(p_E, |\mathbf{p}| = p)$-function.

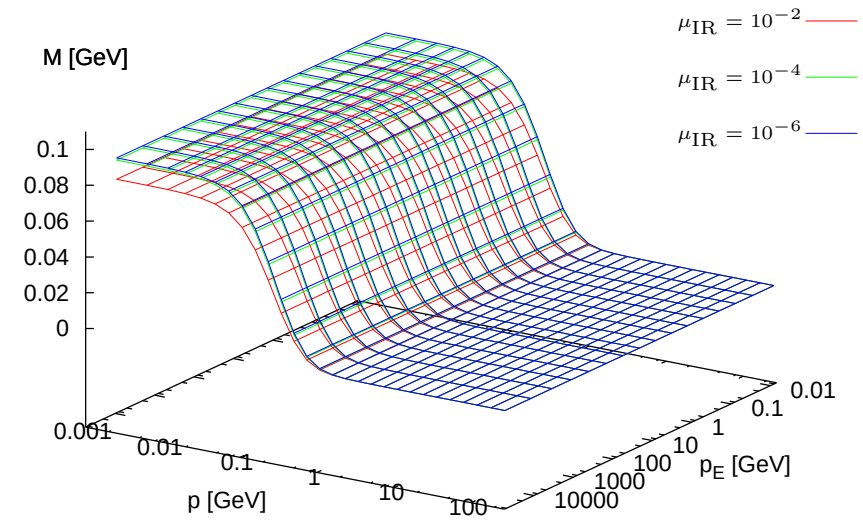

Figure 4.5: Plot Analogous to figure 4.3. The shown mass function $M(p_E, |\mathbf{p}| = p)$ converges with decreasing infrared regulator.

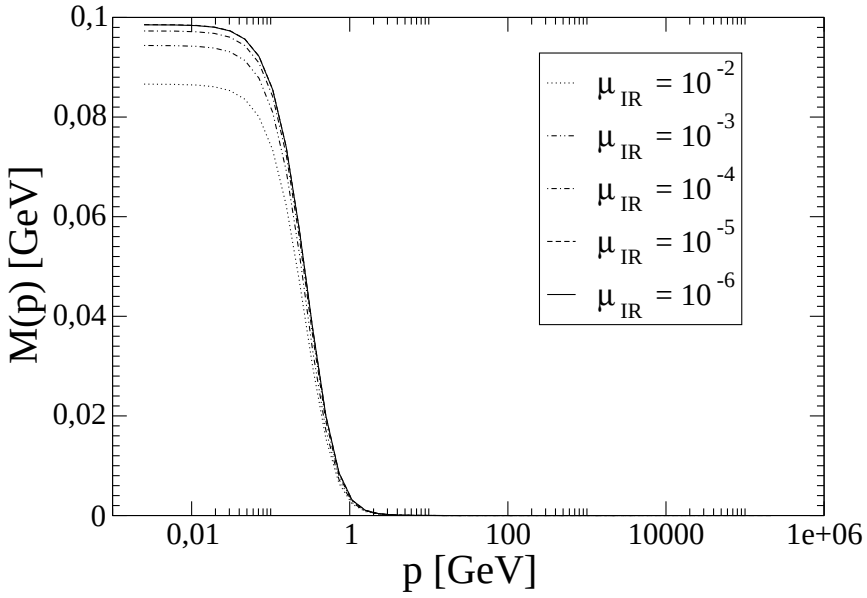

Figure 4.6: Like figure 4.5 but with suppressed frequency coordinate p_E.

Chapter 5

Meson Observables, Diquark Confinement and Radii

In the preceding section we have seen, that at the solution of the gap equation in Coulomb gauge is not sufficient in order to calculate observables in a quantitative satisfactory manner. In this section we therefore aim for qualitative results and employ the solution of the gap equation without transverse gluons and retardation using in the time-time component of the gluon propagator the colour Coulomb potential

$$V_C(\mathbf{k}) = \frac{3/2\ \sigma_c}{\mathbf{k}^4}\ . \tag{5.1}$$

The presented results were published in [AKKW06].

Obviously, also in this case $V_C(\mathbf{k})$ is infrared singular. It is regulated by a parameter $\mu_{\rm IR}$ such that the momentum dependence is modified to

$$V_C(\mathbf{k}) = \frac{3/2\ \sigma_c}{(\mathbf{k}^2)^2} \to \frac{3/2\ \sigma_c}{(\mathbf{k}^2+\mu_{\rm IR}^2)^2}\ . \tag{5.2}$$

In this fashion all quantities and observables become $\mu_{\rm IR}$ dependent and one obtains the final result for some $f(\mu_{\rm IR})$ by taking the limit $f = \lim_{\mu_{\rm IR}\to 0} f(\mu_{\rm IR})$. The result for the mass function is displayed in figure 5 in appropriate units of the Coulomb string tension σ_c.

We employ the Bethe-Salpeter equation in the ladder approximation for meson and diquarks. The appropriate 4-point Green's function fulfils[1]

$$G_{\alpha\beta\gamma\delta}(k,p',p) = k_{\alpha\beta\gamma\delta}(p'-p) + i\int \frac{d^4q}{(2\pi)^4} G_{\tau\xi\gamma\delta}(k,p',q) S_{\xi\sigma}\left(q+\frac{k}{2}\right) S_{\rho\tau}\left(q-\frac{k}{2}\right) k_{\alpha\beta\rho\sigma}(p-q)\ . \tag{5.3}$$

[1]This chapter applies the Minkowski space conventions A.1 .

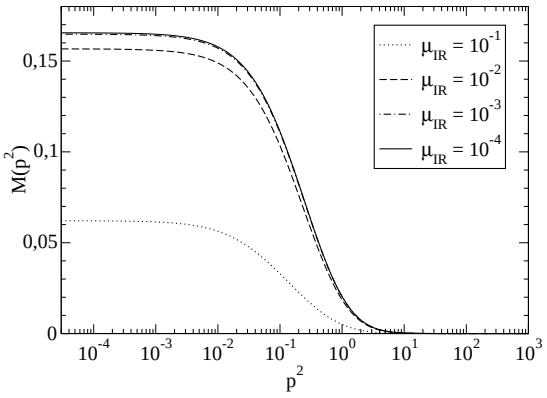

Figure 5.1: The quark mass function $M(p^2)$ for four values of the infrared regulator $\mu_{\rm IR}$. All quantities are given in appropriate units of $\sqrt{\sigma_c}$.

For $G_{\alpha\beta\gamma\delta}$ of the pion we make the ansatz

$$G_{\alpha\beta\gamma\delta}(k,p',p) = \Gamma_{\alpha\beta}\left(p+\frac{k}{2},p-\frac{k}{2}\right)\frac{1}{k^2-m_\pi^2}\Gamma_{\gamma\delta}\left(p'-\frac{k}{2},p'+\frac{k}{2}\right)+\ldots \quad , \tag{5.4}$$

where terms, which are finite on the mass shell, were omitted. Taking only the time-time component of the gluon propagator in the Bethe-Salpeter kernel (4.24) into account, we attain the following BSE at $k^2=m_\pi^2$ for the pion vertex function:

$$\Gamma\left(p+\frac{k}{2},p-\frac{k}{2}\right) = C_f\int\frac{d^4q}{(2\pi)^4}g^2(p-q)\gamma_0 S\left(q+\frac{k}{2}\right)\Gamma\left(q+\frac{k}{2},q-\frac{k}{2}\right)\cdot \\ S\left(q-\frac{k}{2}\right)\gamma_0 D^{00}(p-q)\ . \tag{5.5}$$

Exemplarily we examine the pseudoscalar meson state in greater detail. To simplify this expression, we consider a pion at rest, i.e. choose $k=(m_\pi,0)$. In the instantaneous approximation the pion vertex depends only on the three-momentum, $\Gamma(p+\frac{k}{2},p-\frac{k}{2}) = \Gamma(p,m_\pi)=\Gamma(\mathbf{p},m_\pi)$. Expanding the pion vertex function,

$$\Gamma(\mathbf{p},m_\pi) = \Gamma_p(|\mathbf{p}|)\gamma_5 + m_\pi\Gamma_A(|\mathbf{p}|)\gamma_0\gamma_5 + m_\pi\Gamma_T(|\mathbf{p}|)(\hat{\mathbf{p}}\boldsymbol{\gamma})\gamma_0\gamma_5 \tag{5.6}$$

we obtain three coupled integral equations for Γ_p, Γ_A and Γ_T. For a confining potential these quantities also diverge. We therefore introduce

$$h(|\mathbf{p}|) = \frac{P_p(|\mathbf{p}|)}{\omega(|\mathbf{p}|)} \tag{5.7}$$

and

$$g(|\mathbf{p}|) = \frac{\Gamma_p(|\mathbf{p}|)+2[m(|\mathbf{p}|)+|\mathbf{p}|A(|\mathbf{p}|)]\Gamma_A(|\mathbf{p}|)+2[|\mathbf{p}|+|\mathbf{p}|B(|\mathbf{p}|)]\Gamma_T(|\mathbf{p}|)}{\omega^2(|\mathbf{p}|)-m_\pi^2/4}\ , \tag{5.8}$$

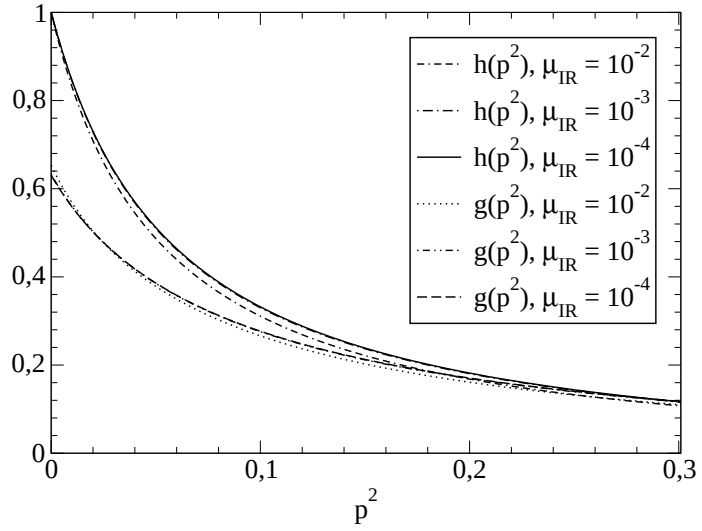

Figure 5.2: Pion Bethe-Salpeter amplitude components g and h as functions of the infrared regulator $\mu_{\rm IR}$. For convenience, the amplitudes are normalised such that $h(0) = 1$. All quantities are given in appropriate units of $\sqrt{\sigma_c}$.

where

$$\omega(|\mathbf{p}|) = \sqrt{[m + |\mathbf{p}|A(|\mathbf{p}|)]^2 + [|\mathbf{p}| + |\mathbf{p}|B(|\mathbf{p}|)]^2} \ . \tag{5.9}$$

The functions $h(|\mathbf{p}|)$ and $g(|\mathbf{p}|)$ are finite and satisfy the coupled integral equations

$$\begin{aligned} h(|\mathbf{p}|)\omega(|\mathbf{p}|) &= \frac{1}{3\pi^2}\int d^3q V_C(k)\left[h(|\mathbf{q}|) + \frac{m_\pi^2}{4\omega(|\mathbf{q}|)}g(|\mathbf{q}|)\right] \\ g(|\mathbf{p}|)\left[\omega(|\mathbf{p}|) - \frac{m_\pi^2}{\omega(|\mathbf{p}|)}\right] &= h(|\mathbf{p}|)+ \\ &\quad \frac{1}{3\pi^2}\int d^3q \frac{V_C(|\mathbf{k}|)}{\tilde{\omega}(|\mathbf{p}|)\tilde{\omega}(|\mathbf{q}|)}\left(M(|\mathbf{p}|)M(|\mathbf{q}|) + (\hat{\mathbf{p}}\hat{\mathbf{q}})|\mathbf{p}||\mathbf{q}|\right)g(|\mathbf{q}|) \ , \end{aligned} \tag{5.10}$$

where we introduced

$$\tilde{\omega}(|\mathbf{p}|) = \sqrt{M^2(|\mathbf{p}|) + \mathbf{p}^2} \ . \tag{5.11}$$

For vector mesons (and correspondingly axial-vector diquarks) the Bethe-Salpeter vertex function has four linearly independent amplitudes. The construction of the four coupled integral equations corresponding to the BSE is analogous to the pseudoscalar case.

The homogeneous BSE in equation (5.5) can be solved by introducing an eigenvalue $\lambda(P^2 = M^2)$ with M the bound-state mass. One then finds M such that $\lambda = 1$ for mesons and $\lambda = 2$ for diquarks. The numerical solution of the BSEs can be performed as in [OVSA02].

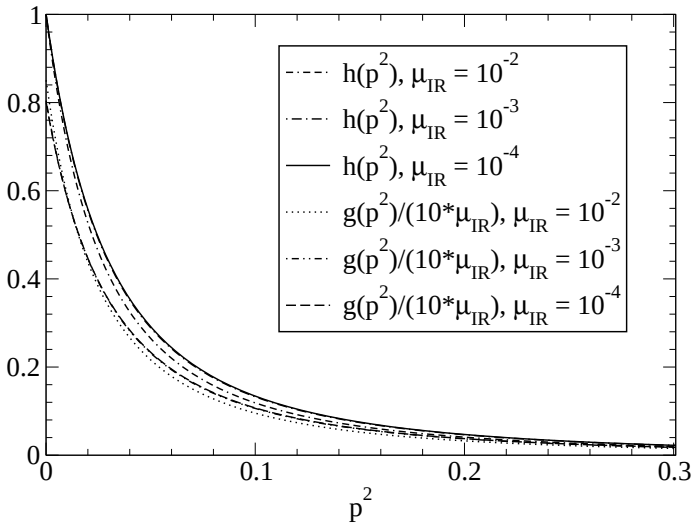

Figure 5.3: Same as fig. 5.2 for the scalar diquark.

We studie the Bethe-Salpeter amplitudes as $\mu_{\rm IR} \to 0$: the results for g and h of (5.10) are presented in figs. 5.2 and 5.3 for the pion and scalar diquark, respectively. For convenience, the normalisation of the amplitudes has been chosen such that $h(0) = 1$. We note, however, that IR-cancellations appearing in the pion case lead to a stable h as well as ratio of g/h, which is not the case (as one would naively expect) in the diquark case: there $g/h \sim \mu_{\rm IR} \to 0$ and $h \sim 1/\sqrt{\mu_{\rm IR}}$.

The curve for $\lambda(P^2)$ gets less inclined with smaller values of the infrared regulator $\mu_{\rm IR}$, and its intersection point with $\lambda = 1$ stabilises in the limit $\mu_{\rm IR} \to 0$. As a consequence, while the meson mass is stable, the mass eigenvalue for the corresponding diquark state (corresponding to $\lambda(M) = 2$) increases like $1/\mu_{\rm IR}$, ultimately completely removing these states from the physical spectrum. We have illustrated these effects in figure 5.4 for values of $10^{-4} \leq \mu_{\rm IR} \leq 10^{-2}$.

Possessing amplitudes we are in the position to compute charge radii. To this end we need to know the electromagnetic form factors for low momenta. The pion electromagnetic form factor $F_\pi(q^2)$ (analogously for the diquarks) is defined in terms of the electromagnetic vertex [GMW84, GMW83]

$$\langle \pi(p') | J_\mu(0) | \pi(p) \rangle = ieQ\ (p_\mu + p'_\mu) F_\pi(q^2)\ , \tag{5.12}$$

where J_μ the electromagnetic current, $Q = 0, \pm 1$ is the pion charge and $q = p' - p$. The form factor is normalised via

$$F_\pi(0) = 1\ , \tag{5.13}$$

which is the same as demanding the charge of the π^+ to be one. The mean square charge

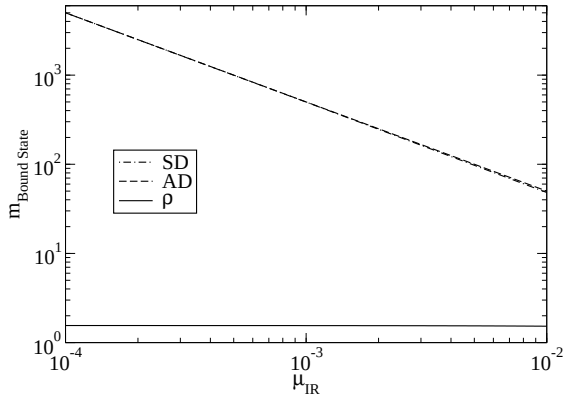

Figure 5.4: The masses of the ρ as well as the scalar (SD) and axial-vector (AD) diquarks as functions of the infrared regulator μ_{IR}. The mass of the π is identically zero for all values of μ_{IR} and therefore not shown in the graph. All quantities are given in appropriate units of $\sqrt{\sigma_c}$.

radius is then given as

$$\langle r^2 \rangle = 6 \frac{\partial F_\pi}{\partial q^2}(q^2 = 0) \ . \tag{5.14}$$

In order to calculate the pion form factor at non-zero momentum transfer we need to know the wave function of a moving pion. The integral equations (5.10) however give only the Bethe-Salpeter wave function for a pion at rest. In a covariant gauge a wave function expanded in covariants does not need any boost. However in our approach we have to boost the wave function. Since we are only interested in low momenta, a Galilean boost is sufficient.

Exemplarily for a π^+ one gets [GMW83]

$$\begin{aligned} F_\pi(-\mathbf{q}^2) = \frac{N_c}{\mathcal{N}^2 E} \int \frac{d^4k}{(2\pi)^4} \mathrm{tr}[& S\left(k_0 + \frac{E}{2}, \mathbf{k}\right) \Gamma\left(\mathbf{k} + \frac{\mathbf{q}}{4}, E\right) S\left(k_0 - \frac{E}{2}, \mathbf{k} + \frac{\mathbf{q}}{2}\right) \gamma_0 \\ & S\left(k_0 - \frac{E}{2}, \mathbf{k} - \frac{\mathbf{q}}{2}\right) \Gamma\left(\mathbf{k} - \frac{\mathbf{q}}{4}, -E\right)] \ , \end{aligned} \tag{5.15}$$

where $\mathcal{N}$ is the Bethe-Salpeter normalisation factor, which can be computed from the normalisation condition (5.13).

For both mesons *and* diquarks we get finite results for the charge radii in the limit $\mu_{\mathrm{IR}} \to 0$. Plots of these pion and scalar diquark radii are shown in figure 5.5. The results for vector-mesons and axial-vector-diquarks are analogous. Consequently though the diquarks are removed from the physical spectrum, which reflects confinement of coloured quark-quark correlations, their charge radii remain finite. Diquarks therefore possess a well-defined size, which adds to the motivation of nucleon studies in a covariant quark-diquark

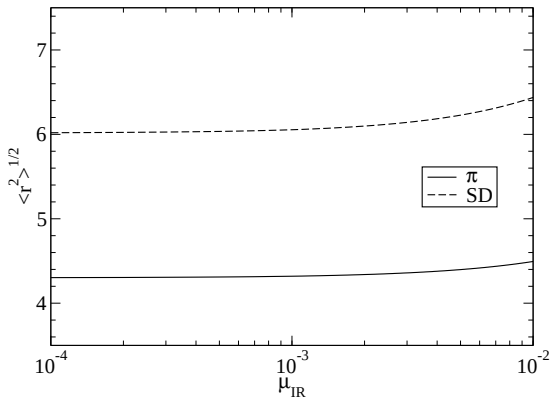

Figure 5.5: Charge radii for π meson as well as scalar diquark (SD) as functions of the infrared regulator μ_{IR}. All quantities are given in appropriate units of $\sqrt{\sigma_c}$.

picture, what is the topic of the following chapter.

Chapter 6

Nucleon Form Factors in a Covariant Diquark-Quark model

In chapter 5 we have seen that although diquarks are confined they can be assigned a finite radius, which suggests that a description of the nucleon using such degrees of freedom might be successful. In the present chapter we take this implication serious and treat at first the Faddeev equation of the nucleon in a diquark-quark approximation, which maintains Poincaré covariance, and use the results to calculate nucleon form factors in this framework. A detailed introduction in the model may be found in [Oet00]. The presented findings have been published in [AHK$^+$05, H$^+$05]. In contrast to the preceding sections we will employ Landau gauge for our calculations. The whole chapter uses Euclidean conventions, cf. A.2.

6.1 Introduction

Since QCD is a quite involved theory in the infrared sector a straightforward deduction of hadronic properties is not possible. To circumvent this difficulty models with a simplified dynamics have been employed in the past, which may contain beside QCD degrees of freedom such of the observable particle spectrum like pions. Three kinds of models were popular over the last decades (a discussion of these can be found in [TW]):

- *Non-relativistic quark models* assume, that baryons are built out of three massive constituent quarks localised in a potential. A success of this model is the simple description of the anomalous magnetic moments of the proton, the neutron and the hyperons. With a suitable quark-quark interaction also a large part of the baryon spectrum can be explained.

- *Bag models* imagine hadrons as colour singlett bag out of perturbative vacuum with relativistic quarks and gluons.

- *Soliton models* picture baryons as a localised lump of energy density, which consists of mesons. One ansatz is the topological soliton, where the baryon number is identified with a topological winding number, which is connected to the boundary conditions for the meson field configurations. An interesting variation are chiral solitons, which are non-linear interacting systems of quarks and pions.

Most of these models describe static and a few dynamic observables quite well on the usual twenty-percent scale of accuracy. However, none of these can be formulated in a covariant manner. A model with this feature could also succeed in the intermediate energy regime. Outstanding observables with an interesting behaviour on such energy scales are the electromagnetic form factors of the nucleon.

In order to understand the structure of the nucleon large experimental and theoretical effort is undertaken [TW]. An important branch is the exploration of the electromagnetic structure [ARZ06, PPV06]. Modern, high-luminosity experimental facilities that employ large momentum transfer reactions are providing remarkable and intriguing new information in this field [Gao03, BL04]. For an example one need only look so far as the discrepancy between the ratio of electromagnetic proton form factors extracted via Rosenbluth separation and that inferred from polarisation transfer. This discrepancy is marked for $Q^2 \gtrsim 2\,\mathrm{GeV}^2$ and grows with increasing Q^2. At such values of momentum transfer, $Q^2 > M^2$, where M is the nucleon's mass, a real understanding of these and other contemporary data require a Poincaré covariant description of the nucleon. This is apparent in applications of relativistic quantum mechanics, e.g. [B$^+$02].

In this chapter we introduce shortly such a model, which we gain by reducing the relativistic three-quark problem, and use it in order to calculate nucleon form factors. The formal setting for such a model was already clarified more than two decades ago [AT77, Glo83]. In the quantum field theory framework the few-body problem is somewhat ill-posed, since a rigorous treatment should take infinitely many degrees of freedom into account. However, the observed spectrum of mesons and baryons advises us that a good physical description is probably possible using the constituent quarks as degrees of freedom. Therefore we consider matrix elements of three quarks between the non-perturbative vacuum and a bound state with certain observable quantum numbers, which we call wave functions, in order to calculate observables (since the QCD vacuum is a non-trivial condensate it contains sea quarks and gluonic fractions). With this conditions the quantum mechanical formulation of the three-body problem can be adopted in the Green's functions formulation.

The starting point of the model is Dyson's equation for the full quark 6-point function G, in symbolic notation written as

$$G = G_0 + G_0 K G \ . \tag{6.1}$$

Here G_0 is the disconnected three-quark propagator and K is the three-quark scattering kernel that contains all two- and three-particle irreducible graphs. The calculation of the three-quark wave function can be simplified enormously by two assumptions:

- Neglect three body interactions, i.e. all 3-particle irreducible contributions to the full 3-quark correlation function.
- Assume that the 2-quark correlation functions can be approximated as a sum over separable[1] terms that are identified with diquark-quark vertex functions.

We detail on the second point in section 6.2. Reference [BCP89] reported a rudimentary study of this Faddeev equation and subsequently more sophisticated analyses have appeared. As already mentioned our approach is based on the one which was taken in reference [Oet00].

As pointed out in chapter 5 diquarks do not survive as asymptotic states, the attraction between quarks in this channel grounds a picture of baryons in which two quarks are always correlated as a colour-$\bar{3}$ diquark pseudoparticle, and binding is effected by the iterated exchange of roles between the bystander and diquark-participant quarks.

It has become apparent that the dominant correlations for ground state octet and decuplet baryons are scalar and axial-vector diquarks, primarily because the associated mass-scales are smaller than the masses of these baryons [Mar02] and the positive parity of the correlations matches that of the baryons. Both scalar and axial-vector diquarks provide attraction in the Faddeev equation; e.g., a scalar diquark alone provides for a bound octet baryon and including axial-vector correlations reduces that baryon's mass.

With the retention of axial-vector diquark correlations a quantitative description of baryon properties is attainable [OHAR98]. However, that possibility necessitates the incorporation of pseudoscalar meson loop contributions because a credible description of baryon properties is otherwise problematic. Such effects contribute materially: to baryon masses [H$^+$02, Tho84, YLTW01]; and charge and magnetic radii, and magnetic moments [HJLT00a, HJLT00b, LTY01].

In the following section we discuss the approximation for the two-quark correlation matrix. In 6.3 we introduce those aspects of the Poincaré covariant Faddeev equations

[1] Separability means that the two-quark correlation matrix is not supposed to contain products between the "ingoing" and "outgoing" momenta.

for the nucleon and Δ that are vital for our analysis, and present the solutions. Section 6.4 describes the formulation of a Ward-Takahashi identity preserving current that is appropriate to a nucleon represented by a solution of the Faddeev equation. With the necessary elements thus specified, the results for the nucleons' electromagnetic form factors are presented and discussed in section 6.5.

6.2 Two-quark correlations

In the preceding section we pointed out that by using the concept of diquarks we effectively assume the two-quark correlation matrix to be separable. As this approximation is mainly borrowed from the Nambu-Jona-Lasinio (NJL) model, we will describe how diquarks arise there and how the diquark-quark picture is realized in other models.

It is well-known that a separable two-quark correlation matrix arises from a separable four-quark scattering kernel. In QCD already the simplest contribution in the perturbative kernel, the gluon exchange, has a non-separable form. By introducing a δ-function in configuration space for the gluon propagator a NJL model with pointlike four-quark interaction is realised. This local current-current interaction can be expressed as an attractive interaction in colour singlet meson and colour triplet diquark channels [AR]. The quark-quark scattering kernel in the scalar channel s can be written as

$$(K^s)_{\alpha\beta,\gamma\delta} = 4G_s(\chi^s)_{\alpha\beta}(\overline{\chi}^s)_{\gamma\delta} \tag{6.2}$$

$$= 4G_s(\gamma^5 C\tau^2\lambda^k)_{\alpha\beta}(C^T\gamma^5\tau^2\lambda^k)_{\gamma\delta} \ . \tag{6.3}$$

Here we only consider an isospin doublet of two quarks that are in a flavour antisymmetric (τ^2) and a colour antitriplet state ($\lambda^k, k = 2, 5, 7$) (the τ^i are Pauli matrices and λ^k are Gell-Mann matrices). C denotes the charge conjugation matrix and G_s regulates the strength in the interaction channel. The scalar diquark propagator can be computed to be

$$(D^s)^{-1}(k^2) = \frac{1}{4G_s} - 2\mathrm{tr}_D \int \frac{d^4q}{(2\pi)^4}(C^T\gamma^5)S(q+\frac{k}{2})(\gamma^5 C)S^T(\frac{k}{2}-q) \ . \tag{6.4}$$

After regularising the divergent integral the inverse propagator has zeros for certain values of k^2. This shows that in the NJL model bound scalar diquarks exist and the propagator can be seen as a scalar propagator, which has the effect of a dressing quark loop incorporated.

Looking at the meson spectrum the axialvector diquarks are analogously supposed to play an important role in the diquark channel. Indeed in [WBAR93] the axialvector diquark propagator has poles, but their appearance varies with the ratio of the coupling

constant in the diquark channel to the coupling constant in the pseudoscalar meson channel.

With scalar and axialvector diquarks introduced in [HK95] the spectrum of octet and decuplet baryons was calculated from the Bethe-Salpeter equation. For the quark exchange kernel a static approximation was used and therefore momentum dependence of the exchanged quark was not taken into account. This approach violates covariance and therefore the rich relativistic structure of models from the type which is used in the present work is approximated by the leading non-relativistic component, which is the s wave. Calculations of static nucleon observables with the scalar diquark sector revealed deficiencies in the magnetic moments, which called for an inclusion of the axialvector diquark. This was done in [IBY95, MBIY02] with better success, what seems to support the separable approximation for the two-quark correlation matrix.

If one overcomes the ladder approximation by including higher order perturbation graphs in the quark-quark scattering kernel, the diquark poles disappear both in the NJL model [HAR97] and in the Munczek-Nemirowsky model [BRVS96]. The latter uses a δ-function for the gluon propagator in momentum space and can be regarded as complementary to the former. This suggests that with a more sophisticated gluon propagator the diquark poles might disappear from the quark-quark scattering amplitude.

However, the phenomenological quality of using a diquark correlator to approximate the two-quark correlation matrix does not rely on the existence of asymptotic diquark states. The diquark correlator is allowed to have no singularities for timelike momenta, which is a possible realization of diquark confinement. One can even employ models with a general, separable diquark correlator which does not have to possess a simple analytic structure, implying that no particle interpretation in terms of a diquark is possible. The reason for this is that the attractive nature of the interaction mechanism in the diquark-quark picture (the quark exchange) is independent of the details of the diquark correlations of the model. This comes from the antisymmetry of the diquark and baryon vertices, which is visible in the colour and flavour factors of the baryon Bethe-Salpeter equation.

Of course the applicability of the diquark-quark picture and the usage of specific diquark correlations has in the end to be judged by comparison to experimental data. This has to include more than the octet and decuplet spectrum as these masses are not very sensitive to the level of sophistication in the treatment.

6.3 Covariant Faddeev equation

The properties of light pseudoscalar and vector mesons are described well by a rainbow-ladder truncation of QCD's Dyson-Schwinger equations [MR03], and the calculation of baryon properties using the solution of a Poincaré covariant Faddeev equation is a desirable extension of that approach. For quarks in the fundamental representation of colour-$SU(3)$:

$$3_c \otimes 3_c \otimes 3_c = (\bar{3}_c \oplus 6_c) \otimes 3_c = 1_c \oplus 8'_c \oplus 8_c \oplus 10_c \,, \tag{6.5}$$

and hence any two quarks in a colour-singlet three-quark bound state must constitute a relative colour-antitriplet. This enables the derivation of a Faddeev equation for the bound state contribution to the three quark scattering kernel because the same kernel that describes mesons so well is also attractive for quark-quark scattering in the colour-$\bar{3}$ channel.

The Faddeev equation thus obtained describes the baryon as a composite of a dressed-quark and nonpointlike diquark with an iterated exchange of roles between the bystander and diquark-participant quarks. The baryon is consequently represented by a Faddeev amplitude:

$$\Psi = \Psi_1 + \Psi_2 + \Psi_3 \,, \tag{6.6}$$

where the subscript identifies the bystander quark and, e.g., $\Psi_{1,2}$ are obtained from Ψ_3 by a correlated, cyclic permutation of all the quark labels.

6.3.1 *Ansätze* for the nucleon and Δ

We employ the simplest realistic representation of the Faddeev amplitudes for the nucleon and Δ. The spin- and isospin-1/2 nucleon is a sum of scalar and axial-vector diquark correlations:

$$\Psi_3(p_i, \alpha_i, \tau_i) = \mathcal{N}_3^{0^+} + \mathcal{N}_3^{1^+}, \tag{6.7}$$

with (p_i, α_i, τ_i) the momentum, spin and isospin labels of the quarks constituting the bound state, and $P = p_1 + p_2 + p_3$ the system's total momentum. We assume isospin symmetry of the strong interaction throughout; i.e., the u- and d-quarks are indistinguishable but for their electric charge. Since it is not possible to combine an isospin-0 diquark with an isospin-1/2 quark to obtain isospin-3/2, the spin- and isospin-3/2 Δ contains only an axial-vector diquark component

$$\Psi_3^{\Delta}(p_i, \alpha_i, \tau_i) = \mathcal{D}_3^{1^+}. \tag{6.8}$$

The scalar diquark piece in equation (6.7) is

$$\mathcal{N}_3^{0^+}(p_i, \alpha_i, \tau_i) \;=\; [\Gamma^{0^+}(\tfrac{1}{2}p_{[12]}; K)]^{\tau_1\tau_2}_{\alpha_1\alpha_2}\, \Delta^{0^+}(K)\, [\mathcal{S}(\ell; P)u(P)]^{\tau_3}_{\alpha_3} \,, \tag{6.9}$$

where: the spinor satisfies

$$(i\gamma\cdot P + M)\,u(P) = 0 = \bar{u}(P)\,(i\gamma\cdot P + M)\,, \tag{6.10}$$

with M the mass obtained by solving the Faddeev equation, and it is also a spinor in isospin space with $\varphi_+ = \mathrm{col}(1,0)$ for the proton and $\varphi_- = \mathrm{col}(0,1)$ for the neutron. The momenta are given as $K = p_1 + p_2 =: p_{\{12\}}$, $p_{[12]} = p_1 - p_2$, $\ell := (-p_{\{12\}} + 2p_3)/3$. Δ^{0^+} is a pseudoparticle propagator for the scalar diquark formed from quarks 1 and 2, and Γ^{0^+} is a Bethe-Salpeter-like amplitude describing their relative momentum correlation. And $\mathcal{S}$, a 4×4 Dirac matrix, describes the relative quark-diquark momentum correlation. These objects are discussed in more detail in secion 6.3.2. The colour antisymmetry of Ψ_3 is implicit in Γ^{J^P}, with the Levi-Civita tensor, $\epsilon_{c_1c_2c_3}$, expressed via the antisymmetric Gell-Mann matrices. Explicitly we define

$$\{H^1 = i\lambda^7, H^2 = -i\lambda^5, H^3 = i\lambda^2\}\,, \tag{6.11}$$

and then we have $\epsilon_{c_1c_2c_3} = (H^{c_3})_{c_1c_2}$. (See equations (6.43), (6.44).)

The axial-vector component in equation (6.7) is

$$\mathcal{N}^{1^+}(p_i,\alpha_i,\tau_i) \;=\; [\mathtt{t}^i\,\Gamma^{1^+}_\mu(\frac{1}{2}p_{[12]};K)]^{\tau_1\tau_2}_{\alpha_1\alpha_2}\,\Delta^{1^+}_{\mu\nu}(K)\,[\mathcal{A}^i_\nu(\ell;P)u(P)]^{\tau_3}_{\alpha_3}\,, \tag{6.12}$$

where the symmetric isospin-triplet matrices are

$$\mathtt{t}^+ = \frac{1}{\sqrt{2}}(\tau^0+\tau^3)\,,\ \mathtt{t}^0 = \tau^1\,,\ \mathtt{t}^- = \frac{1}{\sqrt{2}}(\tau^0-\tau^3)\,, \tag{6.13}$$

with $(\tau^0)_{ij} = \delta_{ij}$ and $\tau^{1,3}$ the usual Pauli matrices, and the other elements in equation (6.12) are straightforward generalisations of those in equation (6.9).

The general form of the Faddeev amplitude for the spin- and isospin-3/2 Δ is complicated. However, isospin symmetry means one can focus on the Δ^{++} with it's simple flavour structure, because all the charge states are degenerate, and consider

$$\mathcal{D}^{1^+}_3 = [\mathtt{t}^+\Gamma^{1^+}_\mu(\frac{1}{2}p_{[12]};K)]^{\tau_1\tau_2}_{\alpha_1\alpha_2}\,\Delta^{1^+}_{\mu\nu}(K)\,[\mathcal{D}_{\nu\rho}(\ell;P)u_\rho(P)\,\varphi_+]^{\tau_3}_{\alpha_3}\,, \tag{6.14}$$

where $u_\rho(P)$ is a Rarita-Schwinger spinor, equation (A.12).

The general forms of the matrices $\mathcal{S}(l;P)$, $\mathcal{A}^i_\nu(l;P)$ and $\mathcal{D}_{\nu\rho}(\ell;P)$, which describe the momentum space correlation between the quark and diquark in the nucleon and the Δ, respectively, are described in reference [OHAR98]. The requirement that $\mathcal{S}(l;P)$ represent a positive energy nucleon; namely, that it be an eigenfunction of $\Lambda_+(P)$, equation (A.9), entails

$$\mathcal{S}(\ell;P) = s_1(\ell;P)\,I_{\rm D} + \Big(i\gamma\cdot\hat{\ell} - \hat{\ell}\cdot\hat{P}\,I_{\rm D}\Big)\;s_2(\ell;P)\,, \tag{6.15}$$

where $(I_{\rm D})_{rs} = \delta_{rs}$, $\hat{l}^2 = 1$, $\hat{P}^2 = -1$. In the nucleon rest frame, $s_{1,2}$ describe, respectively, the upper, lower component of the bound-state nucleon's spinor. Placing the same constraint on the axial-vector component, one has

$$\mathcal{A}^i_\nu(l;P) = \sum_{n=1}^{6} p^i_n(l;P)\,\gamma_5\,A^n_\nu(l;P)\,,\ i=+,0,-\,, \tag{6.16}$$

where ($\hat{l}^\perp_\nu = \hat{l}_\nu + \hat{l}\cdot\hat{P}\,\hat{P}_\nu$, $\gamma^\perp_\nu = \gamma_\nu + \gamma\cdot\hat{P}\,\hat{P}_\nu$)

$$\begin{array}{lll} A^1_\nu = \gamma\cdot\hat{l}^\perp\,\hat{P}_\nu\,, & A^2_\nu = -i\hat{P}_\nu\,, & A^3_\nu = \gamma\cdot\hat{l}^\perp\,\hat{l}^\perp\,, \\ A^4_\nu = i\,\hat{l}^\perp_\mu\,, & A^5_\nu = \gamma^\perp_\nu - A^3_\nu\,, & A^6_\nu = i\gamma^\perp_\nu\gamma\cdot\hat{l}^\perp - A^4_\nu\,. \end{array} \tag{6.17}$$

Finally, requiring also that $\mathcal{D}_{\nu\rho}(\ell;P)$ be an eigenfunction of $\Lambda_+(P)$, one obtains

$$\mathcal{D}_{\nu\rho}(\ell;P) = \mathcal{S}^\Delta(l;P)\,\delta_{\nu\rho} + \gamma_5\mathcal{A}^\Delta_\nu(l;P)\,l^\perp_\rho\,, \tag{6.18}$$

with $\mathcal{S}^\Delta$ and $\mathcal{A}^\Delta_\nu$ given by obvious analogues of equations (6.15) and (6.16), respectively.

One can now write the Faddeev equation satisfied by Ψ_3 as

$$\left[\begin{array}{c} \mathcal{S}(k;P)\,u(P) \\ \mathcal{A}^i_\mu(k;P)\,u(P) \end{array}\right] = -4\int\frac{d^4\ell}{(2\pi)^4}\,\mathcal{M}(k,\ell;P)\left[\begin{array}{c} \mathcal{S}(\ell;P)\,u(P) \\ \mathcal{A}^j_\nu(\ell;P)\,u(P) \end{array}\right], \tag{6.19}$$

where one factor of "2" appears because Ψ_3 is coupled symmetrically to Ψ_1 and Ψ_2, and the necessary colour contraction has been evaluated: $(H^a)_{bc}(H^a)_{cb'} = -2\,\delta_{bb'}$. The kernel in equation (6.19) is

$$\mathcal{M}(k,\ell;P) = \left[\begin{array}{cc} \mathcal{M}_{00} & (\mathcal{M}_{01})^j_\nu \\ (\mathcal{M}_{10})^i_\mu & (\mathcal{M}_{11})^{ij}_{\mu\nu} \end{array}\right] \tag{6.20}$$

with

$$\mathcal{M}_{00} = \Gamma^{0^+}(k_q - \ell_{qq}/2;\ell_{qq})\,S^{\rm T}(\ell_{qq}-k_q)\,\bar{\Gamma}^{0^+}(\ell_q - k_{qq}/2;-k_{qq})\,S(\ell_q)\,\Delta^{0^+}(\ell_{qq})\,, \tag{6.21}$$

where:[2] $\ell_q = \ell + P/3$, $k_q = k + P/3$, $\ell_{qq} = -\ell + 2P/3$, $k_{qq} = -k + 2P/3$ and the superscript "T" denotes matrix transpose; and

$$\begin{aligned} (\mathcal{M}_{01})^j_\nu &= \mathtt{t}^j\,\Gamma^{1^+}_\mu(k_q - \ell_{qq}/2;\ell_{qq}) \\ &\quad\times S^{\rm T}(\ell_{qq}-k_q)\,\bar{\Gamma}^{0^+}(\ell_q - k_{qq}/2;-k_{qq})\,S(\ell_q)\,\Delta^{1^+}_{\mu\nu}(\ell_{qq})\,, \end{aligned} \tag{6.22}$$

$$\begin{aligned} (\mathcal{M}_{10})^i_\mu &= \Gamma^{0^+}(k_q - \ell_{qq}/2;\ell_{qq}) \\ &\quad\times S^{\rm T}(\ell_{qq}-k_q)\,\mathtt{t}^i\,\bar{\Gamma}^{1^+}_\mu(\ell_q - k_{qq}/2;-k_{qq})\,S(\ell_q)\,\Delta^{0^+}(\ell_{qq})\,, \end{aligned} \tag{6.23}$$

$$\begin{aligned} (\mathcal{M}_{11})^{ij}_{\mu\nu} &= \mathtt{t}^j\,\Gamma^{1^+}_\rho(k_q - \ell_{qq}/2;\ell_{qq}) \\ &\quad\times S^{\rm T}(\ell_{qq}-k_q)\,\mathtt{t}^i\,\bar{\Gamma}^{1^+}_\mu(\ell_q - k_{qq}/2;-k_{qq})\,S(\ell_q)\,\Delta^{1^+}_{\rho\nu}(\ell_{qq})\,. \end{aligned} \tag{6.24}$$

[2] This choice is explained by equation (6.55) and the discussion thereabout.

It is illuminating to note that $u(P)$ in equation (6.19) is a normalised average of $\varphi_\pm$ so that, e.g., the proton equation is obtained by projection on the left with $\varphi_+^\dagger$. To illustrate this we note that equation (6.22) generates an isospin coupling between $u(P)_{\varphi_+}$ on the left-hand-side (l.h.s.) of equation (6.19) and, on the r.h.s.,

$$\sqrt{2}\,\mathcal{A}_\nu^+\,u(P)_{\varphi^-} - \mathcal{A}_\nu^0\,u(P)_{\varphi_+}\,. \tag{6.25}$$

This is just the Clebsch-Gordon coupling of isospin-1$\oplus$ isospin-$\frac{1}{2}$ to total isospin-$\frac{1}{2}$ and means that the scalar diquark amplitude in the proton, $(ud)_{0^+}\,u$, is coupled to itself *and* the linear combination:

$$\sqrt{2}\,(uu)_{1^+}\,d - (ud)_{1^+}\,u\,. \tag{6.26}$$

Similar statements are obviously true of the spin couplings.

The Δ's Faddeev equation is

$$\mathcal{D}_{\lambda\rho}(k;P)\,u_\rho(P) \;=\; 4\int\frac{d^4\ell}{(2\pi)^4}\,\mathcal{M}^\Delta_{\lambda\mu}(k,\ell;P)\,\mathcal{D}_{\mu\sigma}(\ell;P)\,u_\sigma(P)\,, \tag{6.27}$$

with

$$\mathcal{M}^\Delta_{\lambda\mu} = \mathtt{t}^+\Gamma^{1^+}_\sigma(k_q-\ell_{qq}/2;\ell_{qq})\,S^{\rm T}(\ell_{qq}-k_q)\,\mathtt{t}^+\bar\Gamma^{1^+}_\lambda(\ell_q-k_{qq}/2;-k_{qq})\,S(\ell_q)\,\Delta^{1^+}_{\sigma\mu}(\ell_{qq}). \tag{6.28}$$

6.3.2 Propagators and diquark amplitudes

To complete the Faddeev equations, equations (6.19) and (6.27), one must specify the dressed-quark propagator, the diquark Bethe-Salpeter amplitudes and the diquark propagators that appear in the kernels. In contrast to the preceding chapters we use in this one Landau gauge.

Dressed-quark propagator

The dressed-quark propagator can be obtained from QCD's gap equation and the general form of the solution is

$$S(p) \;=\; -i\gamma\cdot p\,\sigma_V(p^2)+\sigma_S(p^2) = 1/[i\gamma\cdot p\,A(p^2)+B(p^2)]\,. \tag{6.29}$$

The enhancement of the mass function

$$M(p^2) := \frac{B(p^2)}{A(p^2)} \tag{6.30}$$

is central to the appearance of a constituent-quark mass-scale and an existential prerequisite for Goldstone modes. The mass function evolves with increasing p^2 to reproduce

the asymptotic behaviour familiar from perturbative analyses, cf. section 2.2, and that behaviour is unambiguously evident for $p^2 \gtrsim 10\,\mathrm{GeV}^2$ [AS01].

While numerical solutions of the quark DSE are now readily obtained, the utility of an algebraic form for $S(p)$ when calculations require the evaluation of numerous multidimensional integrals is obvious. An suitable parametrisation of $S(p)$, which exhibits the features described above, has been used extensively in hadron studies [AS01, MR03]. It is expressed via

$$\bar{\sigma}_S(x) = 2\,\bar{m}\,\mathcal{F}(2(x+\bar{m}^2)) + \mathcal{F}(b_1 x)\,\mathcal{F}(b_3 x)\,[b_0 + b_2\mathcal{F}(\epsilon x)]\,, \tag{6.31}$$

$$\bar{\sigma}_V(x) = \frac{1}{x+\bar{m}^2}\,\left[1 - \mathcal{F}(2(x+\bar{m}^2))\right]\,, \tag{6.32}$$

with $x = p^2/\lambda^2$, $\bar{m} = m/\lambda$,

$$\mathcal{F}(x) = \frac{1-\mathrm{e}^{-x}}{x}\,, \tag{6.33}$$

$\bar{\sigma}_S(x) = \lambda\,\sigma_S(p^2)$ and $\bar{\sigma}_V(x) = \lambda^2\,\sigma_V(p^2)$. The mass-scale, $\lambda = 0.566\,\mathrm{GeV}$, and parameter values[3]

$\bar{m}$	b_0	b_1	b_2	b_3
0.00897	0.131	2.90	0.603	0.185

, (6.34)

were fixed in a least-squares fit to light-meson observables [BRT96]. The dimensionless $u = d$ current-quark mass in equation (6.34) corresponds to

$$m_{u,d} = 5.1\,\mathrm{MeV}\,. \tag{6.35}$$

The parametrisation yields a Euclidean constituent-quark mass

$$M^E_{u,d} = 0.33\,\mathrm{GeV}, \tag{6.36}$$

defined as the solution of $p^2 = M^2(p^2)$, whose magnitude is typical of that employed in constituent-quark models. In ref. [BRT96] it is shown that $m_s = 25\,m_{u,d}$ and $M^E_s = 0.49\,\mathrm{GeV}$. It is generally true that $M^E_s - M^E_{u,d} \gtrsim \hat{m}_s - \hat{m}_{u,d}$, where $\hat{m}$ denotes the renormalisation point independent current-quark mass. The constituent-quark mass is an expression of dynamical chiral symmetry breaking, as is the vacuum quark condensate[4] ($\Lambda_{\mathrm{QCD}} = 0.2\,\mathrm{GeV}$)

$$-\langle\bar{q}q\rangle_0^{1\,\mathrm{GeV}^2} = \lambda^3\,\frac{3}{4\pi^2}\,\frac{b_0}{b_1\,b_3}\,\ln\frac{1\,\mathrm{GeV}^2}{\Lambda^2_{\mathrm{QCD}}} = (0.221\,\mathrm{GeV})^3\,. \tag{6.37}$$

[3] $\epsilon = 10^{-4}$ in equation (6.31) acts only to decouple the large- and intermediate-p^2 domains.

[4] The condensate is calculated directly from its gauge invariant definition [MR03] after making allowance for the fact that equations (6.31) and (6.32) yield a chiral-limit quark mass function with anomalous dimension $\gamma_m = 1$. This omission of the additional $\ln(p^2/\Lambda^2_{\mathrm{QCD}})$-suppression that is characteristic of QCD is merely a practical simplification.

The equations (6.31) and (6.32) express the dressed-quark propagator as an entire function. Hence $S(p)$ does not have a Lehmann representation, which is a sufficient condition for confinement.[5] Employing an entire function, whose form is only constrained through the calculation of spacelike observables, can lead to model artefacts when it is employed directly to calculate observables involving large timelike momenta of the order of 1 GeV [A$^+$01]. An improved parametrisation is therefore being sought. Nevertheless, difficulties are not encountered for moderate timelike momenta, and on the domain of the complex plane explored in the present calculation the integral support provided by an equally effective alternative cannot differ significantly from that of this parametrisation.

Diquark Bethe-Salpeter amplitudes

The two-quark correlation function has been calculated in different models. Since they have a strong model dependence we will employ a simple ansatz for it, namely the pole approximation in the scalar and axialvector channel:

$$[M_{qq}(k,q;K)]^{tu}_{rs} = \sum_{J^P=0^+,1^+,\ldots} \bar{\Gamma}^{J^P}(k;-K)\,\Delta^{J^P}(K)\,\Gamma^{J^P}(q;K)\,. \tag{6.38}$$

One practical means of specifying the Γ^{J^P} in equation (6.38) is to employ the solutions of a rainbow-ladder quark-quark Bethe-Salpeter equation (BSE). Using the properties of the Gell-Mann matrices one finds easily that $\Gamma^{J^P}_C := \Gamma^{J^P} C^\dagger$ satisfies exactly the same equation as the J^{-P} colour-singlet meson *but* for a halving of the coupling strength. This makes clear that the interaction in the $\bar{3}_c$ (qq) channel is strong and attractive.[6] Moreover, it follows as a feature of the rainbow-ladder truncation that, independent of the specific form of a model's interaction, the calculated masses satisfy

$$m_{(qq)_{J^P}} > m_{(\bar{q}q)_{J^{-P}}}\,. \tag{6.39}$$

This is a useful guide for all but scalar diquark correlations because the partnered mesons in that case are pseudoscalars, whose ground state masses are constrained to be small by Goldstone's theorem and which therefore provide a weak lower bound. For the correlations relevant herein, models typically give masses (in GeV) [Mar02]:

$$m_{(ud)_{0^+}} = 0.74 - 0.82\,,\; m_{(uu)_{1^+}} = m_{(ud)_{1^+}} = m_{(dd)_{1^+}} = 0.95 - 1.02\,. \tag{6.40}$$

Such values are confirmed by results obtained in simulations of quenched lattice-QCD [HKLW98]. Charge radii have also been computed for the scalar diquark in a Landau

[5] It is a sufficient condition for confinement because of the associated violation of reflection positivity [AS01].

[6] The same analysis shows the interaction to be strong and repulsive in the 6_c (qq) channel.

gauge approach: $r_{(ud)_{0^+}} \approx 1.1\, r_\pi$. The Bethe-Salpeter amplitude is canonically normalised [IZ] via:

$$2\,K_\mu = \left[\frac{\partial}{\partial Q_\mu}\Pi(K,Q)\right]_{Q=K}^{K^2=-m_{J^P}^2}, \tag{6.41}$$

$$\Pi(K,Q) = tr\int\frac{d^4q}{(2\pi)^4}\,\bar{\Gamma}(q;-K)\,S(q+Q/2)\,\Gamma(q;K)\,S^{\rm T}(-q+Q/2). \tag{6.42}$$

A solution of the BSE equation requires a simultaneous solution of the quark-DSE [Mar02]. However, since we have already chosen to simplify the calculations by parametrising $S(p)$, we also employ that expedient with Γ^{J^P}, using the following one-parameter forms:

$$\Gamma^{0^+}(k;K) = \frac{1}{\mathcal{N}^{0^+}}\,H^a\,C i\gamma_5\,i\tau_2\,\mathcal{F}(k^2/\omega_{0^+}^2)\,, \tag{6.43}$$

$$\mathtt{t}^i\Gamma_\mu^{1^+}(k;K) = \frac{1}{\mathcal{N}^{1^+}}\,H^a\,i\gamma_\mu C\,\mathtt{t}^i\,\mathcal{F}(k^2/\omega_{1^+}^2)\,, \tag{6.44}$$

with the normalisation, $\mathcal{N}^{J^P}$, fixed by equation (6.41). These *Ansätze* retain only that single Dirac-amplitude which would represent a point particle with the given quantum numbers in a local Lagrangian density: they are usually the dominant amplitudes in a solution of the rainbow-ladder BSE for the lowest mass J^P diquarks [Mar02].

Diquark propagators

Calculations beyond rainbow-ladder truncation eliminate asymptotic diquark states from the spectrum. It is apparent in reference [BHK$^+$04] that the behaviour of the diquark propagator Δ^{J^P} can be modelled efficiently by simple functions that are free-particle-like at spacelike momenta but pole-free on the timelike axis. Hence we employ

$$\Delta^{0^+}(K) = \frac{1}{m_{0^+}^2}\,\mathcal{F}(K^2/\omega_{0^+}^2)\,, \tag{6.45}$$

$$\Delta_{\mu\nu}^{1^+}(K) = \left(\delta_{\mu\nu}+\frac{K_\mu K_\nu}{m_{1^+}^2}\right)\frac{1}{m_{1^+}^2}\,\mathcal{F}(K^2/\omega_{1^+}^2)\,, \tag{6.46}$$

where the two parameters m_{J^P} are diquark pseudoparticle masses and ω_{J^P} are widths characterising Γ^{J^P}. Herein we require additionally that

$$\frac{d}{dK^2}\left(\frac{1}{m_{J^P}^2}\,\mathcal{F}(K^2/\omega_{J^P}^2)\right)^{-1}\Bigg|_{K^2=0} = 1 \;\Rightarrow\; \omega_{J^P}^2 = \frac{1}{2}\,m_{J^P}^2\,, \tag{6.47}$$

which is a normalisation that accentuates the free-particle-like propagation characteristics of the diquarks *within* the hadron.

6.3.3 Solving the Faddeev equation and choices for nucleon and Δ masses

All elements of the Faddeev equations, equations (6.19) and (6.27), are now completely specified. We solve the equations via the method described in reference [OVSA02]. The masses of the scalar and axial-vector diquarks are the only variable parameters. The axial-vector mass is chosen so as to obtain a desired mass for the Δ, and the scalar mass is subsequently set by requiring a particular nucleon mass.

Two parameter sets are presented in table 6.1. We obtained set A by requiring a precise fit to the experimental nucleon and Δ masses. It has long been known that this is possible: reference [OHAR98] reports octet and decuplet baryon masses in which the rms deviation between the calculated mass and experiment is only 2%. However, it is also known that such an outcome is undesirable because, e.g., studies using the cloudy bag model indicate that the nucleon's mass is reduced by as much as $\delta M_N = -300$ to $-400\,\mathrm{MeV}$ through pion self-energy corrections [PA86]. Furthermore, a perturbative study, using the Faddeev equation, of the mass shift induced by pion exchange between the quark and diquark constituents of the nucleon obtains $\delta M_N = -150$ to $-300\,\mathrm{MeV}$ [Ish98]. We are thus led to set B, which was obtained by fitting to nucleon and Δ masses that are inflated so as to allow for the additional attractive contribution from the pion cloud [H$^+$02].

It is apparent in table 6.1 that a baryon's mass increases with increasing diquark mass, and the fitted diquark mass-scales are commensurate with the anticipated values, cf. equation (6.40), with set B in better accord. If coupling to the axial-vector diquark channel is omitted from equation (6.19), then $M_N^{\mathrm{set\,A}} = 1.15\,\mathrm{GeV}$ and $M_N^{\mathrm{set\,B}} = 1.46\,\mathrm{GeV}$. It is thus clear that axial-vector diquark correlations provide significant attraction in the nucleon. Of course, using our Faddeev equation, the Δ does not exist without axial-vector correlations.

Table 6.1: Mass-scale parameters (in GeV) for the scalar and axial-vector diquark correlations, fixed by fitting nucleon and Δ masses: for set A, a fit to the actual masses was required; whereas for set B the fitted mass was offset to allow for "pion cloud" contributions [H$^+$02]. We also list $\omega_{J^P} = \frac{1}{\sqrt{2}} m_{J^P}$, which is the width-parameter in the $(qq)_{J^P}$ Bethe-Salpeter amplitude, equations (6.43) and (6.44): its inverse is a measure of the diquark's matter radius.

set	M_N	M_Δ	m_{0^+}	m_{1^+}	ω_{0^+}	ω_{1^+}
A	0.94	1.23	0.63	0.84	0.44=1/(0.45 fm)	0.59=1/(0.33 fm)
B	1.18	1.33	0.79	0.89	0.56=1/(0.35 fm)	0.63=1/(0.31 fm)

In set B the amount of attraction provided by axial-vector correlations must be matched by that provided by the pion cloud. This highlights the constructive interference between the contribution of these two effects to a baryons' mass. It is related and noteworthy that $m_{1^+} - m_{0^+}$ is only a reasonable approximation to $M_\Delta - M_N = 0.29\,\mathrm{GeV}$ when pion cloud effects are ignored: set A, $m_{1^+} - m_{0^+} = 0.21\,\mathrm{GeV}$ cf. set B, $m_{1^+} - m_{0^+} = 0.10\,\mathrm{GeV}$. Plainly, understanding the N-Δ mass splitting requires more than merely reckoning the mass-scales of constituent degrees of freedom.

6.4 Electromagnetic current operator

The nucleon's electromagnetic current is

$$J_\mu(P',P) = ie\,\bar{u}(P')\,\Lambda_\mu(q,P)\,u(P)\,, \tag{6.48}$$

$$= ie\,\bar{u}(P')\left(\gamma_\mu F_1(Q^2) + \frac{1}{2M}\,\sigma_{\mu\nu}\,Q_\nu\,F_2(Q^2)\right)u(P)\,, \tag{6.49}$$

where P (P') is the momentum of the incoming (outgoing) nucleon, $Q = P' - P$, and F_1 and F_2 are, respectively, the Dirac and Pauli form factors. They are the primary calculated quantities, from which one obtains the nucleon's electric and magnetic form factors

$$G_E(Q^2) = F_1(Q^2) - \frac{Q^2}{4M^2}F_2(Q^2)\,,\; G_M(Q^2) = F_1(Q^2) + F_2(Q^2)\,. \tag{6.50}$$

In equation (6.48), Λ_μ is the nucleon-photon vertex, which we construct following the systematic procedure of reference [OPS00]. This approach has the merit of automatically providing a conserved current for on-shell nucleons described by Faddeev amplitudes of the type we have calculated. Moreover, the canonical normalisation condition for the nucleons' Faddeev amplitude is equivalent to requiring $F_1(Q^2 = 0) = 1$ for the proton. The vertex has six terms, which are depicted in figure 6.1. Here we describe the key elements in the construction.

In order to make this vertex more explicit, we write the scalar and axial-vector components of the nucleons' Faddeev amplitudes in the form [cf. equation (6.19)]

$$\Psi(k;P) = \left[\begin{array}{c} \Psi^0(k;P) \\ \Psi^i_\mu(k;P) \end{array}\right] = \left[\begin{array}{c} \mathcal{S}(k;P)u(P) \\ \mathcal{A}^i_\mu(k;P)u(P) \end{array}\right], \qquad i = 1,\ldots,4\,. \tag{6.51}$$

For explicit calculations, we work in the Breit frame: $P_\mu = P^{BF}_\mu - Q_\mu/2$, $P'_\mu = P^{BF}_\mu + Q_\mu/2$ and $P^{BF}_\mu = (0,0,0,i\sqrt{M_n^2 + Q^2/4})$, and write the electromagnetic current matrix element

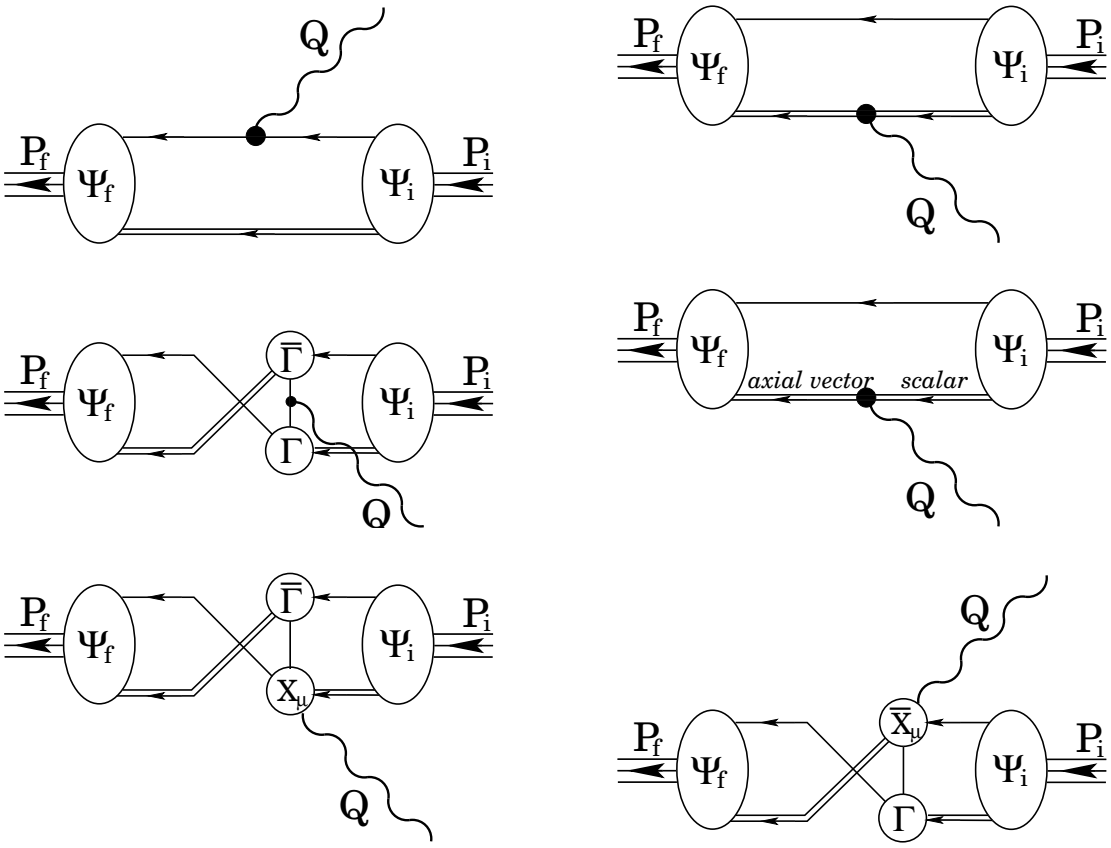

Figure 6.1: Nucleon-photon vertex which ensures a conserved current for on-shell nucleons described by the Faddeev amplitudes, $\Psi_{i,f}$, calculated in section 6.3. The single line represents $S(p)$, the dressed-quark propagator, section 6.3.2, and the double line, the diquark propagator, section 6.3.2; Γ is the diquark Bethe-Salpeter amplitude, section 6.3.2; and the remaining vertices are described in sections. 6.4.1–6.4.5: the top-left image is diagram 1; the top-right, diagram 2; and so on, with the bottom-right image, diagram 6.

as [cf. equation (6.48)]

$$\left\langle P'|\hat{J}^{em}_\mu|P\right\rangle = \Lambda^+(P')\left[\gamma_\mu G_E + M_n\frac{P^{BF}_\mu}{P^2_{BF}}(G_E - G_M)\right]\Lambda^+(P) \tag{6.52}$$

$$= \int \frac{d^4p}{(2\pi)^4}\frac{d^4k}{(2\pi)^4}\,\bar\Psi(-p,P')J^{em}_\mu(p,P';k,P)\Psi(k,P)\,. \tag{6.53}$$

In figure 6.1 we have broken the current, $J^{em}_\mu(p,P';k,P)$, into a sum of six parts, each of which we now make precise.

6.4.1 Coupling to the quark

In this section we deal with diagram 1. The one-body term is expressed as

$$J_\mu^{qu} \;=\; S(p_q)\hat{\Gamma}_\mu^{qu}(p_q;k_q)S(k_q)\left(\Delta^{0^+}(k_s)+\Delta^{1^+}(k_s)\right)(2\pi)^4\delta^4(p-k-\hat{\eta}Q)\,, \quad (6.54)$$

where $\hat{\Gamma}_\mu^{qu}(p_q;k_q) = Q_q\,\Gamma_\mu(p_q;k_q)$, with $Q_q = \mathrm{diag}[2/3,-1/3]$ being the quark electric charge matrix, and $\Gamma_\mu(p_q;k_q)$ is given in equation (6.57).

Here and in the diagrams 2 and 4 the denotation

$$\begin{aligned} k_q &= \eta P + k\,, & p_q &= \eta P' + p\,,\\ k_d &= \hat{\eta} P - k\,, & p_d &= \hat{\eta} P' - p\,, \end{aligned} \quad (6.55)$$

with $\eta+\hat{\eta}=1$ is used. The results reported were obtained with $\eta = 1/3$, which provides a single quark with one-third of the baryon's total momentum, but, as our approach is manifestly Poincaré covariant, the precise value is immaterial. Nevertheless, numerical results converge more quickly with this natural choice.

This represents the photon coupling directly to the bystander quark and is obtained explicitly from the equations (6.52) and (6.54). It is a necessary condition for current conservation that the quark-photon vertex satisfy the Ward-Takahashi identity:

$$Q_\mu\, i\Gamma_\mu(\ell_1,\ell_2) = S^{-1}(\ell_1) - S^{-1}(\ell_2)\,, \quad (6.56)$$

where $Q = \ell_1 - \ell_2$ is the photon momentum flowing into the vertex. Since the quark is dressed the vertex is not bare; i.e., $\Gamma_\mu(\ell_1,\ell_2) \neq \gamma_\mu$. It can be obtained by solving an inhomogeneous Bethe-Salpeter equation, which was the procedure adopted in the DSE calculation that successfully predicted the electromagnetic pion form factor [MT00]. However, since we have parametrised $S(p)$, we use the Ball-Chiu construction of the vertex [BC80]

$$i\Gamma_\mu(\ell_1,\ell_2) = i\Sigma_A(\ell_1^2,\ell_2^2)\,\gamma_\mu + 2k_\mu\left[i\gamma\cdot k_\mu\,\Delta_A(\ell_1^2,\ell_2^2) + \Delta_B(\ell_1^2,\ell_2^2)\right]; \quad (6.57)$$

with $k = (\ell_1+\ell_2)/2$, $Q = (\ell_1-\ell_2)$ and

$$\Sigma_F(\ell_1^2,\ell_2^2) = \frac{1}{2}\left[F(\ell_1^2)+F(\ell_2^2)\right],\; \Delta_F(\ell_1^2,\ell_2^2) = \frac{F(\ell_1^2)-F(\ell_2^2)}{\ell_1^2-\ell_2^2}\,, \quad (6.58)$$

where $F = A, B$, i.e. the scalar functions in equation (6.29). It is critical that Γ_μ in equation (6.57) satisfies equation (6.56) and very useful that it is completely determined by the dressed-quark propagator. This *ansatz* has been used fruitfully in many hadronic applications [AS01]. Its primary defect is the omission of pion cloud contributions. But since one of our goals is to draw attention to consequences of that omission, this fault is herein a virtue.

6.4.2 Coupling to the diquark

In this section we treat diagram 2. It depicts the photon coupling directly to a diquark correlation. The explicit expression is

$$J_\mu^{dq} \;=\; \Delta^i(p_d)\left[\hat{\Gamma}_\mu^{dq}(p_d;k_d)\right]^{ij}\Delta^j(k_d)S(k_q)(2\pi)^4\delta^4(p-k+\eta Q)\,, \tag{6.59}$$

where $[\hat{\Gamma}_\mu^{dq}(p_d;k_d)]^{ij} = \mathrm{diag}[Q_{0^+}\Gamma_\mu^{0^+}, Q_{1^+}\Gamma_\mu^{1^+}]$, with $Q_{0^+} = 1/3$ and $\Gamma_\mu^{0^+}$ is given in equation (6.62), and $Q_{1^+} = \mathrm{diag}[4/3, 1/3, -2/3]$ where $\Gamma_\mu^{1^+}$ is given in equation (6.64). Naturally, the diquark propagators match the line to which they are attached.

In the case of a scalar correlation, the general form of the diquark-photon vertex is

$$\Gamma_\mu^{0^+}(\ell_1,\ell_2) = 2\,k_\mu\,f_+(k^2,k\cdot Q,Q^2) + Q_\mu\,f_-(k^2,k\cdot Q,Q^2)\,, \tag{6.60}$$

and it must satisfy the Ward-Takahashi identity:

$$Q_\mu\,\Gamma_\mu^{0^+}(\ell_1,\ell_2) = \Pi^{0^+}(\ell_1^2) - \Pi^{0^+}(\ell_2^2)\,,\; \Pi^{J^P}(\ell^2) = \{\Delta^{J^P}(\ell^2)\}^{-1}. \tag{6.61}$$

The evaluation of scalar diquark elastic electromagnetic form factors in reference [Mar04] is a first step toward calculating this vertex. However, in providing only an on-shell component, it is insufficient for our requirements. We therefore adapt equation (6.57) to this case and write

$$\Gamma_\mu^{0^+}(\ell_1,\ell_2) = k_\mu\,\Delta_{\Pi^{0^+}}(\ell_1^2,\ell_2^2)\,, \tag{6.62}$$

which is the minimal *ansatz* that satisfies equation (6.61), is completely determined by quantities introduced already and is free of kinematic singularities. It implements $f_- \equiv 0$, which is a requirement for elastic form factors, and guarantees a valid normalisation of electric charge, i.e.

$$\lim_{\ell'\to\ell}\Gamma_\mu^{0^+}(\ell',\ell) = 2\,\ell_\mu\,\frac{d}{d\ell^2}\,\Pi^{0^+}(\ell^2) \stackrel{\ell^2\sim 0}{=} 2\,\ell_\mu\,, \tag{6.63}$$

owing to equation (6.47). We have to keep in mind that we factored the fractional diquark charge, which therefore appears subsequently in our calculations as a simple multiplicative factor.

For the case in which the struck diquark correlation is axial-vector and the scattering is elastic, the vertex assumes the form [HP99]: [7]

$$\Gamma_{\mu\alpha\beta}^{1^+}(\ell_1,\ell_2) = -\sum_{i=1}^{3}\Gamma_{\mu\alpha\beta}^{[\mathrm{i}]}(\ell_1,\ell_2)\,, \tag{6.64}$$

[7] If the scattering is inelastic the general form of the vertex involves eight scalar functions [SD64]. Absent further constraints and input, we ignore the additional structure in this *ansatz*.

with $(T_{\alpha\beta}(\ell) = \delta_{\alpha\beta} - \ell_\alpha \ell_\beta/\ell^2)$

$$\Gamma^{[1]}_{\mu\alpha\beta}(\ell_1,\ell_2) = (\ell_1+\ell_2)_\mu\, T_{\alpha\lambda}(\ell_1)\, T_{\lambda\beta}(\ell_2)\; F_1(\ell_1^2,\ell_2^2)\,, \tag{6.65}$$

$$\Gamma^{[2]}_{\mu\alpha\beta}(\ell_1,\ell_2) = [T_{\mu\alpha}(\ell_1)\, T_{\beta\rho}(\ell_2)\, \ell_{1\rho} + T_{\mu\beta}(\ell_2)\, T_{\alpha\rho}(\ell_1)\, \ell_{2\rho}]\, F_2(\ell_1^2,\ell_2^2)\,, \tag{6.66}$$

$$\Gamma^{[3]}_{\mu\alpha\beta}(\ell_1,\ell_2) = -\frac{1}{2m_{1^+}^2}\,(\ell_1+\ell_2)_\mu\, T_{\alpha\rho}(\ell_1)\, \ell_{2\rho}\, T_{\beta\lambda}(\ell_2)\, \ell_{1\lambda}\; F_3(\ell_1^2,\ell_2^2)\,. \tag{6.67}$$

This vertex satisfies:

$$\ell_{1\alpha}\,\Gamma^{1^+}_{\mu\alpha\beta}(\ell_1,\ell_2) = 0 = \Gamma^{1^+}_{\mu\alpha\beta}(\ell_1,\ell_2)\,\ell_{2\beta}\,, \tag{6.68}$$

which is a general requirement of the elastic electromagnetic vertex of axial-vector bound states and guarantees that the interaction does not induce a pseudoscalar component in the axial-vector correlation. We note that the electric, magnetic and quadrupole form factors of an axial-vector bound state are expressed [HP99]

$$G_{\mathcal{E}}^{1^+}(Q^2) = F_1 + \frac{2}{3}\,\tau_{1^+}\, G_{\mathcal{Q}}^{1^+}(Q^2)\,,\; \tau_{1^+} = \frac{Q^2}{4\,m_{1^+}^2} \tag{6.69}$$

$$G_{\mathcal{M}}^{1^+}(Q^2) = -F_2(Q^2)\;, \tag{6.70}$$

$$G_{\mathcal{Q}}^{1^+}(Q^2) = F_1(Q^2) + F_2(Q^2) + (1+\tau_{1^+})\, F_3(Q^2)\,. \tag{6.71}$$

Extant knowledge of the form factors in equations (6.64)–(6.67) is limited and thus one has little information about even this rudimentary vertex model. Hence, we employ the following *ansätze*:

$$F_1(\ell_1^2,\ell_2^2) = \Delta_{\Pi^{1^+}}(\ell_1^2,\ell_2^2)\,, \tag{6.72}$$

$$F_2(\ell_1^2,\ell_2^2) = -F_1 + (1-\tau_{1^+})\,(\tau_{1^+}F_1 + 1 - \mu_{1^+})\, d(\tau_{1^+}) \tag{6.73}$$

$$F_3(\ell_1^2,\ell_2^2) = -\,(\chi_{1^+}\,(1-\tau_{1^+})\, d(\tau_{1^+}) + F_1 + F_2)\, d(\tau_{1^+})\,, \tag{6.74}$$

with $d(x) = 1/(1+x)^2$. This construction ensures a valid electric charge normalisation for the axial-vector correlation,

$$\lim_{\ell'\to\ell}\,\Gamma^{1^+}_{\mu\alpha\beta}(\ell',\ell) = T_{\alpha\beta}(\ell)\,\frac{d}{d\ell^2}\,\Pi^{1^+}(\ell^2) \stackrel{\ell^2\sim 0}{=} T_{\alpha\beta}(\ell)\,2\,\ell_\mu\,, \tag{6.75}$$

owing to equation (6.47), and current conservation

$$\lim_{\ell_2\to\ell_1}\, Q_\mu \Gamma^{1^+}_{\mu\alpha\beta}(\ell_1,\ell_2) = 0\,. \tag{6.76}$$

The diquark's static electromagnetic properties follow:

$$G_{\mathcal{E}}^{1^+}(0) = 1\,,\; G_{\mathcal{M}}^{1^+}(0) = \mu_{1^+}\,,\; G_{\mathcal{Q}}^{1^+}(0) = -\chi_{1^+}\,. \tag{6.77}$$

For a pointlike axial-vector we have $\mu_{1^+} = 2$; and $\chi_{1^+} = 1$, which corresponds to an oblate charge distribution. In addition, equations (6.64)–(6.67) with equations (6.72)–(6.74) realise the constraints of reference [BH92], namely, independent of the values of μ_{1^+} and χ_{1^+}, the form factors assume the ratios

$$G_{\mathcal{E}}^{1^+}(Q^2) : G_{\mathcal{M}}^{1^+}(Q^2) : G_{\mathcal{Q}}^{1^+}(Q^2) \stackrel{Q^2\to\infty}{=} (1 - \frac{2}{3}\tau_{1^+}) : 2 : -1\,. \tag{6.78}$$

6.4.3 Coupling to the exchanged quark

Diagram 3 depicts a photon coupling to the quark that is exchanged as one diquark breaks up and another is formed. While this is the first two-loop diagram we have described, no new elements appear in its specification: the dressed-quark-photon vertex was discussed in section 6.4.1. The explicit contribution to the vertex is obtained with

$$J_\mu^{ex} = -\frac{1}{2} S(k_q)\Delta^i(k_d)\Gamma^i(p_1,k_d)S^T(q)\hat{\Gamma}_\mu^{quT}(q',q)S^T(q')\bar{\Gamma}^{jT}(p_2',p_d)\Delta^j(p_d)S(p_q)\,, \tag{6.79}$$

wherein the vertex $\hat{\Gamma}_\mu^{qu}$ appeared in equation (6.54). The full contribution is obtained by summing over the superscripts i, j, which can each take the values 0^+, 1^+.

It is noteworthy that the process of quark exchange provides the attraction necessary in the Faddeev equation to bind the nucleon. It also guarantees that the Faddeev amplitude has the correct antisymmetry under the exchange of any two dressed-quarks. This key feature is absent in models with elementary (noncomposite) diquarks.

6.4.4 Scalar ↔ axialvector transition

This contribution differs from diagram 2 in expressing the contribution to the nucleons' form factors owing to an electromagnetically induced transition between scalar and axialvector diquarks:

$$J_\mu^{dq} \;=\; \Delta^i(p_d)\left[\hat{\Gamma}_\mu^{dq}(p_d;k_d)\right]^{ij}\Delta^j(k_d)S(k_q)(2\pi)^4\delta^4(p-k+\eta Q)\,, \tag{6.80}$$

where $[\hat{\Gamma}_\mu^{dq}(p_d;k_d)]^{i=j} = 0$, and $[\hat{\Gamma}_\mu^{dq}(p_d;k_d)]^{1,2} = \Gamma_{SA}$, which is given in equation (6.81), and $[\hat{\Gamma}_\mu^{dq}(p_d;k_d)]^{2,1} = \Gamma_{AS}$. Naturally, the diquark propagators match the line to which they are attached.

The transition vertex is a rank-2 pseudotensor and can therefore be expressed

$$\Gamma_{SA}^{\gamma\alpha}(\ell_1,\ell_2) = -\Gamma_{AS}^{\gamma\alpha}(\ell_1,\ell_2) = \frac{i}{M_N}\,\mathcal{T}(\ell_1,\ell_2)\,\varepsilon_{\gamma\alpha\rho\lambda}\ell_{1\rho}\ell_{2\lambda}\,, \tag{6.81}$$

where γ, α are, respectively, the vector indices of the photon and axial-vector diquark. For simplicity we proceed under the assumption that

$$\mathcal{T}(\ell_1, \ell_2) = \kappa_{\mathcal{T}} \,, \tag{6.82}$$

i.e. a constant, for which a typical value is [OAS00]:

$$\kappa_{\mathcal{T}} \sim 2 \,. \tag{6.83}$$

In the nucleons' rest frame, a outstanding piece of the Faddeev amplitude that describes an axial-vector diquark inside the bound state can be characterised as containing a bystander quark whose spin is antiparallel to that of the nucleon, with the axial-vector diquark's parallel. The interaction pictured in this diagram does not affect the bystander quark but the transformation of an axial-vector diquark into a scalar effects a flip of the quark spin within the correlation. After this transformation, the spin of the nucleon must be formed by summing the spin of the bystander quark, which is still aligned antiparallel to that of the nucleon, and the orbital angular momentum between that quark and the scalar diquark.[8] This argument, while not sophisticated, does motivate an expectation that diagram 4 will strongly impact on the nucleons' magnetic form factors.

6.4.5 Seagull contributions

The two-loop diagrams 5 and 6 are the so-called "seagull" terms, which appear as partners to diagram 3 and arise because binding in the nucleons' Faddeev equations is effected by the exchange of *nonpointlike* diquark correlations [OPS00].

The explicit expression for their contribution to the nucleons' form factors is given by

$$\begin{aligned} J_\mu^{sg} &= \frac{1}{2} S(k_q) \Delta^i(k_d) \left(X_\mu^i(p_q, q', k_d) S^T(q') \bar{\Gamma}^{jT}(p_2', p_d) \right. \\ &\quad \left. - \Gamma^i(p_1, k_d) S^T(q) \bar{X}_\mu^j(-k_q, -q, p_d) \right) \Delta^j(p_d) S(p_q) \,, \end{aligned} \tag{6.84}$$

where, again, the superscripts are summed. In equations (6.79) and (6.84) the momenta are

$$\begin{aligned} q &= \hat{\eta} P - \eta P' - p - k \,, & q' &= \hat{\eta} P' - \eta P - p - k \,, \\ p_1 &= (p_q - q)/2 \,, & p_2' &= (-k_q + q')/2 \,, \\ p_1' &= (p_q - q')/2 \,, & p_2 &= (-k_q + q)/2 \,. \end{aligned} \tag{6.85}$$

[8] A less prominent component of the amplitude has the bystander quark's spin parallel to that of the nucleon while the axial-vector diquark's is antiparallel: this $q^\uparrow \oplus (qq)^\downarrow_{1^+}$ system has one unit of angular momentum. That momentum is absent in the $q^\uparrow \oplus (qq)_{0^+}$ system. Other combinations also contribute via diagram 3 but all mediated processes inevitably require a modification of spin and/or angular momentum.

The new elements in these diagrams are the couplings of a photon to two dressed-quarks as they either separate from (diagram 5) or combine to form (diagram 6) a diquark correlation. As such they are components of the five point Schwinger function which describes the coupling of a photon to the quark-quark scattering kernel. This Schwinger function could be calculated, as is evident from the recent computation of analogous Schwinger functions relevant to meson observables [CM02, CM03]. However, such a calculation provides valid input only when a uniform truncation of the DSEs has been employed to calculate each of the elements described hitherto. We must instead employ an algebraic parametrisation [OPS00], which for Diagram 5 reads

$$\begin{aligned} X_\mu^{J^P}(k,Q) &= e_{\rm by}\,\frac{4k_\mu - Q_\mu}{4k\cdot Q - Q^2}\,\left[\Gamma^{J^P}(k-Q/2) - \Gamma^{J^P}(k)\right] \\ &+ e_{\rm ex}\,\frac{4k_\mu + Q_\mu}{4k\cdot Q + Q^2}\,\left[\Gamma^{J^P}(k+Q/2) - \Gamma^{J^P}(k)\right], \end{aligned} \tag{6.86}$$

with k the relative momentum between the quarks in the initial diquark, $e_{\rm by}$ the electric charge of the quark which becomes the bystander and $e_{\rm ex}$, the charge of the quark that is reabsorbed into the final diquark. Diagram 6 has

$$\begin{aligned} \bar{X}_\mu^{J^P}(k,Q) &= -e_{\rm by}\,\frac{4k_\mu - Q_\mu}{4k\cdot Q - Q^2}\,\left[\bar{\Gamma}^{J^P}(k+Q/2) - \bar{\Gamma}^{J^P}(k)\right] \\ &- e_{\rm ex}\,\frac{4k_\mu + Q_\mu}{4k\cdot Q + Q^2}\,\left[\bar{\Gamma}^{J^P}(k-Q/2) - \bar{\Gamma}^{J^P}(k)\right], \end{aligned} \tag{6.87}$$

where $\bar{\Gamma}^{J^P}(\ell)$ is the charge-conjugated amplitude, equation (A.11). These terms vanish if the diquark correlation is represented by a momentum-independent Bethe-Salpeter-like amplitude, i.e. the diquark is pointlike.

It is naturally possible to use more complicated *ansätze*. However, like equation (6.62), equations. (6.86) and (6.87) are simple forms, free of kinematic singularities and sufficient to ensure the nucleon-photon vertex satisfies the Ward-Takahashi identity when the composite nucleon is obtained from the Faddeev equation.

6.5 Nucleon electromagnetic form factors: results

6.5.1 Remarks

In order to place the calculation of baryon observables on the same footing as the study of mesons, the proficiency evident in [MR03, CM03] will need to be applied to every line and vertex that appears in figure 6.1. This is a feasible but tedious task. In the meantime, herein we present a study whose merits include a capacity to explore the potential of the

Faddeev equation truncation of the baryon three-body problem and elucidate the role of additional correlations, such as those associated with pseudoscalar mesons.

It is worthwhile to summarise our input before presenting the results. One element is the dressed-quark propagator, section 6.3.2. The form we use expresses the features that were found in recent studies [ADFM04]. It carries no free parameters, because its behaviour was fixed in analyses of meson observables, and is basic to a description of light- and heavy-quark mesons that is accurate to better than 10% [IKR99].

We proposed that the nucleon is at heart composed of a dressed-quark and nonpointlike diquark with binding effected by an iterated exchange of roles between the bystander and diquark-participant quarks. This picture is realised via a Poincaré covariant Faddeev equation, section 6.3.1, which incorporates scalar and axial-vector diquark correlations. There are two parameters, sections. 6.3.2 and 6.3.2: the mass-scales associated with these correlations. They are fixed by fitting to specified nucleon and Δ masses, section 6.3.3, and thus at this point there are still no free parameters with which to influence the nucleons' form factors.

With the constituents and the bound states' structure defined, only a specification of the nucleons' electromagnetic interaction remained. Its formulation was guided almost exclusively by a requirement that the nucleon-photon vertex satisfy a Ward-Takahashi identity. Since the scalar diquark's electromagnetic properties are readily resolved, our result, figure 6.1, depends on three parameters that are all tied to properties of the axial-vector diquark correlation: μ_{1^+} and χ_{1^+}, respectively, the axial-vector diquarks' magnetic dipole and electric quadrupole moments; and $\kappa_{\mathcal{T}}$, the strength of electromagnetic axial-vector $\leftrightarrow$ scalar diquark transitions. Hence, with our calculations we exhibit and interpret the dependence of the nucleons' form factors on these three parameters, and also on the nucleons' intrinsic quark structure as expressed in the Poincaré covariant Faddeev amplitudes.

6.5.2 Calculated results and discussion

Static properties and form factors

The slope of the form factors at the origin is conventionally expressed in terms of a nucleon radius $\sqrt{\langle r^2\rangle}$,

$$F(t) = F(0)\left(1 + \frac{1}{6}\langle r^2\rangle t + ...\right) \ , \tag{6.88}$$

which is rooted in the non-relativistic description of the scattering process in which a pointlike charged particle interact with a given charge distribution $\rho(r)$.

In terms of the Sachs form factors the nucleons' charge and magnetic radii can then be written as

$$r_N^2 := -6\,\frac{d}{ds}\ln G_E^N(s)\bigg|_{s=0},\ (r_N^\mu)^2 := -6\,\frac{d}{ds}\ln G_M^N(s)\bigg|_{s=0}, \tag{6.89}$$

where $N = n, p$.

In table 6.2 we report charge radii calculated for a range of values of the parameters that characterise the axial-vector diquarks' electromagnetic form factors, secion 6.4.2, centred on the point-particle values of $\mu_{1^+} = 2$ and $\chi_{1^+} = 1$, equation (6.77), and $\kappa_{\mathcal{T}} = 2$, equation (6.83).

Table 6.2: Charge radii, in fm, calculated using the diquark mass-scale parameters in table 6.1 for a range of axial-vector-diquark–photon vertex parameters, centred on the point-particle values of $\mu_{1^+} = 2$ and $\chi_{1^+} = 1$, equation (6.77), and $\kappa_{\mathcal{T}} = 2$, equation (6.83). Columns labelled σ give the percentage-difference from results obtained with the reference values. $r_n := -\sqrt{-\langle r_n^2\rangle}$. Values inferred from experiment are [MMD96]: $r_p = 0.847$ and $r_n = -0.336$.

			set A				set B			
μ_{1^+}	χ_{1^+}	$\kappa_{\mathcal{T}}$	r_p	$\sigma^A_{r_p}$	r_n	$\sigma^A_{r_n}$	r_p	$\sigma^B_{r_p}$	r_n	$\sigma^B_{r_n}$
1	1	2	0.599	-1.2	0.185	-4.1	0.596	0.2	0.171	1.2
2	1	2	0.606		0.193		0.595		0.169	
3	1	2	0.614	1.3	0.200	3.6	0.593	-0.3	0.167	-1.2
2	0	2	0.593	-2.2	0.179	-7.3	0.575	-3.4	0.145	-14.2
2	2	2	0.620	2.3	0.205	6.2	0.614	3.2	0.191	13.0
2	1	1	0.606	0.0	0.189	-2.1	0.595	0.0	0.167	-1.2
2	1	3	0.606	0.0	0.196	1.6	0.595	0.0	0.172	1.8

The radii, particularly that of the neutron, are most sensitive to changes in the axial-vector diquarks' electric quadrupole moment, χ_{1^+}. This is not surprising given that χ_{1^+} is the only model parameter that speaks directly of the axial-vector diquarks' electric charge distribution. The radii's insensitivity to $\kappa_{\mathcal{T}}$, the strength of the scalar $\leftrightarrow$ axial-vector transition, is concordant with the discussion in section 6.4.4. With the reference values given in equations (6.77) and (6.83), set A underestimates the proton radius by 30% and the magnitude of the neutron radius by 43%, while for set B these differences are 32% and 50%, respectively.

Table 6.3 presents results for the nucleons' magnetic radii. They are insensitive to the axial-vector diquarks' quadrupole moment but react to the diquarks' magnetic moment

Table 6.3: Magnetic radii, in fm, calculated with the diquark mass-scales in table 6.1 and the parameter range described in table 6.2. Columns labelled σ give the percentage-difference from results obtained with the reference values: $\mu_{1^+} = 2$, $\chi_{1^+} = 1$, $\kappa_{\mathcal{T}} = 2$. Values inferred from experiment are [MMD96]: $r_p^\mu = 0.836$ and $r_n^\mu = 0.889$.

			set A				set B			
μ_{1^+}	χ_{1^+}	$\kappa_{\mathcal{T}}$	r_p^μ	$\sigma^A_{r_p^\mu}$	r_n^μ	$\sigma^A_{r_n^\mu}$	r_p^μ	$\sigma^B_{r_p^\mu}$	r_n^μ	$\sigma^B_{r_n^\mu}$
1	1	2	0.456	-2.4	0.467	-1.3	0.442	-1.6	0.446	-0.7
2	1	2	0.467		0.473		0.449		0.449	
3	1	2	0.477	2.1	0.478	1.1	0.454	1.1	0.454	1.1
2	0	2	0.467	0.0	0.473	0.0	0.449	0.0	0.449	0.0
2	2	2	0.467	0.0	0.473	0.0	0.449	0.0	0.449	0.0
2	1	1	0.470	0.6	0.480	1.3	0.453	0.9	0.459	2.2
2	1	3	0.465	-0.4	0.472	-0.2	0.445	-0.9	0.446	-0.7

as one would anticipate: increasing in magnitude as μ_{1^+} increases. Moreover, consistent with expectation, section 6.4.4, these radii also respond to changes in $\kappa_{\mathcal{T}}$, decreasing as this parameter is increased. With the reference values in equations (6.77) and (6.83), both sets underestimate r_N^μ by approximately 40%.

Table 6.4 lists results for the nucleons' magnetic moments. They, too, are insensitive to the axial-vector diquarks' quadrupole moment but react to the diquarks' magnetic moment, increasing quickly in magnitude as μ_{1^+} increases. As anticipated in section 6.4.4, the nucleons' moments respond strongly to alterations in the strength of the scalar $\leftrightarrow$ axial-vector transition, increasing rapidly as $\kappa_{\mathcal{T}}$ is increased. Set A, which is fitted to the experimental values of M_N and M_Δ, describes the nucleons' moments quite well: κ_p is 15% too large; and $|\mu_n|$, 16% too small. On the other hand, set B, which is fitted to baryon masses that are inflated so as to make room for pion cloud effects, overestimates κ_p by 47% and $|\mu_n|$ by 18%.

Nucleon electromagnetic form factors associated with the tabulated values of static properties are presented in Figs. 6.2–6.4. These figures confirm and augment the information in tables 6.2–6.4. Consider, e.g., the electric form factors. One observes that the differences between results obtained with set A and set B generally outweigh those delivered by variations in the parameters characterising the axial-vector diquark's electromagnetic properties. The proton's electric form factor, in particular, is largely insensitive to these parameters, and it is apparent that the nucleon's electric form factor only responds notably to variations in χ_{1^+}, figure 6.3. The nucleons' magnetic form factors exhibit the

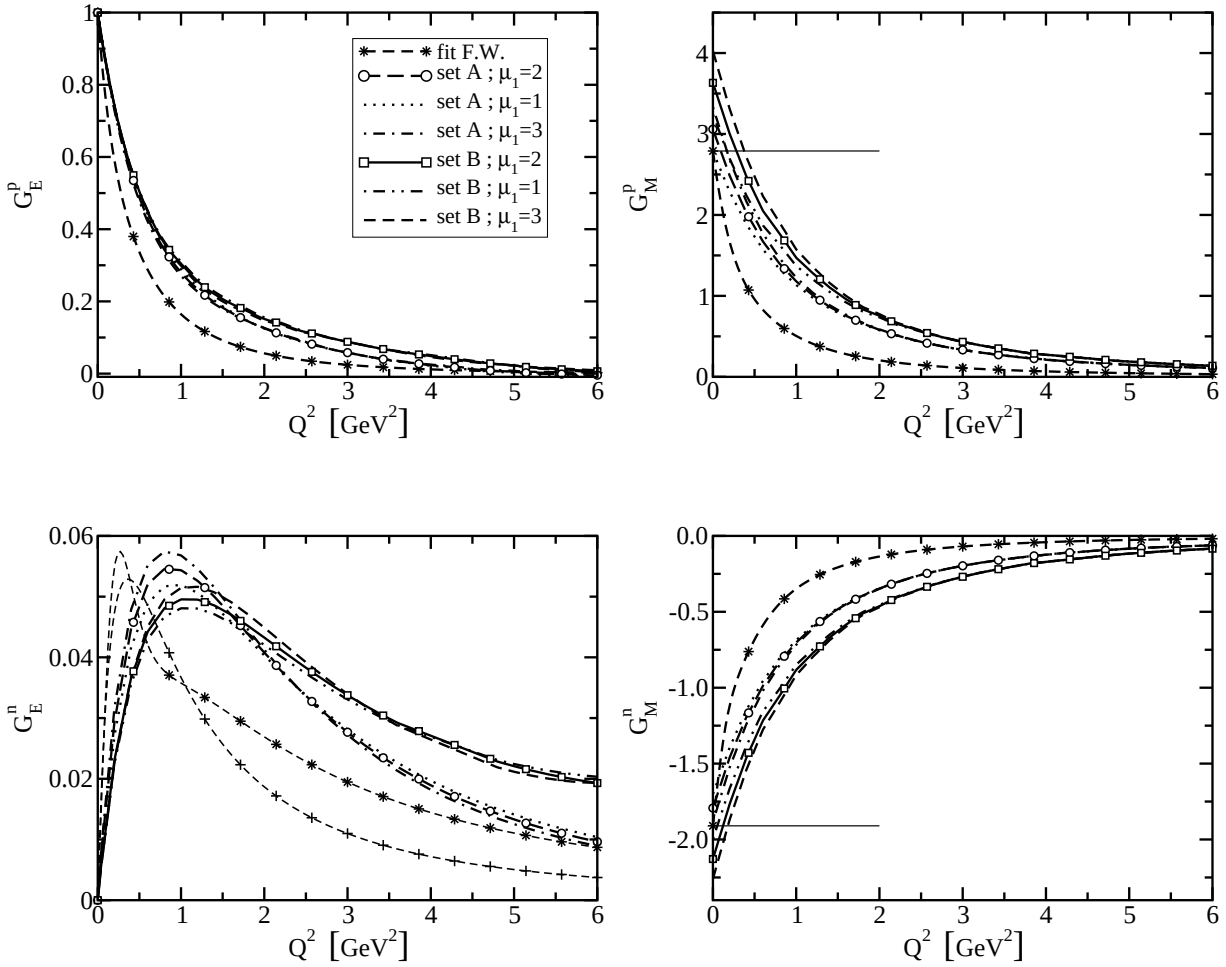

Figure 6.2: Response of nucleon form factors to variations in the magnetic moment of the axial-vector diquark: $\mu_{1^+} = 1, 2, 3$; with $\chi_{1^+} = 1$, $\kappa_{\mathcal{T}} = 2$. The legend in the top-left panel applies to all; the dashed-line marked by "$*$" is a fit to experimental data [FW03] and the dashed-line marked by "$+$" in the lower-left panel is the fit to $G_E^n(Q^2)$ of reference [G$^+$71]; and the horizontal lines in the right panels mark the experimental value of the nucleon's magnetic moment.

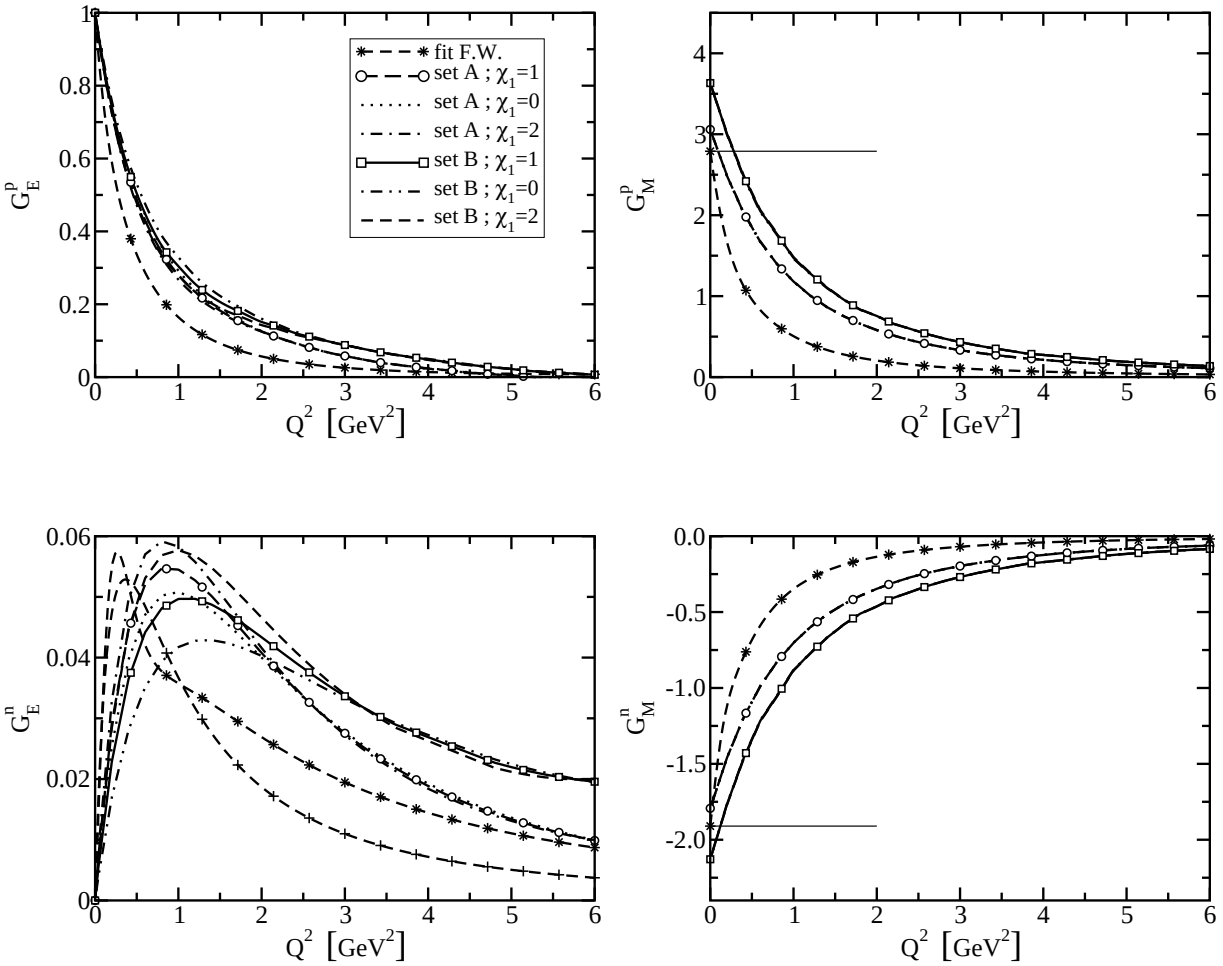

Figure 6.3: Response of nucleon form factors to variations in the electric quadrupole moment of the axial-vector diquark: $\chi_{1^+} = 0, 1, 2$; with $\mu_{1^+} = 2$, $\kappa_{\mathcal{T}} = 2$. The other features are described in the caption of figure 6.2.

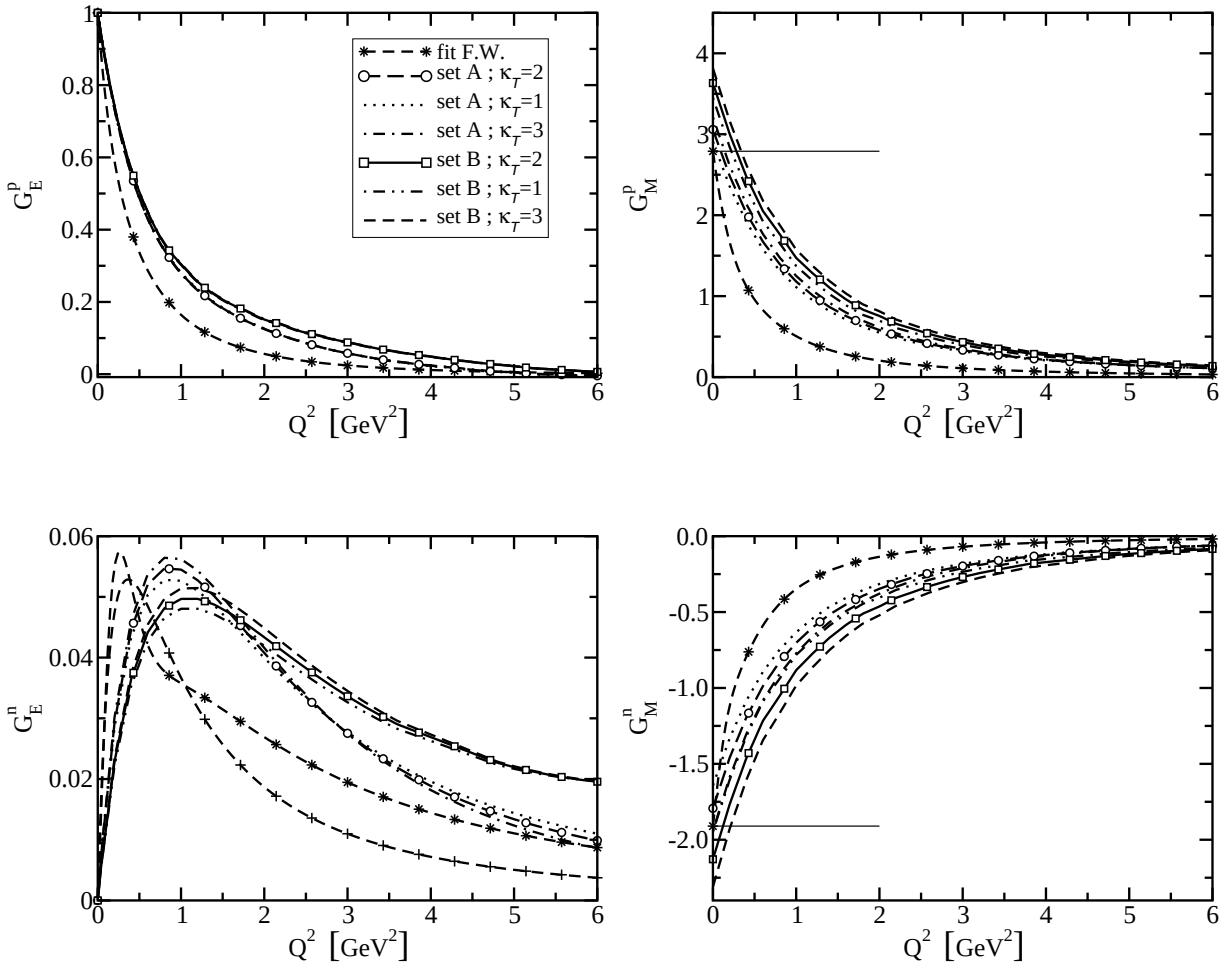

Figure 6.4: Response of nucleon form factors to variations in the strength of the electromagnetic axial-vector $\leftrightarrow$ scalar diquark transition: $\kappa_{\mathcal{T}} = 1, 2, 3$; with $\mu_{1^+} = 2$, $\chi_{1^+} = 1$. The other features are described in the caption of figure 6.2.

Table 6.4: Magnetic moments, in nuclear magnetons, calculated with the diquark mass-scales in table 6.1 and the parameter range described in table 6.2. Columns labelled σ give the percentage-difference from results obtained with the reference values: $\mu_{1^+} = 2$, $\chi_{1^+} = 1$, $\kappa_{\mathcal{T}} = 2$. Experimental values are: $\kappa_p := \mu_p - 1 = 1.79$ and $\mu_n = -1.91$.

			set A				set B			
μ_{1^+}	χ_{1^+}	$\kappa_{\mathcal{T}}$	κ_p	$\sigma^A_{\kappa_p}$	$\lvert\mu_n\rvert$	$\sigma^A_{\lvert\mu_n\rvert}$	κ_p	$\sigma^B_{\kappa_p}$	$\lvert\mu_n\rvert$	$\sigma^B_{\lvert\mu_n\rvert}$
1	1	2	1.79	-15.3	1.70	-5.1	2.24	-21.9	2.00	-6.2
2	1	2	2.06		1.79		2.63		2.13	
3	1	2	2.33	15.4	1.88	5.1	3.02	21.9	2.26	6.1
2	0	2	2.06	0.0	1.79	0.0	2.63	0.0	2.13	0.0
2	2	2	2.06	0.0	1.79	0.0	2.63	0.0	2.13	0.0
2	1	1	1.91	-8.4	1.64	-8.4	2.45	-10.1	1.95	-8.5
2	1	3	2.21	8.4	1.85	8.3	2.82	10.1	2.31	8.5

greatest sensitivity to the axial-vector diquarks's electromagnetic properties but in this case, too, the differences between set A and set B are more significant. For $Q^2 \gtrsim 4\,\mathrm{GeV}^2$ there is no sensitivity to the diquarks' electromagnetic parameters in any curve. This is naturally because our parametrisation expresses the perturbative limit, equation (6.78). It is thus apparent from these figures that the behaviour of the nucleons' form factors is primarily determined by the information encoded in the Faddeev amplitudes.

Our results show that the nucleons' electromagnetic properties are sensitive to the strength of axial-vector diquark correlations in the bound state and react to the electromagnetic properties of these correlations. In all cases the dependence is readily understood intuitively. However, taken together our results indicate that one cannot readily tune the model's parameters to provide a uniformly good account of nucleon properties: something more than dressed-quark and -diquark degrees of freedom is required.

Chiral corrections

It is appropriate now to examine effects that arise through coupling to pseudoscalar mesons. As with baryon masses, there are two types of contributions from meson loops to electromagnetic form factors: regularisation-scheme-dependent terms, which are analytic in the neighbourhood of $\hat{m} = 0$, and nonanalytic scheme-independent terms. For the static properties presented in tables 6.2–6.4, the leading-order scheme-independent contributions

are [KM01]

$$\langle r^2_{\substack{p\\n}}\rangle^{1-loop}_{NA} = \mp\frac{1+5g_A^2}{32\pi^2 f_\pi^2}\,\ln\left(\frac{m_\pi^2}{M_N^2}\right), \tag{6.90}$$

$$\langle (r^\mu_N)^2\rangle^{1-loop}_{NA} = -\frac{1+5g_A^2}{32\pi^2 f_\pi^2}\,\ln\left(\frac{m_\pi^2}{M_N^2}\right) + \frac{g_A^2\,M_N}{16\pi f_\pi^2\mu_v}\frac{1}{m_\pi}, \tag{6.91}$$

$$(\mu_{\substack{p\\n}})^{1-loop}_{NA} = \mp\frac{g_A^2\,M_N}{4\pi^2 f_\pi^2}\,m_\pi, \tag{6.92}$$

where $g_A = 1.26$, $f_\pi = 0.0924\,\mathrm{GeV} = 1/(2.13\,\mathrm{fm})$, $\mu_v = \mu_p - \mu_n$. Clearly, the radii diverge in the chiral limit, a frequently advertised aspect of chiral corrections.

While these scheme-independent terms are fixed, at physical values of the pseudoscalar meson masses they do not usually provide the dominant contribution to observables: that is provided by the regularisation-parameter-dependent terms. This is apparent for baryon masses in reference [H$^+$02] and for the pion charge radius in reference [ABR95]. It is particularly important here, as is made plain by a consideration of the neutron charge radius. From equation (6.90), one obtains

$$\langle r_n^2\rangle^{1-loop}_{NA} = -\,(0.48\,\mathrm{fm})^2, \tag{6.93}$$

which is more than twice the experimental value. On the other hand, the contribution from the low energy constants is [KM01]

$$\langle r_n^2\rangle^{1-loop}_{lec} = +\,(0.69\,\mathrm{fm})^2, \tag{6.94}$$

which is four-times larger in magnitude than the experimental value and has the opposite sign. This emphasises the delicate cancellation that is arranged in chiral perturbation theory to fit the neutron's charge radius. In this instance the remaining important piece is the neutron's Foldy term: $3\mu_n/(2M_n^2) = -(0.35\,\mathrm{fm})^2$, which is also a fitted quantity. Moreover, for the magnetic radii it is established that, at the physical pion mass, the leading chiral limit behaviour is not a good approximation [KM01]. Additional discussion of issues that arise in formulating a chiral expansion in the baryon sector and its convergence may be found in reference [FGS04].

Since regularisation-parameter-dependent parts of the chiral loops are important we follow reference [ALTY04] and estimate the corrections using modified formulae that incorporate a single parameter which mimics the effect of regularising the integrals. Thus

Table 6.5: Row 1 – static properties calculated with set B diquark masses, table 6.1, and $\mu_{1^+} = 2$, $\chi_{1^+} = 1$, $\kappa_{\mathcal{T}} = 2$: charge radii in fm, with r_n defined in table 6.2; and magnetic moments in nuclear magnetons. Row 2 adds the corrections of equations (6.95)–(6.97) with $\lambda = 0.3\,\mathrm{GeV}$. ς in row n, is the rms relative-difference between the entries in row n and 3.

	r_p	r_n	r_p^μ	r_n^μ	μ_p	$-\mu_n$	ς
q-(qq) core	0.595	0.169	0.449	0.449	3.63	2.13	0.39
$+\pi$-loop correction	0.762	0.506	0.761	0.761	3.05	1.55	0.23
experiment	0.847	0.336	0.836	0.889	2.79	1.91	

equations (6.90) and (6.91) are rewritten

$$\langle r^2_{\substack{p\\n}}\rangle^{1-loop^R}_{NA} = \mp \frac{1+5g_A^2}{32\pi^2 f_\pi^2}\,\ln(\frac{m_\pi^2}{m_\pi^2+\lambda^2})\,, \tag{6.95}$$

$$\langle (r_N^\mu)^2\rangle^{1-loop^R}_{NA} = -\frac{1+5g_A^2}{32\pi^2 f_\pi^2}\,\ln(\frac{m_\pi^2}{m_\pi^2+\lambda^2}) + \frac{g_A^2\,M_N}{16\pi f_\pi^2 \mu_v}\frac{1}{m_\pi}\,\frac{2}{\pi}\arctan(\frac{\lambda}{m_\pi})\,, \tag{6.96}$$

$$(\mu_{\substack{p\\n}})^{1-loop^R}_{NA} = \mp \frac{g_A^2\,M_N}{4\pi^2 f_\pi^2}\,m_\pi\,\frac{2}{\pi}\arctan(\frac{\lambda^3}{m_\pi^3})\,, \tag{6.97}$$

wherein λ is a regularisation mass-scale, for which a typical value is $\sim 0.4\,\mathrm{GeV}$ [ALTY04]. As required the loop contributions vanish when the pion mass is much larger than the regularisation scale: very massive states must decouple from low-energy phenomena.

We return now to the calculated values of the nucleons' static properties, tables 6.2–6.4, and focus on the set B results obtained with $\mu_{1^+} = 2$, $\chi_{1^+} = 1$, $\kappa_{\mathcal{T}} = 2$. Recall that set B was chosen to give inflated values of the nucleon and Δ masses in order to make room for chiral corrections, and therefore one may consistently apply the corrections in equations (6.92), (6.95) and (6.96) to the static properties. With $\lambda = 0.3\,\mathrm{GeV}$ this yields the second row in table 6.5: the regularised chiral corrections reduce the rms relative-difference significantly. This crude analysis suggests that a veracious description of baryons can be obtained using dressed-quark and -diquark degrees of freedom augmented by a sensibly regulated pseudoscalar meson cloud.

Form factor ratios

In figure 6.5 we plot the ratio $\mu_p\,G_E^p(Q^2)/G_M^p(Q^2)$. The behaviour of the experimental data at small Q^2 is readily understood. In the neighbourhood of $Q^2 = 0$,

$$\mu_p\,\frac{G_E^p(Q^2)}{G_M^p(Q^2)} = 1 - \frac{Q^2}{6}\,\left[(r_p)^2 - (r_p^\mu)^2\right]\,, \tag{6.98}$$

and because $r_p \approx r_p^\mu$ the ratio varies by less than 10% on $0 < Q^2 < 0.6\,\mathrm{GeV}^2$, if the form factors are approximately dipole. This is evidently true of the experimental data. In our calculation, without chiral corrections, table 6.2 and 6.3, $r_p > r_p^\mu$. Hence the ratio must fall immediately with increasing Q^2. Incorporating pion loops, we obtain the results in Row 2 of table 6.5, which have $r_p \approx r_p^\mu$. The small Q^2 behaviour of this ratio is thus materially affected by the proton's pion cloud.

True pseudoscalar mesons are not pointlike and therefore pion cloud contributions to form factors diminish in magnitude with increasing Q^2. For example, in a study of the $\gamma N \to \Delta$ transition [SL01], pion cloud contributions to the M1 form factor fall from 50% of the total at $Q^2 = 0$ to $\lesssim 10\%$ for $Q^2 \gtrsim 2\,\mathrm{GeV}^2$. Hence, the evolution of $\mu_p\, G_E^p(Q^2)/G_M^p(Q^2)$ on $Q^2 \gtrsim 2\,\mathrm{GeV}^2$ is primarily determined by the quark core of the proton. This is evident in figure 6.5, which illustrates that, on $Q^2 \in (1,5)\,\mathrm{GeV}^2$, $\mu_p\, G_E^p(Q^2)/G_M^p(Q^2)$ is sensitive to the parameters defining the axial-vector-diquark–photon vertex. The response diminishes with increasing Q^2 because our parametrisation expresses the perturbative limit, equation (6.78).

The behaviour of $\mu_p\, G_E^p(Q^2)/G_M^p(Q^2)$ on $Q^2 \gtrsim 2\,\mathrm{GeV}^2$ is determined either by correlations expressed in the Faddeev amplitude, the electromagnetic properties of the constituent degrees of freedom, or both. The issue is decided by the fact that the magnitude and trend of the results are not materially affected by the axial-vector-diquarks' electromagnetic parameters. This observation suggests strongly that the ratio's evolution is due primarily to spin-isospin correlations in the nucleon's Faddeev amplitude. One might question this conclusion, and argue instead that the difference between the results depicted for set A cf. set B originates in the larger quark-core nucleon mass obtained with set B (table 6.1) which affects $G_E^p(Q^2)$ through equation (6.50). We checked and that is not the case. Beginning with the set B results for $F_{1,2}$ we calculated the electric form factor using the set A nucleon mass and then formed the ratio. The result is very different from the internally consistent set A band in figure 6.5; e.g., it drops more steeply and lies uniformly below, and crosses zero for $Q^2 \approx 3.7\,\mathrm{GeV}^2$.

It is noteworthy that set B, which anticipates pion cloud effects, is in reasonable agreement with both the trend and magnitude of the polarisation transfer data [J$^+$00, G$^+$01, G$^+$02]. It should be stressed that neither this nor the Rosenbluth [W$^+$94] data played any role in the preceding analysis or discussion.

The extension of the calculation for set B to higher momenta is displays in figure 6.6. The form factor ration passes through zero at $Q^2 \approx 6.5 GeV^2$. This prediction still awaits an experimental test. In our model the existence of the zero is robust but its location depends on the model's parameters.

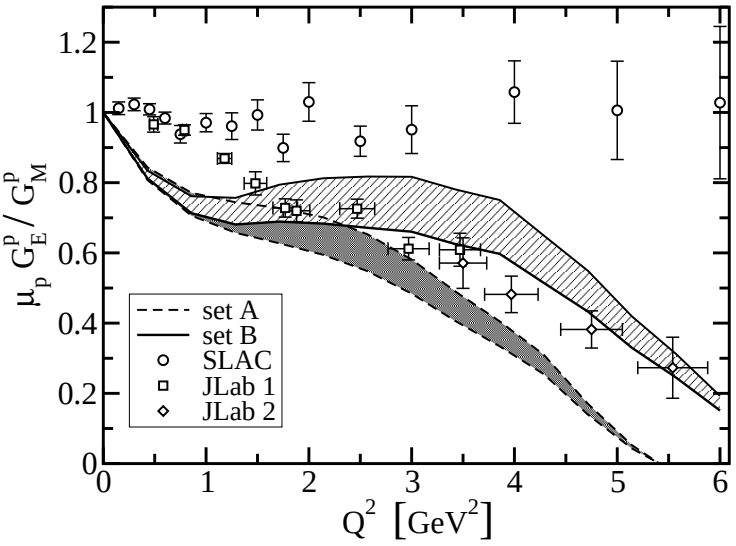

Figure 6.5: Proton form factor ratio: $\mu_p\, G_E^p(Q^2)/G_M^p(Q^2)$. Calculated results: *lower band* - set A in table 6.1; and *upper band* - set B. For both bands, $G_E^p(Q^2)$ was calculated using the point-particle values: $\mu_{1^+} = 2$ and $\chi_{1^+} = 1$, equation (6.77), and $\kappa_{\mathcal{T}} = 2$, equation (6.83); i.e., the reference values in tables 6.2–6.4. Variations in the axial-vector diquark parameters used to evaluate $G_E^p(Q^2)$ have little effect on the plotted results. The width of the bands reflects the variation in $G_M^p(Q^2)$ with axial-vector diquark parameters and, in both cases, the upper border is obtained with $\mu_{1^+} = 3$, $\chi_{1^+} = 1$ and $\kappa_{\mathcal{T}} = 2$, while the lower has $\mu_{1^+} = 1$. The data are: *squares* - reference [J$^+$00]; *diamonds* - reference [G$^+$02]; and *circles* - reference [W$^+$94].

We have also examined the proton's Dirac and Pauli form factors in isolation. On the domain covered, neither $F_1(Q^2)$ nor $F_2(Q^2)$ show any sign they have achieved the asymptotic behaviour anticipated from perturbative QCD.

In figure 6.7 we depict weighted ratios of these form factors. Our numerical results are consistent with

$$\sqrt{Q^2}\,\frac{F_2(Q^2)}{F_1(Q^2)} \approx \text{constant},\ 2 \lesssim Q^2(\text{GeV}^2) \lesssim 6\,, \tag{6.99}$$

as are the polarisation transfer data (however, a calculation for set B and higher momenta indicates that this relations fails for $Q^2 \gtrsim 6\text{GeV}^2$, cf. figure 6.8) . Such behaviour has been argued to indicate the presence of substantial orbital angular momentum in the proton [MF02, RJ04]. Orbital angular momentum is not a Poincaré invariant. However, if absent in a particular frame, it will almost inevitably appear in another frame related via a Poincaré transformation. Nonzero quark orbital angular momentum is the necessary

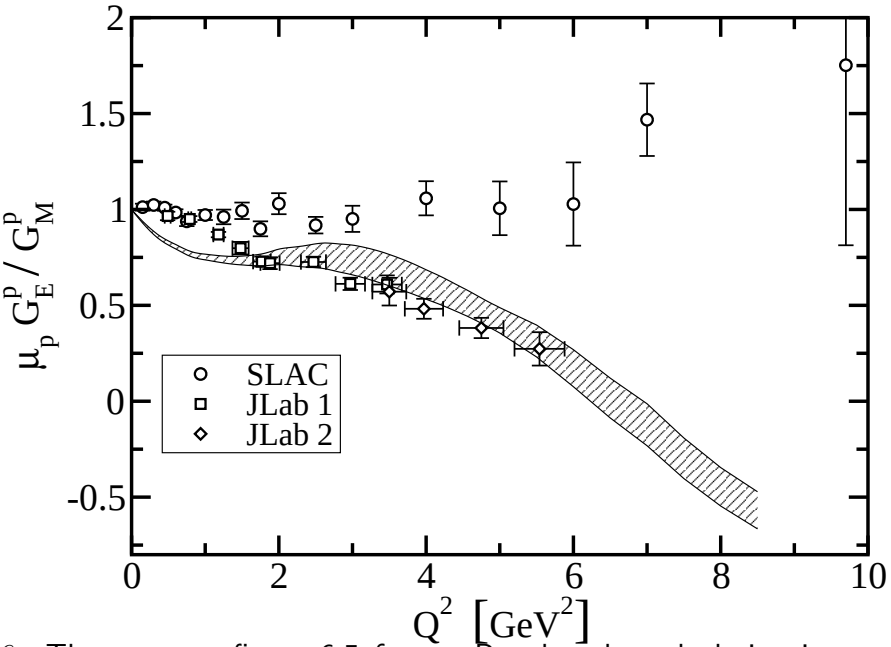

Figure 6.6: The same as figure 6.5 for set B only: the calculation is expanded to higher momenta.

outcome of a Poincaré covariant description. This is why the covariant Faddeev amplitude describing a nucleon is a matrix-valued function with a rich structure that, in the nucleons' rest frame, corresponds to a relativistic wave function with s-wave, p-wave and even d-wave components [Oet00]. The result in figure 6.7 is not significantly influenced by details of the diquarks' electromagnetic properties. Instead, the behaviour is primarily governed by correlations expressed in the proton's Faddeev amplitude and, in particular, by the amount of intrinsic quark orbital angular momentum [BKR03]. This phenomenon is analogous to that observed in connection with the pion's electromagnetic form factor. In that instance axial-vector components of the pion's Bethe-Salpeter amplitude are responsible for the large Q^2 behaviour of the form factor: they alone ensure $Q^2 F_\pi(Q^2) \approx$ constant for truly ultraviolet momenta [MR98]. These components are required by covariance [MRT98] and signal the presence of quark orbital angular momentum in the pseudoscalar pion.

In figure 6.9 we plot another weighted ratio of Pauli and Dirac form factors. A perturbative QCD analysis [BJY03] that considers effects arising from both the proton's leading- and subleading-twist light-cone wave functions, the latter of which represents quarks with one unit of orbital angular momentum, suggests

$$\frac{Q^2}{[\ln Q^2/\Lambda^2]^2}\,\frac{F_2(Q^2)}{F_1(Q^2)} = \text{constant},\ Q^2 \gg \Lambda^2\,, \tag{6.100}$$

where Λ is a mass-scale that corresponds to an upper-bound on the domain of nonpertur-

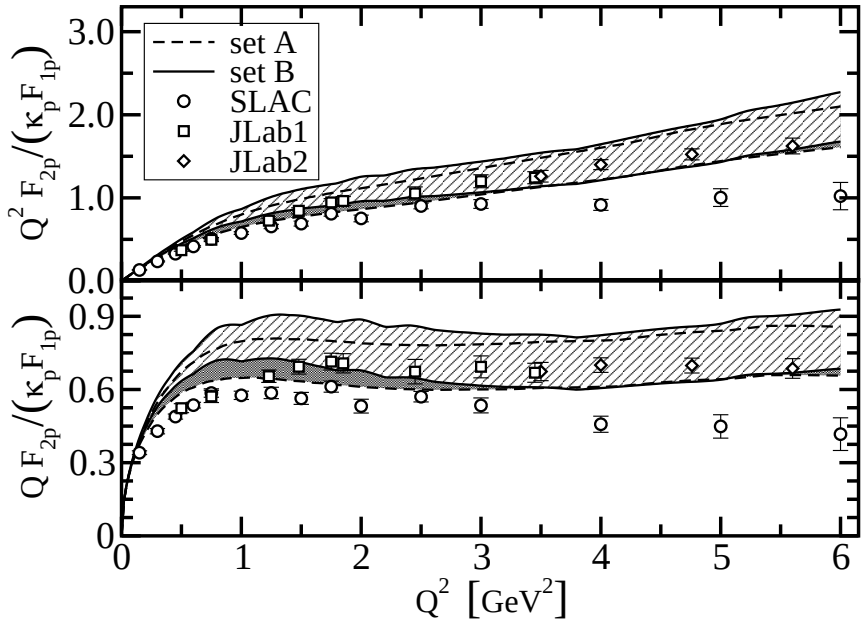

Figure 6.7: Proton Pauli/Dirac form factor ratios. The data are as described in figure 6.5, as are the bands except that here the upper border is obtained with $\mu_{1^+} = 1$, $\chi_{1^+} = 1$ and $\kappa_{\mathcal{T}} = 2$, and the lower with $\mu_{1^+} = 3$.

bative (soft) momenta. This scaling hypothesis is not predictive unless the value of Λ is known *a priori*. However, Λ cannot be computed in perturbation theory.

A scale of this type is not an elemental input to our calculation. It is instead a derivative quantity that expresses the net integrated effect of many basic features, among which are the mass-scale characterising quark-dressing and that implicit in the support of the Faddeev amplitude. Extending our calculation to larger Q^2 is not a problem in principle, and the numerical challenge are met by choosing something more powerful than a single desktop computer.

One needs an estimate of a reasonable value for Λ. The nucleon's mass, M_N, is one natural mass-scale in our calculation. Other relevant mass-scales are those which characterise the electromagnetic size of the nucleon and its constituents. A dipole mass-scale for the proton is approximately 0.85 GeV. The dressed-quark-photon-vertex is characterised by a monopole mass-scale of 0.8 GeV [BKR03] and the diquark-photon vertices by monopole mass-scales $\sqrt{3}\, m_{J^P} \approx 1.0$ - 1.5 GeV, equations (6.62) and (6.72).

As an adjunct one can consider the dressed-quark mass function, defined in equa-

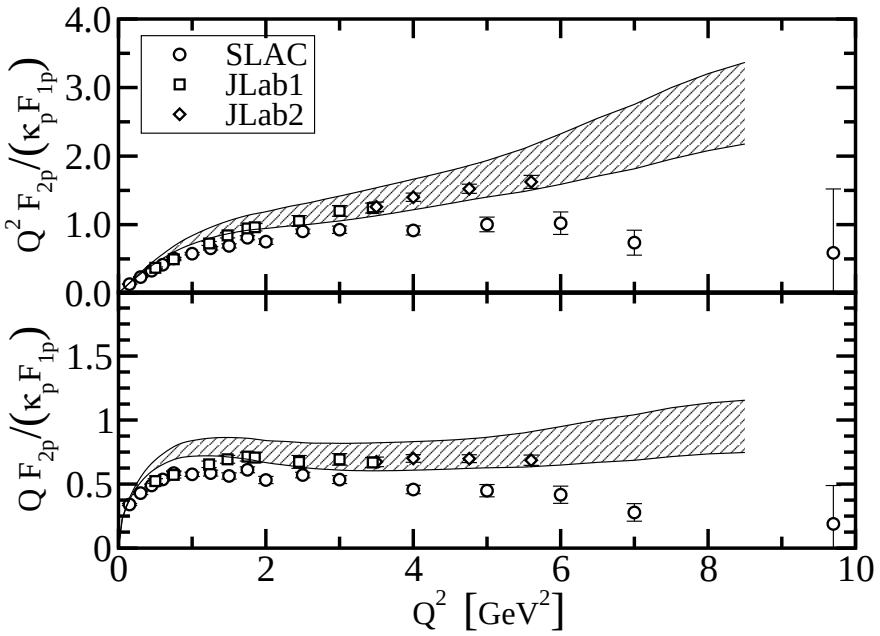

Figure 6.8: The same as figure 6.7 for set B only: the calculation is expanded to higher momenta.

tion (6.30) and discussed thereabout. A nonzero mass function in the chiral limit is an essentially nonperturbative phenomenon. Hence the ratio

$$R_u^0(Q^2) := \frac{M_{\hat{m}=0}(Q^2)}{M_{\hat{m}_u}(Q^2)} \tag{6.101}$$

vanishes on the perturbative-Q^2 domain. For $Q^2 = 0$, on the other hand, calculations typically yield [HKRW05] $R_u^0(0) = 0.96$; i.e., the mass function's behaviour is almost completely nonperturbative. The Q^2-evolution of $R_u^0(Q^2)$ can therefore guide in demarcating the nonperturbative domain. Reference [BPRT03] provides a mass-function that agrees pointwise with quenched-QCD lattice data and gives a unique chiral-limit mass function. From these results one finds that $R_u^0(Q^2 > 4M_N^2) < 0.5\, R_u^0(0)$. Therefore perturbative effects are dominant in the u-quark mass function on $Q^2 \in (4M_N^2, \infty)$. On the other hand, $0.8 < R_u^0(Q^2 < M_N^2)$ and hence the u-quark mass function is principally nonperturbative on $Q^2 \in [0, M_N^2]$.

Together these observations suggest that, in our model and in QCD, a judicious estimate of the least-upper-bound on the domain of soft momenta is $\Lambda = M_N$, and this is the value employed in figure 6.9: the figure does not provide compelling evidence for equation (6.100) on the domain up to $6\,\mathrm{GeV}^2$. One can attempt to *fit* equation (6.100) to the calculated results or data, and [BJY03] $\Lambda = \Lambda_{\mathrm{fit}} \approx 0.3\,\mathrm{GeV}$, provides fair agreement. However, this value is significantly smaller than the natural scales we have identified in the

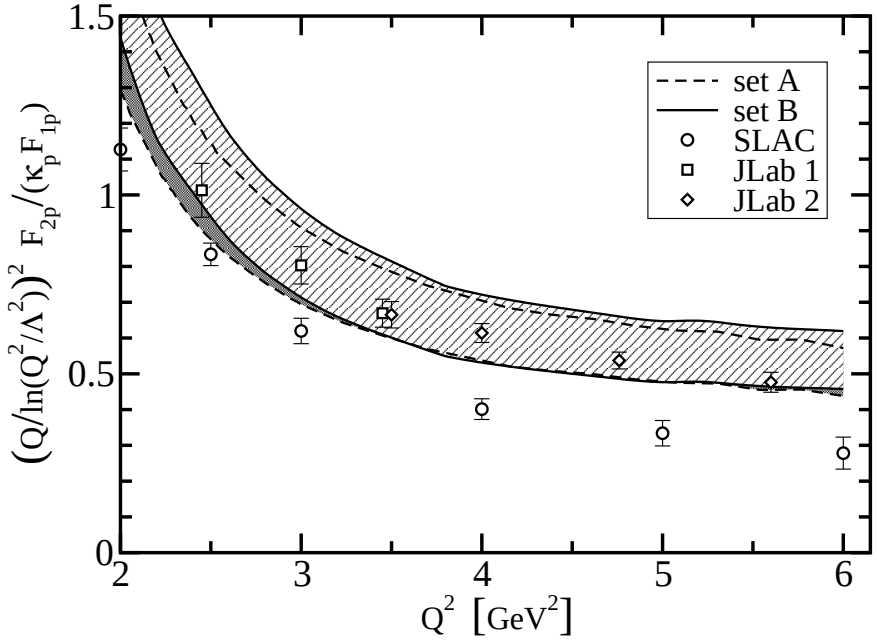

Figure 6.9: Weighted proton Pauli/Dirac form factor ratio, calculated with $\Lambda = M_N = 0.94$ GeV. The bands are as described in figure 6.7, as are the data.

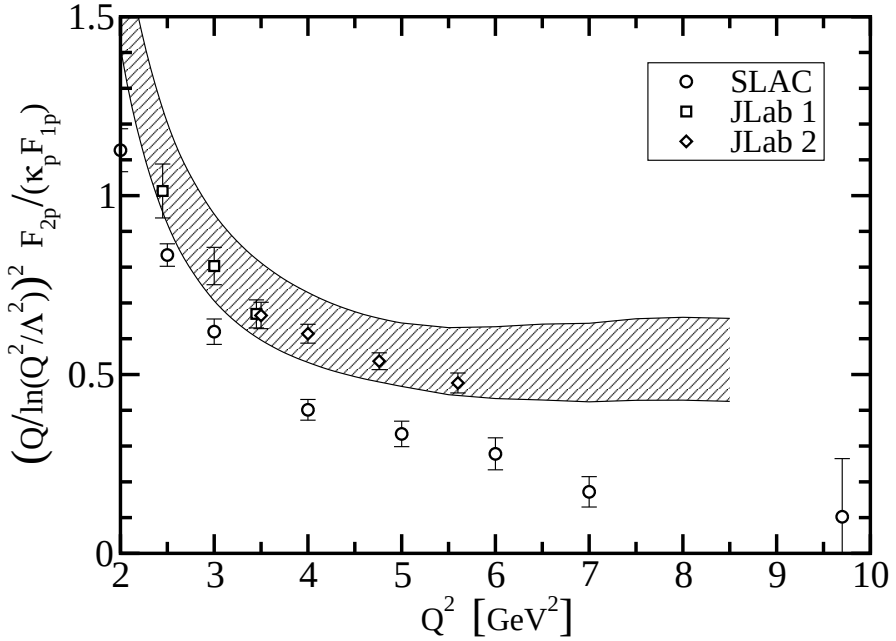

Figure 6.10: The same as figure 6.9 for set B only: the calculation is expanded to higher momenta.

model and $R_u^0(\Lambda^2_{\text{fit}}) = 0.98\, R_u^0(0)$. In figure 6.10 we extended the calculations for set B to higher momenta. The results hint that the relation (6.100) may be valid for $Q^2 \gtrsim 6\,\text{GeV}^2$.

Chapter 7

Epilogue

In this thesis we have treated the elementary two-point function of quarks in QCD within Coulomb gauge and implications for hadronic observables and models. We have presented results for the rainbow truncated gap equation in the chiral limit keeping only the instantaneous time-time component of the gluon propagator. Since in Coulomb gauge this quantity corresponds to the colour Coulomb potential, which is calculated in lattice gauge theory, our ansatz is based on these numbers. Regulating the appearing infrared divergence we extract a mass function, which gives a third of the desired constituent quark mass in the infrared. To improve upon this we introduce transverse components with retardation in the gluon propagator ansatz, which is inspired by recent calculations in the Hamiltonian picture. However, the mass function shows no considerable increase after this extension. An explanation for this can be traced in the fact that a sizeable contribution has to come from a dressing of the quark-gluon vertex. An infrared analysis for the quark-gluon vertex carried out in Landau gauge [AFLE06], which showed an infrared enhancement, can be analogously performed in Coulomb gauge. However, a computation of the quark-gluon vertex is tedious and even a one-loop calculation awaits completion [Lic].

Hence Coulomb gauge calculations involving the quark propagator are currently limited to qualitative studies only. We obtain solutions of the homogeneous Bethe-Salpeter equation for the pseudoscalar and vector mesons as well as for scalar and axialvector diquarks. In the limit of a vanishing infrared regulator the diquark masses diverge, while meson masses and radii of both mesons and diquarks remain finite and well-defined. This suggests that diquarks might be reasonable degrees of freedom in describing baryons, especially the nucleon.

Taking this implication serious we subsequently treat the Faddeev equation of the nucleon in a diquark-quark approximation, which maintains Poincaré covariance, and use the results to calculate nucleon form factors in this framework. In contrast to the chapters

before we employ Landau gauge for these examinations.

We solved the covariant Faddeev equations numerically to obtain masses and amplitudes for the nucleon and Δ. Two parameters appear in the model Faddeev equation: masses of the scalar and axial-vector diquark correlations. They were fixed by fitting stipulated masses of the baryons. We interpreted the masses and Faddeev amplitudes thus obtained as representing properties of the baryons' "quark core," and argued that this should be augmented in a consistent fashion by chiral-loop corrections.

We explained subsequently the formulation of a nucleon-photon vertex, which automatically ensures the vector Ward-Takahashi identity is fulfilled for on-shell nucleons described by the calculated Faddeev amplitudes. This guarantees current conservation. The vertex *Ansatz* involves three parameters. Two of these specify electromagnetic properties of axial-vector diquarks and a third measures the strength of electromagnetically induced axial-vector- $\leftrightarrow$ scalar-diquark transitions. These quantities are also properties of the nucleons' quark core.

The elements just described are sufficient for a calculation of the quark contribution to the nucleons' electromagnetic form factors. We explored a reasonable range of nucleon-photon-vertex parameter values and found that an accurate description of the nucleons' static properties was not possible with the core components alone. However, this mismatch with experiment was greatly reduced by the inclusion of chiral corrections.

We calculated ratios of the proton's form factors. On the whole domain of nucleon-photon-vertex parameter values explored, the calculated behaviour of $G_E^p(Q^2)/G_M^p(Q^2)$ for $Q^2 \gtrsim 2\,\mathrm{GeV}^2$ agrees with that inferred from contemporary polarisation transfer data. Moreover, with the same insensitivity to parameters, the ratio was seen to give $\sqrt{Q^2}F_2(Q^2)/F_1(Q^2) \approx$ constant on $Q^2 \in [2,6]\,\mathrm{GeV}^2$. For higher momenta this relation seems to fail. Since the parameters in the nucleon-photon vertex do not influence these outcomes, we judge they are manifestations of features intrinsic to the nucleon's Faddeev amplitude. In the nucleon's rest frame, this amplitude corresponds to a relativistic wave function with s-, p- and even d-wave quark orbital angular momentum components.

In our view baryons can realistically be seen as a dominant Poincaré covariant quark core, augmented by pseudoscalar meson cloud contributions that, e.g., make a noticeable contribution to form factors for $Q^2 \lesssim 2\,\mathrm{GeV}^2$. Meson compositeness ensures that such contributions diminish with increasing Q^2. Hence future experiments at larger Q^2 will serve as an instructive probe of correlations in baryon wave functions, i.e. their Faddeev amplitudes. Combined with further knowledge about QCD's quark propagator, the structure of the 2-quark correlations and a more sophisticated treatment of chiral corrections this is likely to make clear if quarks and diquarks are suitable degrees of freedom for describing

the nucleon.

Appendix A

Units and Conventions

In this work we use natural units, i.e.

$$\hbar = c = 1 \ . \tag{A.1}$$

A.1 Conventions in Minkowski space

In Minkowski space our metric is $g = \mathrm{diag}[1, -1, -1, -1]$. A collection of relations for the γ-matrices can be found in the appendix of [IZ]. They satisfy

$$\{\gamma_\mu, \gamma_\nu\} = 2\, g_{\mu\nu} \ . \tag{A.2}$$

A.2 Euclidean conventions

In our Euclidean formulation:

$$p \cdot q = \sum_{i=1}^{4} p_i q_i \, ; \tag{A.3}$$

$$\{\gamma_\mu, \gamma_\nu\} = 2\,\delta_{\mu\nu} \, ; \ \gamma_\mu^\dagger = \gamma_\mu \, ; \ \sigma_{\mu\nu} = \frac{i}{2}[\gamma_\mu, \gamma_\nu] \, ; \ \mathrm{tr}[\gamma_5\gamma_\mu\gamma_\nu\gamma_\rho\gamma_\sigma] = -4\,\epsilon_{\mu\nu\rho\sigma} \, , \epsilon_{1234} = 1 \, . \tag{A.4}$$

A positive energy spinor satisfies

$$\bar{u}(P,s)\,(i\gamma \cdot P + M) = 0 = (i\gamma \cdot P + M)\,u(P,s) \, , \tag{A.5}$$

where $s = \pm$ is the spin label. It is normalised:

$$\bar{u}(P,s)\,u(P,s) = 2M \tag{A.6}$$

and may be expressed explicitly:

$$u(P,s) = \sqrt{M - i\mathcal{E}} \begin{pmatrix} \chi_s \\ \dfrac{\vec{\sigma}\cdot\vec{P}}{M - i\mathcal{E}}\chi_s \end{pmatrix} , \tag{A.7}$$

with $\mathcal{E} = i\sqrt{\vec{P}^2 + M^2}$,

$$\chi_+ = \begin{pmatrix} 1 \\ 0 \end{pmatrix} , \ \chi_- = \begin{pmatrix} 0 \\ 1 \end{pmatrix} . \tag{A.8}$$

For the free-particle spinor, $\bar{u}(P,s) = u(P,s)^\dagger\gamma_4$.

The spinor can be used to construct a positive energy projection operator:

$$\Lambda_+(P) := \frac{1}{2M}\sum_{s=\pm} u(P,s)\,\bar{u}(P,s) = \frac{1}{2M}\left(-i\gamma\cdot P + M\right). \tag{A.9}$$

A negative energy spinor satisfies

$$\bar{v}(P,s)\left(i\gamma\cdot P - M\right) = 0 = \left(i\gamma\cdot P - M\right) v(P,s)\,, \tag{A.10}$$

and possesses properties and satisfies constraints obtained via obvious analogy with $u(P,s)$.

A charge-conjugated Bethe-Salpeter amplitude is obtained via

$$\bar{\Gamma}(k;P) = C^\dagger\,\Gamma(-k;P)^{\rm T}\,C\,, \tag{A.11}$$

where "T" denotes a transposing of all matrix indices and $C = \gamma_2\gamma_4$ is the charge conjugation matrix, $C^\dagger = -C$.

In describing the Δ resonance we employ a Rarita-Schwinger spinor to unambiguously represent a covariant spin-3/2 field. The positive energy spinor is defined by the following equations:

$$\left(i\gamma\cdot P + M\right) u_\mu(P;r) = 0\,,\ \gamma_\mu u_\mu(P;r) = 0\,,\ P_\mu u_\mu(P;r) = 0\,, \tag{A.12}$$

where $r = -3/2, -1/2, 1/2, 3/2$. It is normalised:

$$\bar{u}_\mu(P;r')\,u_\mu(P;r) = 2M\,, \tag{A.13}$$

and satisfies a completeness relation

$$\frac{1}{2M}\sum_{r=-3/2}^{3/2} u_\mu(P;r)\,\bar{u}_\nu(P;r) = \Lambda_+(P)\,R_{\mu\nu}\,, \tag{A.14}$$

where

$$R_{\mu\nu} = \delta_{\mu\nu}I_{\rm D} - \frac{1}{3}\gamma_\mu\gamma_\nu + \frac{2}{3}\hat{P}_\mu\hat{P}_\nu I_{\rm D} - i\frac{1}{3}[\hat{P}_\mu\gamma_\nu - \hat{P}_\nu\gamma_\mu]\,, \tag{A.15}$$

with $\hat{P}^2 = -1$, which is very useful in simplifying the positive energy Δ's Faddeev equation.

Appendix B

Gauge potential, field strength and E- and B-fields

This subsections details on conventions used in chapter 3. Given a field $\phi(x)$ we define the gauge transformation via

$$\phi(x) \to g(x)\phi(x) \ , \tag{B.1}$$

where $g(x) = \exp(ig_0\alpha^a(x)T^a)$ and g_0 is the bare coupling constant. For the covariant derivative $D_\mu = \partial_\mu - ig_0A_\mu$ to transform correctly, i.e. $D_\mu \to gD_\mu$, the gauge potential $A_\mu = A^a_\mu T^a$ has to transform like

$$A_\mu \to gA_\mu g^{-1} - \frac{i}{g_0}(\partial_\mu g)g^{-1} \ . \tag{B.2}$$

Acting on a field operator $\phi = \phi^a T^a$ the covariant derivative reads

$$[D_\mu\phi]^a = \partial_\mu\phi^a + g_0 f^{abc}A^b_\mu\phi^c \ . \tag{B.3}$$

The field strength tensor can be defined by the commutator of the covariant derivative,

$$\frac{1}{g_0}[[D_\mu, D_\nu]\phi]_a = f^{abc}F^b_{\mu\nu}\phi^c \ , \tag{B.4}$$

and hence

$$F^b_{\mu\nu} = \partial_\mu A^b_\nu - \partial_\nu A^b_\nu + g_0 f^{bde}A^d_\mu A^e_\nu \ . \tag{B.5}$$

The electric and magnetic fields are defined in terms of the field strength tensor by

$$E^a_k = F^a_{0k} \ , \ B^a_k = -\frac{1}{2}\varepsilon_{ijk}F^a_{ij} \ . \tag{B.6}$$

In terms of the gauge potential they are therefore

$$E^a_k = -\partial_k A^a_0 + \partial_0 A^a_k + g_0 f^{abc}A^b_0 A^c_k \ , \tag{B.7}$$

$$B^a_k = -\varepsilon_{ifk}\left[\partial_i A^a_j + g_0\frac{1}{2}f^{abc}A^b_i A^c_j\right] \ . \tag{B.8}$$

Appendix C

Numerical method employed in solving the gap equation with transverse gluons and retardation, eqs. (4.43)-(4.45)

We solve the integral equations by iteration. To this end the involved integrals have to be computed accurately.

For the infrared regulator going to zero the first non-trivial task is the numerical computation of the angular integrals and especially those which contain the Richardson potential. They exhibit a singular behaviour at the right side of the integration domain. To improve the calculation precision we split off the infrared k^{-4}-behaviour from the Richardson potential, where the angular integrals can be computed analytically. Still we encounter a pronounced behaviour for $|\mathbf{q}| \approx |\mathbf{p}|$ for the remaining parts. An integral substitution can be performed that introduces exponential suppression for the integration region near the right boundary. The price we have to pay using this method is the numerical computation of the error function and the numerical determination of the root of a well-behaved function in order to find the integration limit. These tasks are well feasible with standard techniques [PFTV].

For the integration over the magnitude of the three-momentum we divide the integration interval in four regions. This procedure is governed by the peak at the position $|\mathbf{q}| = |\mathbf{p}|$, which is sampled symmetrically by a relatively small interval. For the sake of reaching a high precision in the subtraction procedure of renormalisation we choose a point with a magnitude higher than the renormalisation coordinate and the last mesh point of the propagator functions, from which on the integration to infinity is performed.

The remaining two intervals are integrated with the help of Gaussian quadrature and a logarithmic mapping, that accumulates summation points at the left and right boundarys of the integration domain.

The integrands in the coordinate q_E, which we call the frequency coordinate, are peaked at $q_E = 0\,\mathrm{GeV}$ and at the point p_E. The width of these peaks depend for the former on the *propagator functions* together with the magnitude of the three-momentum integration variable and for the latter on the gluon energy. Evidently one has to allow for changes in the functions in questions and therefore we repeat the following procedure up to convergence:

- We perform the frequency integration with an adaptive Gauss-Kronrod integrator [PDKUK] and store the integration points.
- Using this information we compute the kernel of the integral equation and iterate it a given number of times.

This algorithm can be parallelised well in the mesh points of the frequency coordinate p_E. The time needed for convergence increases with decreasing infrared regulator. One can lower it considerably by extrapolating successive calculated values for single mesh points to a higher iteration number (which does not affect the criterion or quality of convergence) or by using the ε-algorithm.

Bibliography

[A+01] Ahlig, S. [u. a.]: Production processes as a tool to study parameterizations of quark confinement. In: *Phys. Rev.* D64 (2001), S. 014004

[ABR95] Alkofer, Reinhard ; Bender, Axel ; Roberts, Craig D.: Pion loop contribution to the electromagnetic pion charge radius. In: *Int. J. Mod. Phys.* A10 (1995), S. 3319–3342

[ADFM04] Alkofer, R. ; Detmold, W. ; Fischer, C. S. ; Maris, P.: Analytic properties of the Landau gauge gluon and quark propagators. In: *Phys. Rev.* D70 (2004), S. 014014

[Adl69] Adler, Stephen L.: Axial vector vertex in spinor electrodynamics. In: *Phys. Rev.* 177 (1969), S. 2426–2438

[Adl86] Adler, Stephen L.: Gap equation models for chiral symmetry breaking. In: *Prog. Theor. Phys. Suppl.* 86 (1986), S. 12

[AFLE06] Alkofer, Reinhard ; Fischer, Christian S. ; Llanes-Estrada, Felipe J.: Dynamically induced scalar quark confinement. (2006). – hep-ph/0607293

[AG06] Alkofer, R. ; Greensite, J.: Quark confinement: The hard problem of hadron physics. (2006). – hep-ph/0610365

[AHK+05] Alkofer, R. ; Holl, A. ; Kloker, M. ; Krassnigg, A. ; Roberts, C. D.: On nucleon electromagnetic form factors. In: *Few Body Syst.* 37 (2005), S. 1–31

[AKKW06] Alkofer, R. ; Kloker, M. ; Krassnigg, A. ; Wagenbrunn, R. F.: Aspects of the confinement mechanism in Coulomb-gauge QCD. In: *Phys. Rev. Lett* 96 (2006), S. 022001

[Alk88] Alkofer, Reinhard: Chirale Symmetriebrechung und der chirale Phasenuebergang in instantanen Naeherungen zur Quantenchromodynamik in Coulombeichung. (1988). – PhD thesis, Technische Universitaet Muenchen

[ALTY04] Ashley, J. D. ; Leinweber, D. B. ; Thomas, Anthony W. ; Young, R. D.: Nucleon electromagnetic form factors from lattice QCD. In: *Eur. Phys. J.* A19 (2004), S. 9–14

[ALYO+83] Amer, A. ; Le Yaouanc, A. ; Oliver, L. ; Pene, O. ; Raynal, J. C.: Instability of the chiral invariant vacuum due to gluon exchange. In: *Z. Phys.* C17 (1983), S. 61

[AR] Alkofer, R. ; Reinhardt, H.: Chiral quark dynamics. . – Berlin, Germany: Springer (1995) 114 p. (Lecture notes in physcis)

[ARZ06] Arrington, J. ; Roberts, C. D. ; Zanotti, J. M.: Nucleon electromagnetic form factors. (2006). – nucl-th/0611050

[AS01] Alkofer, Reinhard ; von Smekal, Lorenz: The infrared behavior of QCD Green's functions: Confinement, dynamical symmetry breaking, and hadrons as relativistic bound states. In: *Phys. Rept.* 353 (2001), S. 281

[AT77] Afnan, I. R. ; Thomas, Anthony W.: Fundamentals of three-body scattering theory. In: *Top. Curr. Phys.* 2 (1977), S. 1–47

[B+02] Boffi, S. [u. a.]: Covariant electroweak nucleon form factors in a chiral constituent quark model. In: *Eur. Phys. J.* A14 (2002), S. 17–21

[Baa97] van Baal, Pierre: Gribov ambiguities and the fundamental domain. (1997). – hep-th/9711070

[BC80] Ball, James S. ; Chiu, Ting-Wai: Analytic properties of the vertex function in gauge theories. 1. In: *Phys. Rev.* D22 (1980), S. 2542

[BCP89] Burden, C. J. ; Cahill, R. T. ; Praschifka, J.: Baryon structure and QCD: Nucleon calculations. In: *Austral. J. Phys.* 42 (1989), S. 147–159

[BD] Bjorken, J.D. ; Drell, S.D.: Relativistic Quantum Fields. . – (McGraw-Hill, new York, 1965) sects. 19.3 and 19.8

[BH92] Brodsky, Stanley J. ; Hiller, John R.: Universal properties of the electromagnetic interactions of spin one systems. In: *Phys. Rev.* D46 (1992), S. 2141–2149

[BHK+04] Bhagwat, M. S. ; Holl, A. ; Krassnigg, A. ; Roberts, C. D. ; Tandy, P. C.: Aspects and consequences of a dressed-quark-gluon vertex. In: *Phys. Rev.* C70 (2004), S. 035205

[BJY03] Belitsky, Andrei V. ; Ji, Xiang-dong ; Yuan, Feng: A perturbative QCD analysis of the nucleon's Pauli form factor F2(Q**2). In: *Phys. Rev. Lett.* 91 (2003), S. 092003

[BKR03] Bloch, J. C. R. ; Krassnigg, A. ; Roberts, C. D.: Regarding proton form factors. In: *Few Body Syst.* 33 (2003), S. 219–232

[BL04] Burkert, V. D. ; Lee, T. S. H.: Electromagnetic meson production in the nucleon resonance region. In: *Int. J. Mod. Phys.* E13 (2004), S. 1035–1112

[BPRT03] Bhagwat, M. S. ; Pichowsky, M. A. ; Roberts, C. D. ; Tandy, P. C.: Analysis of a quenched lattice-QCD dressed-quark propagator. In: *Phys. Rev.* C68 (2003), S. 015203

[BRT96] Burden, C. J. ; Roberts, Craig D. ; Thomson, Mark J.: Electromagnetic Form Factors of Charged and Neutral Kaons. In: *Phys. Lett.* B371 (1996), S. 163–168

[BRVS96] Bender, A. ; Roberts, Craig D. ; Von Smekal, L.: Goldstone Theorem and Diquark Confinement Beyond Rainbow- Ladder Approximation. In: *Phys. Lett.* B380 (1996), S. 7–12

[Bur82] Burnel, A.: Choice of a gauge in the light of Dirac quantization. In: *Phys. Rev.* D26 (1982), S. 442–454

[BZ99] Baulieu, Laurent ; Zwanziger, Daniel: Renormalizable non-covariant gauges and Coulomb gauge limit. In: *Nucl. Phys.* B548 (1999), S. 527–562

[CL] Cheng, T. P. ; Li, L. F.: Gauge theory of elementary particle physics. . – Oxford, Uk: Clarendon (1984) 536 P. (Oxford Science Publications)

[CM02] Cotanch, Stephen R. ; Maris, Pieter: QCD based quark description of pi pi scattering up to the sigma and rho region. In: *Phys. Rev.* D66 (2002), S. 116010

[CM03] Cotanch, Stephen R. ; Maris, Pieter: Ladder Dyson-Schwinger calculation of the anomalous gamma 3pi form factor. In: *Phys. Rev.* D68 (2003), S. 036006

[CMZ02] Cucchieri, Attilio ; Mendes, Tereza ; Zwanziger, Daniel: SU(2) running coupling constant and confinement in minimal Coulomb and Landau gauges. In: *Nucl. Phys. Proc. Suppl.* 106 (2002), S. 697–699

[Cuc06] Cucchieri, Attilio: Lattice results in Coulomb gauge. (2006). – hep-lat/0612004

[CZ02a] Cucchieri, Attilio ; Zwanziger, Daniel: Fit to gluon propagator and Gribov formula. In: *Phys. Lett.* B524 (2002), S. 123–128

[CZ02b] Cucchieri, Attilio ; Zwanziger, Daniel: Numerical study of gluon propagator and confinement scenario in minimal Coulomb gauge. In: *Phys. Rev.* D65 (2002), S. 014001

[CZ02c] Cucchieri, Attilio ; Zwanziger, Daniel: Renormalization group calculation of color Coulomb potential. In: *Phys. Rev.* D65 (2002), S. 014002

[CZ03] Cucchieri, Attilio ; Zwanziger, Daniel: Gluon propagator and confinement scenario in Coulomb gauge. In: *Nucl. Phys. Proc. Suppl.* 119 (2003), S. 727–729

[D+04] Davies, C. T. H. [u. a.]: High-precision lattice QCD confronts experiment. In: *Phys. Rev. Lett.* 92 (2004), S. 022001

[Dir] Dirac, P.A.M.: Lectures on Quantum Mechanics. . – Yeshiva University, 1964

[DM85] Davis, A. C. ; Matheson, A. M.: The stability of the chiral vacuum. In: *Phys. Lett.* B165 (1985), S. 395

[E+04] Eidelman, S. [u. a.]: Review of particle physics. In: *Phys. Lett.* B592 (2004), S. 1

[ERS06] Epple, D. ; Reinhardt, H. ; Schleifenbaum, W.: Confining solution of the Dyson-Schwinger equations in Coulomb gauge. (2006). – hep-th/0612241

[FGMS83] Fomin, P. I. ; Gusynin, V. P. ; Miransky, V. A. ; Sitenko, Yu. A.: Dynamical symmetry breaking and particle mass generation in gauge field theories. In: *Riv. Nuovo Cim.* 6N5 (1983), S. 1–90

[FGS04] Fuchs, Thomas ; Gegelia, Jambul ; Scherer, Stefan: Structure of the nucleon in chiral perturbation theory. In: *Eur. Phys. J.* A19 (2004), S. 35–42

[Fis03] Fischer, Christian S.: Non-perturbative propagators, running coupling and dynamical mass generation in ghost - antighost symmetric gauges in QCD. (2003). – PhD thesis, hep-ph/0304233

[Fis06] Fischer, Christian S.: Infrared properties of QCD from Dyson-Schwinger equations. In: *J. Phys.* G32 (2006), S. R253–R291

[FR04a] Feuchter, C. ; Reinhardt, H.: Quark and gluon confinement in Coulomb gauge. (2004). – hep-th/0402106

[FR04b] Feuchter, C. ; Reinhardt, H.: Variational solution of the Yang-Mills Schroedinger equation in Coulomb gauge. In: *Phys. Rev.* D70 (2004), S. 105021

[FW03] Friedrich, J. ; Walcher, T.: A coherent interpretation of the form factors of the nucleon in terms of a pion cloud and constituent quarks. In: *Eur. Phys. J.* A17 (2003), S. 607–623

[G+71] Galster, S. [u. a.]: Elastic electron - deuteron scattering and the electric neutron form-factor at four momentum transfers 5-fm$^{-2} \leq q^2 \leq$ 14-fm^{-2}. In: *Nucl. Phys.* B32 (1971), S. 221–237

[G+01] Gayou, O. [u. a.]: Measurements of the elastic electromagnetic form factor ratio $\mu_p G_E^p / G_M^p$ via polarization transfer. In: *Phys. Rev.* C64 (2001), S. 038202

[G+02] Gayou, O. [u. a.]: Measurement of G(E(p))/G(M(p)) in e(pol.) p $\rightarrow$ e p(pol.) to $Q^2 = 5.6$-GeV^2. In: *Phys. Rev. Lett.* 88 (2002), S. 092301

[Gao03] Gao, Hai-yan: Nucleon electromagnetic form factors. In: *Int. J. Mod. Phys.* E12 (2003), S. 1–40

[Glo83] Gloeckle, W: The Quantum Mechanical Few-Body Problem. In: *Springer, Berlin, Germany* (1983)

[GMW83] Govaerts, J. ; Mandula, J. E. ; Weyers, J.: Pion properties in QCD. In: *Phys. Lett.* B130 (1983), S. 427

[GMW84] Govaerts, J. ; Mandula, J. E. ; Weyers, J.: A model for chiral symmetry breaking in QCD. In: *Nucl. Phys.* B237 (1984), S. 59

[GO03] Greensite, Jeff ; Olejnik, Stefan: Coulomb energy, vortices, and confinement. In: *Phys. Rev.* D67 (2003), S. 094503

[GOZ05] Greensite, Jeff ; Olejnik, Stefan ; Zwanziger, Daniel: Center vortices and the Gribov horizon. In: *JHEP* 05 (2005), S. 070

[Gri78] Gribov, V. N.: Quantization of non-Abelian gauge theories. In: *Nucl. Phys.* B139 (1978), S. 1

[GT] Gitman, D. M. ; Tyutin, I. V.: Quantization of fields with constraints. . – Berlin, Germany: Springer (1990) 291 p. (Springer series in nuclear and particle physics)

[GT02] Greensite, Jeff ; Thorn, Charles B.: Gluon chain model of the confining force. In: *JHEP* 02 (2002), S. 014

[H+02] Hecht, M. B. [u. a.]: Nucleon mass and pion loops. In: *Phys. Rev.* C65 (2002), S. 055204

[H+05] Holl, A [u. a.]: On nucleon electromagnetic form factors: A precis. In: *Nucl. Phys.* A755 (2005), S. 298–302

[HAR97] Hellstern, G. ; Alkofer, R. ; Reinhardt, H.: Diquark confinement in an extended NJL model. In: *Nucl. Phys.* A625 (1997), S. 697–712

[HJLT00a] Hackett-Jones, Emily J. ; Leinweber, D. B. ; Thomas, Anthony W.: Incorporating chiral symmetry and heavy quark theory in extrapolations of octet baryon charge radii. In: *Phys. Lett.* B494 (2000), S. 89–99

[HJLT00b] Hackett-Jones, Emily J. ; Leinweber, D. B. ; Thomas, Anthony W.: Incorporating chiral symmetry in extrapolations of octet baryon magnetic moments. In: *Phys. Lett.* B489 (2000), S. 143–147

[HK95] Hanhart, C. ; Krewald, S.: Faddeev approach to the octet and decuplet baryons. In: *Phys. Lett.* B344 (1995), S. 55–60

[HKLW98] Hess, M. ; Karsch, F. ; Laermann, E. ; Wetzorke, I.: Diquark masses from lattice QCD. In: *Phys. Rev.* D58 (1998), S. 111502

[HKRW05] Holl, A. ; Krassnigg, A. ; Roberts, C. D. ; Wright, S. V.: On the complexion of pseudoscalar mesons. In: *Int. J. Mod. Phys.* A20 (2005), S. 1778–1784

[HP99] Hawes, F. T. ; Pichowsky, M. A.: Electromagnetic form factors of light vector mesons. In: *Phys. Rev.* C59 (1999), S. 1743–1750

[IBY95] Ishii, N. ; Bentz, W. ; Yazaki, K.: Baryons in the NJL model as solutions of the relativistic Faddeev equation. In: *Nucl. Phys.* A587 (1995), S. 617–656

[IKR99] Ivanov, Mikhail A. ; Kalinovsky, Yu. L. ; Roberts, Craig D.: Survey of heavy-meson observables. In: *Phys. Rev.* D60 (1999), S. 034018

[Ish98] Ishii, N.: Meson exchange contributions to the nucleon mass in the Faddeev approach to the NJL model. In: *Phys. Lett.* B431 (1998), S. 1–7

[IZ] Itzykson, C. ; Zuber, J. B.: Quantum field theory. . – New York, Usa: Mcgraw-hill (1980) 705 P.(International Series In Pure and Applied Physics)

[J+00] Jones, M. K. [u. a.]: G(E(p))/G(M(p)) ratio by polarization transfer in e(pol.) p → e p(pol.). In: *Phys. Rev. Lett.* 84 (2000), S. 1398–1402

[KM01] Kubis, Bastian ; Meissner, Ulf-G.: Low energy analysis of the nucleon electromagnetic form factors. In: *Nucl. Phys.* A679 (2001), S. 698–734

[Kug] Kugo, T.: Eichtheorie. . – Springer, 1997

[Lei] Leibbrandt, G.: Noncovariant gauges: Quantization of Yang-Mills and Chern- Simons theory in axial type gauges. . – Singapore, Singapore: World Scientific (1994) 212 p

[Lic] Lichtenegger, Klaus: Private communication.

[LM04] Langfeld, Kurt ; Moyaerts, Laurent: Propagators in Coulomb gauge from SU(2) lattice gauge theory. In: *Phys. Rev.* D70 (2004), S. 074507

[LTY01] Leinweber, D. B. ; Thomas, Anthony W. ; Young, R. D.: Chiral symmetry and the intrinsic structure of the nucleon. In: *Phys. Rev. Lett.* 86 (2001), S. 5011–5014

[LW96] Leibbrandt, George ; Williams, Jimmy: Split Dimensional Regularization for the Coulomb Gauge. In: *Nucl. Phys.* B475 (1996), S. 469–483

[Mar02] Maris, P.: Effective masses of diquarks. In: *Few Body Syst.* 32 (2002), S. 41–52

[Mar04] Maris, Pieter: Electromagnetic properties of diquarks. In: *Few Body Syst.* 35 (2004), S. 117–127

[MBIY02] Mineo, H. ; Bentz, W. ; Ishii, N. ; Yazaki, K.: Axial vector diquark correlations in the nucleon: Structure functions and static properties. In: *Nucl. Phys.* A703 (2002), S. 785–820

[MF02] Miller, Gerald A. ; Frank, Michael R.: Q**2 independence of QF(2)/F(1), Poincare invariance and the non-conservation of helicity. In: *Phys. Rev.* C65 (2002), S. 065205

[MMD96] Mergell, P. ; Meissner, Ulf G. ; Drechsel, D.: Dispersion theoretical analysis of the nucleon electromagnetic form-factors. In: *Nucl. Phys.* A596 (1996), S. 367–396

[Moy04] Moyaerts, Laurent: A Numerical Study of Quantum Forces: Casimir Effect, Vortices and Coulomb Gauge Yang-Mills Theory. (2004). – PhD thesis, Universitaet Tuebingen

[MR98] Maris, Pieter ; Roberts, Craig D.: Pseudovector components of the pion, pi0 $\rightarrow \gamma\ \gamma$, and F(pi)(q**2). In: *Phys. Rev.* C58 (1998), S. 3659–3665

[MR03] Maris, Pieter ; Roberts, Craig D.: Dyson-Schwinger equations: A tool for hadron physics. In: *Int. J. Mod. Phys.* E12 (2003), S. 297–365

[MRT98] Maris, Pieter ; Roberts, Craig D. ; Tandy, Peter C.: Pion mass and decay constant. In: *Phys. Lett.* B420 (1998), S. 267–273

[MT00] Maris, Pieter ; Tandy, Peter C.: The quark photon vertex and the pion charge radius. In: *Phys. Rev.* C61 (2000), S. 045202

[NJL61a] Nambu, Yoichiro ; Jona-Lasinio, G.: Dynamical model of elementary particles based on an analogy with superconductivity. I. In: *Phys. Rev.* 122 (1961), S. 345–358

[NJL61b] Nambu, Yoichiro ; Jona-Lasinio, G.: Dynamical model of elementary particles based on an analogy with superconductivity. II. In: *Phys. Rev.* 124 (1961), S. 246–254

[NNST07] Nakagawa, Y. ; Nakamura, A. ; Saito, T. ; Toki, H.: Infrared behavior of the Faddeev-Popov operator in Coulomb gauge QCD. In: *Phys. Rev.* D75 (2007), S. 014508

[NS06] Nakamura, A. ; Saito, T.: Color confinement in Coulomb gauge QCD. In: *Prog. Theor. Phys.* 115 (2006), S. 189–200

[OAS00] Oettel, M. ; Alkofer, R. ; von Smekal, L.: Nucleon properties in the covariant quark diquark model. In: *Eur. Phys. J.* A8 (2000), S. 553–566

[Oet00] Oettel, Martin: Baryons as relativistic bound states of quark and diquark. (2000). – PhD thesis, nucl-th/0012067

[OHAR98] Oettel, M. ; Hellstern, G. ; Alkofer, R. ; Reinhardt, H.: Octet and decuplet baryons in a covariant and confining diquark-quark model. In: *Phys. Rev.* C58 (1998), S. 2459–2477

[OPS00] Oettel, Martin ; Pichowsky, Mike ; von Smekal, Lorenz: Current conservation in the covariant quark-diquark model of the nucleon. In: *Eur. Phys. J.* A8 (2000), S. 251–281

[OVSA02] Oettel, M. ; Von Smekal, L. ; Alkofer, R.: Relativistic three-quark bound states in separable two- quark approximation. In: *Comput. Phys. Commun.* 144 (2002), S. 63

[PA86] Pearce, B. C. ; Afnan, I. R.: The renormalized pi N N coupling constant and the P wave phase shifts in the cloudy bag model. In: *Phys. Rev.* C34 (1986), S. 991

[PDKUK] Piessens, R. ; de Doncker-Kapenga, E. ; Ueberhuber, C.W. ; Kahaner, D.K.: Quadpack. . – Berlin Heidelberg, Germany: Springer (1983) 301 p. (Springer series in computational mathematics)

[PFTV] Press, W.H. ; Flannery, B.P. ; Teukolsky, S.A. ; Vetterlink, W.T.: Numerical Recipes.

[Pok] Pokorski, S.: Gauge field theories. . – Cambridge, Uk: Univ. Pr. (2000) 609 P. (Cambridge Monographs On Mathematical Physics)

[Pol76] Politzer, H. D.: Effective quark masses in the chiral limit. In: *Nucl. Phys.* B117 (1976), S. 397

[PPV06] Perdrisat, C. F. ; Punjabi, V. ; Vanderhaeghen, M.: Nucleon electromagnetic form factors. (2006). – hep-ph/0612014

[PS] Peskin, Michael E. ; Schroeder, D. V.: An Introduction to quantum field theory. . – Reading, USA: Addison-Wesley (1995) 842 p

[RF05] Reinhardt, H. ; Feuchter, C.: On the Yang-Mills wave functional in Coulomb gauge. In: *Phys. Rev.* D71 (2005), S. 105002

[Ric79] Richardson, John L.: The heavy quark potential and the upsilon, J / psi systems. In: *Phys. Lett.* B82 (1979), S. 272

[RJ04] Ralston, John P. ; Jain, Pankaj: QCD form factors and hadron helicity non-conservation. In: *Phys. Rev.* D69 (2004), S. 053008

[SBZ03] Stodolsky, L. ; van Baal, Pierre ; Zakharov, V. I.: Defining in the finite volume Hamiltonian formalism. In: *Phys. Lett.* B552 (2003), S. 214–222

[Sch] Schrieffer, J. R.: Theory of superconductivity. . – (Benjamin, New York, 1964) sect. 8.5

[SD64] Salam, Abdus ; Delbourgo, Robert: Renormalizable electrodynamics of scalar and vector mesons. II. In: *Phys. Rev.* 135 (1964), S. B1398–B1427

[SK06] Szczepaniak, Adam P. ; Krupinski, Pawel: Coulomb energy and gluon distribution in the presence of static sources. In: *Phys. Rev.* D73 (2006), S. 034022

[SL01] Sato, T. ; Lee, T. S. H.: Dynamical study of the Delta excitation in N(e,e' pi) reactions. In: *Phys. Rev.* C63 (2001), S. 055201

[SS01] Suzuki, Alfredo T. ; Schmidt, Alexandre G. M.: First results for the Coulomb gauge integrals using NDIM. In: *Eur. Phys. J.* C19 (2001), S. 391–396

[Tho84] Thomas, Anthony W.: Chiral Symmetry and the Bag Model: A New Starting Point for Nuclear Physics. In: *Adv. Nucl. Phys.* 13 (1984), S. 1–137

[Tho02] Thorn, Charles B.: A worldsheet description of planar Yang-Mills theory. In: *Nucl. Phys.* B637 (2002), S. 272–292

[TW] Thomas, Anthony W. ; Weise, Wolfram: The Structure of the Nucleon. . – Berlin, Germany: Wiley-VCH (2001) 389 p

[W+94] Walker, R. C. [u. a.]: Measurements of the proton elastic form-factors for 1-GeV/$c^2 \leq Q^2 \leq$ 3-GeV/C^2 at SLAC. In: *Phys. Rev.* D49 (1994), S. 5671–5689

[WBAR93] Weiss, C. ; Buck, A. ; Alkofer, R. ; Reinhardt, H.: Diquark electromagnetic form-factors in a Nambu-Jona- Lasinio model. In: *Phys. Lett.* B312 (1993), S. 6–12

[YLTW01] Young, R. D. ; Leinweber, D. B. ; Thomas, Anthony W. ; Wright, S. V.: Systematic correction of the chiral properties of quenched QCD. (2001). – hep-lat/0111041

[Ynd] Yndurain, F.J.: Quantum Chromodynamics. . – New York, USA: Springer (1983) 227 p.

[Zwa82] Zwanziger, Daniel: Nonperturbative modification of the Faddeev–Popov formula and banishment of the naive vacuum. In: *Nucl. Phys.* B209 (1982), S. 336

[Zwa97] Zwanziger, Daniel: Lattice Coulomb Hamiltonian and static color-Coulomb field. In: *Nucl. Phys.* B485 (1997), S. 185–240

[Zwa03] Zwanziger, Daniel: No confinement without Coulomb confinement. In: *Phys. Rev. Lett.* 90 (2003), S. 102001

Danksagung

Ich möchte mich bei allen bedanken, die zum Gelingen meiner Dissertation beigetragen haben.

An erster Stelle danke ich meinem Betreuer Herrn Prof. Dr. Reinhard Alkofer für das Interesse an meiner Arbeit. Herrn Prof. Dr. Müther danke ich für die Betreuung von Tübinger Seite aus.

Für die Zusammenarbeit an einem Teil des Coulomb-Eichung-Projekts danke ich Andreas Krassnigg und Robert Wagenbrunn. Für nutzbringende Diskussionen zum Thema Quark-DSE danke ich Dominik Nickel. Für die sehr angenehme Atmosphäre in unserem Büro und viele Tipps in Sachen Computer danke ich Laurent Moyaerts.

Sebastian Weiß und Christian Korn danke ich für die gemeinsame, wertvolle Studien- und Freizeit.

Den Tübinger und Grazer Arbeitsgruppen möchte ich für die angenehme Atmosphäre und die gemeinsamen Freizeitaktivitäten danken. Als ein besonderes Highlight sei das zeitweise wöchentliche Fußballspielen mit Prof. Dr. Reinhardt erwähnt.

Dem Graduiertenkolleg “Hadronen im Vakuum, in Kernen und Sternen” danke ich für die interessanten Vorlesungs- und Vortragsreihen, die meine Aufmerksamkeit auch auf Themengebiete gelenkt haben, welche nicht in unmittelbarem Zusammenhang zu meiner Arbeit stehen. Ferner danke ich dem Graduiertenkolleg für die gewährte finanzielle Unterstützung.

Abschließend gilt mein ganz besonderer Dank meinen Eltern für ihre unermüdliche, persönliche wie finanzielle Unterstützung und ihren Rückhalt.

Lebenslauf

Persönliche Daten

Name:	Markus Kloker
geboren:	13.04.1977, Blaubeuren, Deutschland
Staatsangehörigkeit:	deutsch
Familienstand:	ledig

Ausbildung

1996	Abitur am mathematisch-naturwissenschaftlichen Gymnasium Blaubeuren, Durchschnittsnote: 1,1.
08/1996-09/1997	Zivildienst, Katholische Sozialstation Tübingen
10/1997-07/2000	Studium der Physik an der Univ. Tübingen
18.04.2000	Vordiplom, Durchschnittsnote sehr gut
08/2000-05/2001	Zwei Auslandssemester an der University of Maryland, College Park
06/2001-01/2004	Studium der Physik an der Univ. Tübingen
02/2003-01/2004	Diplomarbeit: "Der Zerfall des ungeladenen Σ-Hyperons in einem kovarianten Diquark-Quark-Modell"
30.01.2004	Diplom in Physik, Gesamtnote sehr gut
02/2004-03/2005	Beginn der Dissertation *The QCD Quark Propagator in Coulomb Gauge and some Implications for Hadronic Physics* am Institut für Physik, Univ. Tübingen
04/2005-03/2007	Wechsel mit Prof. R. Alkofer an das Institut für Physik der Univ. Graz und Fertigstellung der Dissertation Betreuer: Prof. H. Müther (Univ. Tübingen), Prof. R. Alkofer (Univ. Graz)

Stipendien und Beschäftigungen

02/2004-03/2004	Wissenschaftliche Hilfskraft, Univ. Tübingen
04/2004-06/2004	Wissenschaftlicher Angestellter, Univ. Tübingen
07/2004-03/2005	Stipendium des europäischen Graduiertenkollegs *Hadronen im Vakuum, in Kernen und Sternen*, Univ. Tübingen
04/2005-03/2007	Wissenschaftlicher Mitarbeiter, Univ. Graz

Akademische Lehrer

Alkofer, Bei-Lok Hu, Clement, Einstein, Fischer, Gates, Gönnenwein, Hartman, Hübener, Kaul,Kelly, Kern, Langfeld, Müther, Pfister, Plies, Reinhardt, Skuja, Staudt, Wagner, Wolff